



KARAZIN UNIVERSITY
CLASSICS AHEAD OF TIME

ISSN 2221-5646 (Print),
ISSN 2523-4641 (Online)

VISNYK OF V.N.KARAZIN
KHARKIV NATIONAL UNIVERSITY

**Ser. MATHEMATICS, APPLIED
MATHEMATICS AND MECHANICS**



Том 100 ' 2024

Вісник Харківського національного
університету імені В.Н.Каразіна
серія

**МАТЕМАТИКА,
ПРИКЛАДНА МАТЕМАТИКА
І МЕХАНІКА**

Volume 100, 2024

ISSN 2221-5646 (Print)
ISSN 2523-4641 (Online)

Міністерство освіти і науки України

ВІСНИК

Харківського національного
університету імені В. Н. Каразіна

Серія

«Математика, прикладна математика і механіка»

Серія започаткована 1965 р.

Том 100



Visnyk of V. N. Karazin Kharkiv National University
Ser. "Mathematics, Applied Mathematics and Mechanics"

Vol. 100

Харків
2024

До Віснику включено статті з математичного аналізу, математичної фізики, диференціальних рівнянь, математичної теорії керування та механіки, які містять нові теоретичні результати у зазначених галузях і мають прикладне значення. УДК 51+531/534](062.552).

Для викладачів, наукових працівників, аспірантів, працюючих у відповідних або суміжних сферах.

Вісник є фаховим виданням у галузі фізико-математичних наук, категорія «Б» за спеціальностями 111 - Математика та 113 - Прикладна математика (Наказ МОН України №1643 від 28.12.2019 р.).

Затверджено до друку рішенням Вченої ради Харківського національного університету імені В. Н. Каразіна (протокол № 26 від 23 грудня 2024 р.).

Головний редактор—Коробов В.І.—д-р ф.-м. наук, проф., ХНУ ім. В.Н. Каразіна, Україна

Члени редакційної колегії:

Кадець В.М.—д-р ф.-м. наук, проф., ХНУ імені В.Н. Каразіна, Україна

Фаворов С.Ю.—д-р ф.-м. наук, проф., ХНУ імені В.Н. Каразіна, Україна

Єгорова І.Є.—д-р ф.-м. наук, проф., ФТІНТ НАН України

Пастур Л.А.—д-р ф.-м. наук, проф., акад. НАН України, ФТІНТ НАН України

Хруслов Є.Я.—д-р ф.-м. наук, проф., акад. НАН України, ФТІНТ НАН України

Шепельський Д.Г.—д-р ф.-м. наук, проф., ФТІНТ НАН України та

ХНУ імені В.Н. Каразіна, Україна

Когут П.І.—д-р ф.-м. наук, проф., Дніпровський національний університет

імені Олеса Гончара, м.Дніпро, Україна

Чуйко С.М.—д-р ф.-м. наук, проф., Інститут прикладної математики і

механіки НАН України, м.Слов'янськ, Україна

Домбровський А.—д-р ф.-м. наук, проф., Університет Щецина, Польща

Карлович Ю.І.—д-р ф.-м. наук, проф., Університет Морелос, Мехіко, Мексика

Корбич Йозеф—д-р ф.-м. наук, проф., чл.-кор. ПАН, Університет Зіелона Гора, Польща

Нгуєн Хоа Шон—д-р ф.-м. наук, проф., Академія наук та технології В'єтнама,

Інститут математики, Ханой, В'єтнам

Поляков А.І.—д-р ф.-м. наук, проф., ІНРІА Національний дослідницький інститут

інформатики та автоматички, Ле-Шене, Франція

Скляр Г.М.—д-р ф.-м. наук, проф., Університет Щецина, Польща

Відповідальний секретар — Резуненко О.В., д-р ф.-м. наук

ХНУ імені В.Н. Каразіна, Україна

Editor-in-Chief — V.I. Korobov—Dr. Sci., Prof., V.N. Karazin Kharkiv National University, Ukraine

Associate Editors:

S.Yu. Favorov—Dr. Sci., Prof., V.N. Karazin Kharkiv National University, Ukraine

V.M. Kadets—Dr. Sci., Prof., V.N. Karazin Kharkiv National University, Ukraine

I.E. Egorova—Dr. Sci., Prof., B.Verkin Institute for Low Temperature Physics

and Engineering, Ukraine

E.Ya. Khruslov—Dr. Sci., Prof., academician of NASU,

B.Verkin Institute for Low Temperature Physics and Engineering, Ukraine

L.A. Pastur—Dr. Sci., Prof., academician of NASU,

B.Verkin Institute for Low Temperature Physics and Engineering, Ukraine

D.G. Shepelsky—Dr. Sci., Prof., B.Verkin Institute for Low Temperature Physics

and Engineering, Ukraine

S.M. Chujko—Dr. Sci., Prof., Donbas State Pedagogical University, Ukraine

P.I. Kogut—Dr. Sci., Prof., Oles Honchar Dnipro National University, Ukraine

Andrzej Dabrowski—Dr. Sci., Prof., University of Szczecin, Poland

Yu. Karlovich—Dr. Sci., Prof., Morelos University, Mexico

Jozef Korbicz—Dr. Sci., Prof., corresponding member of PAS, University of Zielona Gora, Poland

Nguyen Khoa Son—Dr. Sci., Prof., Vietnamese Academy of Science and Technology,

Institute of Mathematics, Hanoi, Vietnam

A.E. Polyakov—Dr. Sci., Prof., INRIA Institut National de Recherche

en Informatique et en Automatique, Le Chesnay, France

G.M. Sklyar—Dr. Sci., Prof., University of Szczecin, Poland

Responsible Editor—A.V. Rezounenko, Dr. Sci., Prof.,

V.N. Karazin Kharkiv National University, Ukraine

Адреса редакційної колегії: 61022, Харків, майдан Свободи, 4, ХНУ імені В.Н. Каразіна, ф-т математики і інформатики, к. 7-27, т. 7075240, 7075135, **e-mail:** vestnik-khnu@ukr.net

Інтернет: <http://vestnik-math.univer.kharkov.ua>; http://periodicals.karazin.ua/mech_math

Статті пройшли внутрішнє та зовнішнє рецензування.

Ідентифікатор медіа у Реєстрі суб'єктів у сфері медіа: R30-04455 (Рішення № 1538

від 09.05.2024 р. Національної ради України з питань телебачення і радіомовлення.

Протокол № 15).

©Харківський національний університет
імені В. Н. Каразіна, оформлення, 2024


ЗМІСТ

Чуйко С. М., Несмелова О. В., Чуйко О. В. Нелінійні крайові задачі для вироджених диференціально-алгебраїчних систем у не-критичному випадку	4
Акалігво Е., Оєм А., Бабанрінса О. Математичне моделювання та віртуальне проектування метаматеріалів для зниження шуму та вібрації у побудованих конструкціях	19
Коробов В. І., Возняк О. С. Оптимальне за часом керування на підпростір для двовимірної та тривимірної системи	48
Чоке-Ріверо А. Е., Вукашинац Т. Метод функції керованості Коробова за допомогою ортогональних поліномів на $[0, \infty)$	61


CONTENTS

S. M. Chuiko, O. V. Nesmelova, O. V. Chuiko. Nonlinear boundary value problems for degenerate differential-algebraic systems in the noncritical case	4
E. Akaligwo, A. Oyem, O. Babanrinsa. Mathematical Modelling and Virtual Design of Metamaterials for Reducing Noise and Vibration in Built-Up Structures	19
V. I. Korobov, O. S. Vozniak. Time-optimal control on a subspace for the two and three-dimensional system	48
A. E. Choque-Rivero, T. Vukašinac. Korobov's controllability function method via orthogonal polynomials on $[0, \infty)$	61


С. М. Чуйко

професор, доктор фізико-математичних наук
завідувач кафедри математики та інформатики
Донбаський державний педагогічний університет
Батюка, 19, Слов'янськ Донецької області, Україна, 84116
chujko-slav@ukr.net  <http://orcid.org/0000-0001-7186-0129>

О. В. Несмєлова

доцент, доктор фізико-математичних наук
заступник директора з наукової роботи
Інститут прикладної математики і механіки НАН України
Батюка, 19, Слов'янськ Донецької області, Україна, 84116
star-o@ukr.net  <http://orcid.org/0000-0003-2542-5980>

О. В. Чуйко

доцент, кандидат фізико-математичних наук
доцент кафедри методики навчання математики та методики навчання інформатики
Донбаський державний педагогічний університет
Батюка, 19, Слов'янськ Донецької області, Україна, 84116
chujko-e@ukr.net  <http://orcid.org/0000-0002-6032-490X>

Нелінійні крайові задачі для вироджених диференціально-алгебраїчних систем у некритичному випадку

Нами отримані умови існування та схема побудови розв'язків слабконелінійної крайової задачі для виродженої диференціально-алгебраїчної системи у некритичному випадку. Крайову умову визначає слабконелінійний векторний функціонал. Лінійна частина поставленої задачі являє собою лінійну нетерову крайову задачу для виродженої диференціально-алгебраїчної системи. Лінійні диференціально-алгебраїчні крайові задачі досліджені у монографіях S. Campbell, J.R. Magnus, A.M. Samoilenko та В.П. Яковця. У роботах А.М. Самойленка та О.А. Бойчука з використанням центральної канонічної форми отримані необхідні і достатні умови існування розв'язків нелінійних диференціально-алгебраїчних крайових задач. Нами отримані необхідні і достатні умови існування розв'язків нелінійних диференціально-алгебраїчних систем без використання центральної канонічної форми, що дає можливість досліджувати розв'язність диференціально-алгебраїчних крайових задач у залежності від довільних неперервних функцій. Такий підхід значно урізноманітнює класифікацію нелінійних диференціально-алгебраїчних крайових задач у критичних і некритичних випадках.

Постановка слабконелінійної диференціально-алгебраїчної крайової задачі, дослідженої нами, узагальнює крайові задачі, досліджені в роботах Ю.О. Митро-

© Чуйко С. М., Несмєлова О. В., Чуйко О. В., 2024; CC BY 4.0 license

польського, А.М. Самойленка, а також О.А. Бойчука. Досліджено випадок, коли диференціально-алгебраїчна система не розв'язна відносно похідної, при цьому запропоновані заміни невідомої, які приводять вихідну систему до нелінійної диференціально-алгебраїчної системи, розв'язної відносно похідної. Наприкінці статті наведено приклад нелінійної диференціально-алгебраїчної антиперіодичної крайової задачі для рівняння типу Ріккати, який демонструє конструктивність отриманих необхідних і достатніх умов існування розв'язків нелінійних диференціально-алгебраїчних систем. Отримані результати можна перенести на задачі про знаходження умов існування та схеми побудови розв'язків нелінійної виродженої диференціально-алгебраїчної крайової задачі у критичних випадках, а також на задачі про знаходження умов стійкості таких розв'язків.

Ключові слова: нелінійна крайова задача; вироджена диференціально-алгебраїчна система; некритичний випадок; рівняння типу Ріккати.

2020 Mathematics Subject Classification: 34B15

1. Постановка задачі

Досліджуємо задачу про знаходження умов існування та побудову розв'язків [1]

$$z(t, \varepsilon) : z(\cdot, \varepsilon) \in \mathbb{C}^1[a, b], \quad z(t, \cdot) \in \mathbb{C}[0, \varepsilon_0]$$

нелінійної диференціально-алгебраїчної крайової задачі

$$A(t)z'(t, \varepsilon) = B(t)z(t, \varepsilon) + f(t) + \varepsilon Z(z, t, \varepsilon), \quad (1)$$

$$\ell z(\cdot, \varepsilon) = \alpha + \varepsilon J(z(\cdot, \varepsilon), \varepsilon). \quad (2)$$

Розв'язки крайової задачі (1), (2) шукаємо в малому околі розв'язку

$$z_0(t) \in \mathbb{C}^1[a, b]$$

нетерової ($n \neq k$) породжуючої диференціально-алгебраїчної задачі [9, 3]

$$A(t)z'_0(t) = B(t)z_0(t) + f(t), \quad \ell z_0(\cdot) = \alpha \in \mathbb{R}^q. \quad (3)$$

Тут

$$A(t), B(t) \in \mathbb{C}_{m \times n}[a, b]$$

— неперервні матриці, $f(t) \in \mathbb{C}[a, b]$ — неперервний вектор; $Z(z, t, \varepsilon)$ — нелінійна функція, неперервно-диференційовна за невідомою $z(t, \varepsilon)$ у малому околі розв'язку породжуючої задачі, неперервна по $t \in [a, b]$ і неперервно-диференційовна по малому параметру; $\ell z(\cdot, \varepsilon)$ — лінійний та $J(z(\cdot, \varepsilon), \varepsilon)$ — нелінійний векторний функціонали

$$\ell z(\cdot, \varepsilon), \quad J(z(\cdot, \varepsilon), \varepsilon) : \mathbb{C}[a, b] \rightarrow \mathbb{R}^q,$$

причому другий функціонал неперервно-диференційовний за невідомою $z(t, \varepsilon)$ та неперервний по малому параметру ε у малому околі розв'язку породжуючої задачі та на відрізку $[0, \varepsilon_0]$.

Нелінійна диференціально-алгебраїчна крайова задача (1), (2) узагальнює численні постановки нелінійних нетерових крайових задач [1, 4].

2. Умови розв'язності лінійної крайової задачі для виродженої диференціально-алгебраїчної системи

За умови [3]

$$P_{A^*(t)} \neq 0 \quad (4)$$

система (3) не розв'язна відносно похідної; тут $P_{A^*(t)}$ — матриця-ортопроектор [1]:

$$P_{A^*(t)} : \mathbb{R}^m \rightarrow \mathbb{N}(A^*(t)).$$

Припустимо, що матриця $A(t)$ має сталий ранг, а саме:

$$1 \leq \text{rank } A(t) = \sigma_0.$$

Як відомо [3], довільна $(m \times n)$ — матриця $A(t)$ у певному базисі може бути представлена у вигляді

$$A(t) = R_0(t) \cdot J_{\sigma_0} \cdot S_0(t), \quad J_{\sigma_0} := \begin{pmatrix} I_{\sigma_0} & O \\ O & O \end{pmatrix}, \quad R_0(t) \in \mathbb{C}_{m \times m}[a, b];$$

тут $R_0(t)$ і $S_0(t)$ — невироджені матриці:

$$S_0(t) \in \mathbb{C}_{n \times n}[a, b].$$

Невироджена заміна змінної $y(t) = S_0(t)z(t)$ приводить систему (3) до вигляду

$$J_{\sigma_0} y'(t) = C_0(t)y(t) + R_0^{-1}(t)f(t); \quad (5)$$

тут

$$C_0(t) := (J_{\sigma_0} S_0'(t) + R_0^{-1}(t)B(t)) S_0^{-1}(t) := \begin{pmatrix} C_{11}^{(0)}(t) & C_{12}^{(0)}(t) \\ C_{21}^{(0)}(t) & C_{22}^{(0)}(t) \end{pmatrix}.$$

Заміна змінної

$$y(t) = \text{col } (u(t), v(t)) \in \mathbb{C}_n^1[a, b], \quad u(t) \in \mathbb{C}_{\sigma_0}^1[a, b], \quad v(t) \in \mathbb{C}_{n-\sigma_0}^1[a, b]$$

приводить систему (5) до вигляду

$$u'(t) = C_{11}^{(0)}(t)u(t) + C_{12}^{(0)}(t)v(t) + g_1^{(0)}(t), \quad (6)$$

$$C_{21}^{(0)}(t)u(t) + C_{22}^{(0)}(t)v(t) + g_2^{(0)}(t) = 0, \quad (7)$$

Тут $P_{D_0^*}(t)$ — матриця-ортопроектор:

$$P_{D_0^*}(t) : \mathbb{R}^{m-\sigma_0} \rightarrow \mathbb{N}(D_0^*(t)),$$

крім того

$$R_0^{-1}(t)f(t) := \text{col} \left(g_1^{(0)}(t), g_2^{(0)}(t) \right).$$

Рівняння (7) розв'язне тоді і тільки тоді, коли [1, 3]

$$P_{D_0^*}(t)g_2^{(0)}(t) \equiv 0;$$

в цьому випадку загальний розв'язок рівняння (7)

$$y(t) = P_{D_{\rho_0}} \varphi(t) - D_0^+(t)g_2^{(0)}(t),$$

$$D_0(t) := \begin{bmatrix} C_{21}^{(0)}(t); C_{21}^{(0)}(t) \end{bmatrix} \in \mathbb{R}^{(m-\sigma_0) \times n}, \quad \varphi(t) \in \mathbb{C}_{\rho_0}[a, b]$$

визначає $P_{D_{\rho_0}}(t) - (n \times \rho_0)$ - матриця, утворена із ρ_0 лінійно-незалежних стовпців $P_{D_0}(t)$ - матриці-ортопроектора:

$$P_{D_0}(t) : \mathbb{R}^n \rightarrow \mathbb{N}(D_0(t)).$$

Позначивши блоки матриці $P_{D_{\rho_0}}(t)$ і добутку $D_0^+(t)g_2^{(0)}(t)$:

$$P_{D_{\rho_0}}(t) := \text{col} (P_1^{(0)}(t), P_2^{(0)}(t)), \quad D_0^+(t)g_2^{(0)}(t) = - \text{col} \left(f_1^{(1)}(t), f_2^{(1)}(t) \right),$$

приходимо до задачі про побудову розв'язків

$$\varphi(t) \in \mathbb{C}_{\rho_0}^1[a, b]$$

лінійної диференціально-алгебраїчної системи

$$A_1(t)\varphi'(t) = B_1(t)\varphi(t) + f_1(t), \quad A_1(t) := P_1^{(0)}(t) \in \mathbb{R}^{\sigma_0 \times \rho_0}; \quad (8)$$

тут

$$B_1(t) := C_{11}^{(0)}(t)P_1^{(0)}(t) + C_{12}^{(0)}(t)P_2^{(0)}(t) - A_1'(t),$$

крім того

$$\text{rank } A_1(t) := \sigma_1 = \sigma_0 \leq \rho_0,$$

$$f_1(t) := C_{11}^{(0)}(t)f_1^{(1)}(t) + C_{12}^{(0)}(t)f_2^{(1)}(t) + g_1^{(0)}(t) - \left(f_1^{(1)}(t) \right)'. \quad (9)$$

За умови [3]

$$P_{A^*} \neq 0, \quad P_{A_1^*} \equiv 0, \quad P_{D_0^*}f_1(t) \equiv 0$$

система (8) розв'язна відносно похідної

$$\frac{d\varphi}{dt} = A_1^+(t)B_1(t)\varphi + \mathfrak{F}_1(t, \nu_1(t)), \quad \nu_1(t) \in \mathbb{C}_{\rho_1}[a; b]; \quad (10)$$

тут

$$\mathfrak{F}_1(t, \nu_1(t)) := A_1^+(t)f_1(t) + P_{A_{e_1}}(t)\nu_1(t).$$

Крім того $P_{A_1^*}(t)$ — неперервна [5] матриця-ортопроектор:

$$P_{A_1^*}(t) : \mathbb{R}^{\sigma_0} \rightarrow \mathbb{N}(A_1^*(t)),$$

$P_{A_{\rho_1}}(t)$ — $(n \times \rho_1)$ — матриця, утворена із ρ_1 лінійно-незалежних стовпців $(\rho_0 \times \rho_0)$ -вимірної неперервної [5] матриці-ортопроектора

$$P_{A_1}(t) : \mathbb{R}^{\rho_0} \rightarrow \mathbb{N}(A_1(t)).$$

Позначимо $U_1(t)$ нормальну фундаментальну матрицю

$$U_1'(t) = A_1^+(t)B_1(t)U_1(t), \quad U_1(a) = I_{\rho_1}$$

отриманої традиційної системи звичайних диференціальних рівнянь (10). За умови (9) система (10), а відповідно і система (3), має розв'язок вигляду [3]

$$z(t, c_{\rho_1}) = X_1(t)c_{\rho_1} + P_{D_{\rho_0}}S_0^{-1}(t)K \left[\mathfrak{F}_1(s, \nu_1(s)) \right] (t) - S_0^{-1}(t)D_0^+(t)g_2^{(0)}(t), \quad c_{\rho_1} \in \mathbb{R}^{\rho_1},$$

де

$$X_1(t) := S_0^{-1}(t)P_{D_{\rho_0}}U_1(t), \quad K \left[\mathfrak{F}_1(s, \nu_1(s)) \right] (t) := X_0(t) \int_a^t X_0^{-1}(s) \mathfrak{F}_1(s, \nu_1(s)) ds.$$

Таким чином, за умови (9) лінійна диференціально-алгебраїчна система (3) має розв'язок вигляду

$$z(t, c_{\rho_1}) = X_1(t)c_{\rho_1} + K \left[f(s), \nu_1(s) \right] (t), \quad X_1(t) := P_{D_{\rho_0}}S_0^{-1}(t)U_1(t), \quad c_{\rho_1} \in \mathbb{R}^{\rho_1},$$

де

$$K \left[f(s), \nu_1(s) \right] (t) := P_{D_{\rho_0}}S_0^{-1}(t)K \left[\mathfrak{F}_1(s, \nu_1(s)) \right] (t) - S_0^{-1}(t)D_0^+(t)g_2^{(0)}(t)$$

— узагальнений оператор Гріна задачі Коші $z(a) = 0$ для диференціально-алгебраїчної системи (3). У випадку (9) будемо казати, що для лінійної диференціально-алгебраїчної системи (3) має місце виродження першого порядку [3].

Зафіксуємо довільну неперервну вектор функцію

$$\nu_1(t) \in \mathbb{C}_{\rho_1}[a, b].$$

Підставляючи загальний розв'язок

$$z(t, c_{\rho_1}) = X_1(t)c_{\rho_1} + K \left[f(s), \nu_1(s) \right] (t), \quad c_{\rho_1} \in \mathbb{R}^{\rho_1},$$

задачі Коші $z(a) = c_{\rho_1}$ для диференціально-алгебраїчного рівняння (3) у крайову умову (3), приходимо до лінійного алгебраїчного рівняння

$$Q c_{\rho_1} = \alpha - \ell K \left[f(s), \nu_1(s) \right] (\cdot). \quad (11)$$

Рівняння (11) розв'язне тоді і тільки тоді, коли

$$P_{Q_d^*} \left\{ \alpha - \ell K \left[f(s), \nu_1(s) \right] (\cdot) \right\} = 0. \quad (12)$$

Тут P_{Q^*} — ортопроектор: $\mathbb{R}^q \rightarrow \mathbb{N}(Q^*)$; матриця $P_{Q_d^*}$ утворена з d лінійно-незалежних рядків ортопроектора P_{Q^*} , крім того

$$Q := \ell X_1(\cdot) \in \mathbb{R}^{q \times \rho_1}.$$

За умови (12) і тільки за неї, загальний розв'язок рівняння (11)

$$c = Q^+ \left\{ \alpha - \ell K \left[f(s), \nu_1(s) \right] (\cdot) \right\} + P_{Q_r} c_r, \quad c_r \in \mathbb{R}^r$$

визначає загальний розв'язок диференціально-алгебраїчної крайової задачі (3)

$$z(t, c_r) = X_r(t) c_r + X_1(t) Q^+ \left\{ \alpha - \ell K \left[f(s), \nu_1(s) \right] (\cdot) \right\} + K \left[f(s), \nu_1(s) \right] (t).$$

Тут P_Q — матриця-ортопроектор:

$$\mathbb{R}^{\rho_1} \rightarrow \mathbb{N}(Q);$$

матриця $P_{Q_{r_1}} \in \mathbb{R}^{\rho_1 \times r}$ утворена з r лінійно-незалежних стовпців ортопроектора P_Q . Таким чином, доведена наступна лема [3].

Лема. За умови (9) лінійна диференціально-алгебраїчна система (3) має розв'язок вигляду

$$z(t, c_{\rho_1}) = X_1(t) c_{\rho_1} + K \left[f(s), \nu_1(s) \right] (t), \quad X_1(t) := P_{D_{\rho_0}} S_0^{-1}(t) U_1(t), \quad c_{\rho_1} \in \mathbb{R}^{\rho_1},$$

де

$$K \left[f(s), \nu_1(s) \right] (t) := P_{D_{\rho_0}} S_0^{-1}(t) K \left[\mathfrak{F}_1(s, \nu_1(s)) \right] (t) - S_0^{-1}(t) D_0^+(t) g_2^{(0)}(t)$$

— узагальнений оператор Гріна задачі Коші $z(a) = 0$ для диференціально-алгебраїчної системи (3). За умови (12) і тільки за неї для фіксованої неперервної вектор-функції $\nu_1(t) \in \mathbb{C}_{\rho_1}[a, b]$ загальний розв'язок диференціально-алгебраїчної крайової задачі (3)

$$z(t, c_r) = X_r(t) c_r + G \left[f(s); \nu_1(s); \alpha \right] (t), \quad c_r \in \mathbb{R}^r$$

визначає узагальнений оператор Гріна диференціально-алгебраїчної крайової задачі (3)

$$G \left[f(s); \nu_1(s); \alpha \right] (t) := X_1(t) Q^+ \left\{ \alpha - \ell K \left[f(s), \nu_1(s) \right] (\cdot) \right\} + K \left[f(s), \nu_1(s) \right] (t).$$

3. Умови розв'язності нелінійної крайової задачі для виродженої диференціально-алгебраїчної системи

Припустимо, що породжуюча крайова задача (3) вироджена і некритична ($P_{Q^*} = 0$), при цьому породжуюча задача (3) розв'язна для довільних неоднорідностей $f(t)$ і α . Загальний розв'язок породжуючої диференціально-алгебраїчної крайової задачі (3) для фіксованої неперервної вектор-функції $\nu_1(t) \in \mathbb{C}[a, b]$ має вигляд

$$z(t, c_{\rho_1}) = X_1(t)c_{\rho_1} + K \left[f(s), \nu_1(s) \right] (t).$$

Розв'язки крайової задачі (1), (2) шукаємо в малому околі розв'язку породжуючої задачі:

$$z(t, \varepsilon) = z_0(t, c_r) + x(t, \varepsilon).$$

Для знаходження вектора

$$x(t, \varepsilon) : x(\cdot, \varepsilon) \in \mathbb{C}^1[a, b], \quad x(t, \cdot) \in \mathbb{C}^1[0, \varepsilon_0], \quad x(t, 0) \equiv 0$$

приходимо до задачі

$$A(t)x'(t, \varepsilon) = B(t)x(t, \varepsilon) + \varepsilon Z(z_0(t, c_r) + x(t, \varepsilon), t, \varepsilon), \quad (13)$$

$$\ell x(\cdot, \varepsilon) = \varepsilon J(z_0(\cdot, c_r) + x(\cdot, \varepsilon), \varepsilon). \quad (14)$$

Невироджена заміна змінної

$$y(t) = S_0(t)x(t)$$

приводить систему (13) до вигляду

$$J_{\sigma_0} y'(t) = C_0(t)y(t) + \varepsilon R_0^{-1}(t)Z(z_0(t, c_r) + x(t, \varepsilon), t, \varepsilon). \quad (15)$$

Заміна змінної

$$y(t) = \text{col } (u(t), v(t)) \in \mathbb{C}_n^1[a, b],$$

$$u(t) \in \mathbb{C}_{\sigma_0}^1[a, b], \quad v(t) \in \mathbb{C}_{n-\sigma_0}^1[a, b]$$

приводить систему (15) до вигляду

$$u'(t) = C_{11}^{(0)}(t)u(t) + C_{12}^{(0)}(t)v(t) + \varepsilon Z_1(z(t, \varepsilon), t, \varepsilon), \quad (16)$$

$$C_{21}^{(0)}(t)u(t) + C_{22}^{(0)}(t)v(t) + \varepsilon Z_2(z_0(t, c_r) + x(t, \varepsilon), t, \varepsilon) = 0; \quad (17)$$

тут

$$\begin{aligned} & R_0^{-1}(t)Z(z_0(t, c_r) + x(t, \varepsilon), t, \varepsilon) := \\ & = \text{col } (Z_1(z_0(t, c_r) + x(t, \varepsilon), t, \varepsilon), Z_2(z_0(t, c_r) + x(t, \varepsilon), t, \varepsilon)). \end{aligned}$$

Рівняння (17) розв'язне тоді і тільки тоді, коли

$$P_{D_0^*}(t)Z_2(z_0(t, c_r) + x(t, \varepsilon), t, \varepsilon) \equiv 0; \quad (18)$$

при цьому загальний розв'язок рівняння (17) має вигляд

$$y(t) = P_{D_{\rho_0}}\mu(t) - D_0^+(t)Z_2(z_0(t, c_r) + x(t, \varepsilon), t, \varepsilon).$$

Позначивши блоки матриці

$$P_{D_{\rho_0}}(t) := \text{col} (P_1^{(0)}(t), P_2^{(0)}(t))$$

і добутку

$$D_0^+(t)Z_2(z_0(t, c_r) + x(t, \varepsilon), t, \varepsilon) = - \text{col} (M(y(t, \varepsilon), t, \varepsilon), N(y(t, \varepsilon), t, \varepsilon)),$$

приходимо до задачі про побудову розв'язків

$$\mu(t) \in \mathbb{C}_{\rho_0}^1[a, b]$$

нелінійної диференціально-алгебраїчної системи

$$A_1(t)\mu'(t) = B_1(t)\mu(t) + \varepsilon Y(y(t, \varepsilon), y'(t, \varepsilon), t, \varepsilon); \quad (19)$$

тут

$$A_1(t) := P_1^{(0)}(t), \quad B_1(t) := C_{11}^{(0)}(t)P_1^{(0)}(t) + C_{12}^{(0)}(t)P_2^{(0)}(t) - \left(P_1^{(0)}(t)\right)';$$

крім того

$$Y(y(t, \varepsilon), y'(t, \varepsilon), t, \varepsilon) := C_{11}^{(0)}(t)M(y(t, \varepsilon), t, \varepsilon) + \\ + C_{12}^{(0)}(t)N(y(t, \varepsilon), t, \varepsilon) + Z_1(z_0(t, c_r) + x(t, \varepsilon), t, \varepsilon) - M_y'(y(t, \varepsilon), t, \varepsilon)\mu'(t).$$

За умови $P_{A_1^*}(t) \equiv 0$ система (19), принаймні однозначно, розв'язна відносно похідної:

$$\frac{d\mu}{dt} = A_1^+(t)B_1(t)\mu + \varepsilon A_1^+(t)Y(y(t, \varepsilon), y'(t, \varepsilon), t, \varepsilon). \quad (20)$$

За умови (9) і (18) система (13) має розв'язок вигляду

$$x(t, c_{\rho_1}(\varepsilon)) = X_1(t)c_{\rho_1}(\varepsilon) + \varepsilon K \left[Z(z(s, \varepsilon), s, \varepsilon), \nu_1(s) \right] (t),$$

де

$$X_1(t) := S_0^{-1}(t)P_{D_{\rho_0}}U_1(t), \quad K \left[Z(z(s, \varepsilon), s, \varepsilon), \nu_1(s) \right] (t) := \\ = S_0^{-1}(t)P_{D_{\rho_0}}U_1(t) \int_a^t U_1^{-1}(s)A_1^+(s)Y(y(s, \varepsilon), y'(s, \varepsilon), s, \varepsilon) ds - \\ - S_0^{-1}(t)D_0^+(t)Z_2(z_0(t, c_r) + x(t, \varepsilon), t, \varepsilon), \quad c_{\rho_1}(\varepsilon) \in \mathbb{R}^{\rho_1}.$$

Таким чином, за умови (9) і (18) розв'язок нелінійної диференціально-алгебраїчної системи (1) має вигляд

$$z(t, c_{\rho_1}) = z_0(t, c_{\rho_1}) + x(t, c_{\rho_1}(\varepsilon)),$$

де

$$z_0(t, c_{\rho_1}) = X_1(t)c_{\rho_1} + K \left[f(s), \nu_1(s) \right] (t).$$

У некритичному випадку задача (1), (2) розв'язна для довільних нелінійностей. Загальний розв'язок диференціально-алгебраїчної крайової задачі (13), (14) для фіксованої неперервної вектор-функції

$$\nu_1(t) \in \mathbb{C}[a, b]$$

має вигляд

$$x(t, \varepsilon) = X_r(t)c_r(\varepsilon) + x^{(1)}(t, \varepsilon),$$

де

$$x^{(1)}(t, \varepsilon) := \varepsilon G \left[Z(z_0(s, c_r) + x(s, \varepsilon), s, \varepsilon); \nu_1(s); J(z_0(\cdot, c_r) + x(\cdot, \varepsilon), \varepsilon) \right] (t).$$

Розв'язки крайової задачі (1), (2) при цьому визначає операторна система

$$z(t, \varepsilon) = z_0(t, c_r) + x(t, \varepsilon), \quad x(t, \varepsilon) = X_r(t)c_r(\varepsilon) + x^{(1)}(t, \varepsilon),$$

$$x^{(1)}(t, \varepsilon) = \varepsilon G \left[Z(z_0(s, c_r) + x(s, \varepsilon), s, \varepsilon); \nu_1(s); J(z_0(\cdot, c_r) + x(\cdot, \varepsilon), \varepsilon) \right] (t).$$

Для побудови розв'язків цієї операторної системи може бути використаний [1] метод простих ітерацій:

$$z_{k+1}(t, \varepsilon) = z_0(t, c_r) + x_{k+1}(t, \varepsilon), \quad k = 0, 1, 2, \dots,$$

$$x_{k+1}(t, \varepsilon) = X_r(t)c_r(\varepsilon) + x_{k+1}^{(1)}(t, \varepsilon), \quad (21)$$

$$x_{k+1}^{(1)}(t, \varepsilon) = \varepsilon G \left[Z(z_0(s, c_r) + x_k(s, \varepsilon), s, \varepsilon); \nu_1(s); J(z_0(\cdot, c_r) + x_k(\cdot, \varepsilon), \varepsilon) \right] (t).$$

Таким чином, доведена наступна теорема.

Теорема. *Припустимо, що диференціально-алгебраїчне рівняння (3) задовольняє вимоги лєми. У некритичному випадку ($P_{Q^*} = 0$) породжуюча задача (3) розв'язна для довільних неоднорідностей диференціально-алгебраїчної системи і крайової умови (3) і для фіксованої неперервної вектор-функції $\nu_1(t) \in \mathbb{C}[a, b]$ має r лінійно-незалежних розв'язків*

$$z_0(t, c_r) = X_r(t)c_r + G \left[f(s); \nu_1(s); \alpha \right] (t), \quad c_r \in \mathbb{R}^r.$$

За умов (9) та (18) для побудови розв'язків нелінійної диференціально-алгебраїчної крайової задачі (1), (2) може бути використана збіжна при $\varepsilon \in [0, \varepsilon_*]$ ітераційна схема (21).

Для визначення величини ε_* може бути використаний метод мажорируючих рівнянь Ляпунова [1, 4]; крім того, конструктивна оцінка величини ε_* може бути знайдена аналогічно [6]. На відміну від статей [7, 8] результат теореми отриманий без використання означення центральної канонічної форми лінійної диференціально-алгебраїчної системи [9].

Приклад. Вимоги теореми задовольняє нелінійна диференціально-алгебраїчна антиперіодична задача для рівняння типу Ріккати

$$A(t) z'(t) = B(t)z(t) + f(t) + \varepsilon Z(z, t, \varepsilon), \quad \ell z(\cdot, \varepsilon) := z(0, \varepsilon) + z(\pi, \varepsilon) = 0, \quad (22)$$

де

$$A(t) := \begin{pmatrix} \cos t & 0 & \sin t \\ -\sin t & 0 & \cos t \\ \cos t & \cos t & \sin t \\ -\sin t & -\sin t & \cos t \end{pmatrix}, \quad B(t) := \begin{pmatrix} -\sin t & \cos t & -\sin t \\ -\cos t & -\sin t & -\cos t \\ -\sin t & \cos t & -\sin t \\ -\cos t & -\sin t & -\cos t \end{pmatrix}.$$

крім того

$$z(t, \varepsilon) := \begin{pmatrix} z_a(t, \varepsilon) \\ z_b(t, \varepsilon) \\ z_c(t, \varepsilon) \end{pmatrix}, \quad Z(z, t, \varepsilon) := \begin{pmatrix} z_a^2(t, \varepsilon) \\ 0 \\ z_a^2(t, \varepsilon) \\ 0 \end{pmatrix}, \quad f(t) := \begin{pmatrix} 0 \\ 1 \\ 0 \\ 1 \end{pmatrix}.$$

Оскільки $P_{A^*(t)} \neq 0$, умова (4) не виконана, при цьому матриця $A(t)$ може бути представлена у вигляді

$$A(t) = R_0(t) \cdot J_{\sigma_0} \cdot S_0(t), \quad J_{\sigma_0} := \begin{pmatrix} I_3 & O \\ O & O \end{pmatrix}, \quad \sigma_0 = 3;$$

тут

$$P_{A^*(t)} = \frac{1}{4} \begin{pmatrix} 1 - \cos 2t & \sin 2t & \cos 2t - 1 & -\sin 2t \\ \sin 2t & 1 + \cos 2t & -\sin 2t & -1 - \cos 2t \\ \cos 2t - 1 & -\sin 2t & 1 - \cos 2t & \sin 2t \\ -\sin 2t & -1 - \cos 2t & \sin 2t & 1 + \cos 2t \end{pmatrix},$$

$$R_0(t) = \begin{pmatrix} \cos t & \sin t & 0 & 0 \\ -\sin t & \cos t & 0 & 0 \\ \cos t & \sin t & \cos t & \sin t \\ -\sin t & \cos t & -\sin t & \cos t \end{pmatrix}, \quad S_0(t) = \begin{pmatrix} 1 & 0 & 0 \\ 0 & 0 & 1 \\ 0 & 1 & 0 \end{pmatrix}$$

— невироджені матриці. У даному випадку матриця

$$A_1(t) = I_3$$

невироджена, тому має місце виродження першого порядку, при цьому

$$P_{A_1}(t) = 0, \quad P_{A_{\rho_1}}(t) = 0,$$

тому шуканий розв'язок

$$z(t, c_3) = X_1(t)c_3 + K \left[f(s) \right] (t), \quad c_3 \in \mathbb{R}^3$$

не залежить від довільної неперервної функції $\nu_1(t)$; тут

$$X_1(t) = \begin{pmatrix} 1 & 0 & t \\ 0 & 0 & 1 \\ e^{-t} - 1 & e^{-t} & 1 - e^{-t} - t \end{pmatrix},$$

а також

$$K \left[f(s) \right] (t) = \begin{pmatrix} \cos t - 1 \\ 0 \\ 1 - e^{-t} \end{pmatrix}$$

— узагальнений оператор Гріна задачі Коші $z(0) = 0$ для лінійної частини диференціально-алгебраїчної системи (22). Загальний розв'язок породжуючої задачі визначає невироджена матриця

$$Q = \begin{pmatrix} 2 & 0 & \pi \\ 0 & 0 & 2 \\ -1 + e^{-\pi} & 1 + e^{-\pi} & 1 - e^{-\pi} - \pi \end{pmatrix},$$

отже, для диференціально-алгебраїчної крайової задачі (22) має місце не критичний випадок. Таким чином, знаходимо єдиний розв'язок породжуючої задачі

$$z_0(t) = G \left[f(s); \alpha \right] (t) = \begin{pmatrix} \cos t \\ 0 \\ 0 \end{pmatrix}$$

— узагальнений оператор Гріна породжуючої задачі для диференціально-алгебраїчної крайової задачі (22). Оскільки $D_0 = 0$, то $D_0^+ = 0$, отже, умова (18) виконана. Умову (9) для диференціально-алгебраїчної системи (22) також виконано. Для побудови розв'язків нелінійної диференціально-алгебраїчної крайової задачі (22) може бути використана ітераційна схема (21), при цьому, поклавши $c_r(\varepsilon) := 0$, отримуємо:

$$x_1(t, \varepsilon) = \begin{pmatrix} x_{1a}(t, \varepsilon) \\ 0 \\ x_{1c}(t, \varepsilon) \end{pmatrix},$$

де

$$x_{1a}(t, \varepsilon) = -\frac{\varepsilon}{12} \left(9 \sin t + \sin 3t \right),$$

$$x_{1c}(t, \varepsilon) = \frac{\varepsilon}{60} \left(15 \cos t - 3 \cos 3t - 15 \sin t + \sin 3t \right).$$

Аналогічно, на другому кроці отримуємо:

$$x_2(t, \varepsilon) = \begin{pmatrix} x_{2a}(t, \varepsilon) \\ 0 \\ x_{2c}(t, \varepsilon) \end{pmatrix},$$

де

$$x_{2a}(t, \varepsilon) = \frac{\varepsilon}{1\ 310\ 400} \left(8400 \varepsilon \cos t + 3080 \varepsilon \cos 3t + 168 \varepsilon \cos 5t - 15\ 120 \sin t - \right.$$

$$\left. -3535 \varepsilon^2 \sin t - 1680 \sin 3t + 945 \varepsilon^2 \sin 3t + 133 \varepsilon^2 \sin 5t + 5 \varepsilon^2 \sin 7t \right),$$

$$x_{2c}(t, \varepsilon) = -\frac{\varepsilon}{1\ 310\ 400} \left(327\ 600 \cos t + 546\ 000 \varepsilon \cos t - 143\ 325 \varepsilon^2 \cos t - \right.$$

$$\left. -65\ 520 \cos t - 29\ 120 \varepsilon \cos t + 12285 \varepsilon^2 \cos 3t - 1680 \varepsilon \cos 5t + 5775 \varepsilon^2 \cos 5t + \right.$$

$$\left. +273 \varepsilon \cos 7t - 327\ 600 \sin t + 546\ 000 \varepsilon \sin t + 143\ 325 \varepsilon \sin t + 21840 \sin 3t - \right.$$

$$\left. -87\ 360 \varepsilon \sin 3t - 4095 \varepsilon^2 \sin 3t - 8400 \varepsilon \sin 5t - 1155 \varepsilon^2 \sin 5t - 39 \varepsilon^2 \sin 7t \right).$$

Таким чином, на другому кроці нами отримано друге наближення до розв'язку крайової задачі (22):

$$z_2(t, \varepsilon) = z_0(t) + (z_1(t, \varepsilon) - z_0(t)) + (z_2(t, \varepsilon) - z_1(t, \varepsilon)).$$

У даному випадку перша скобка першого порядку по ε , а друга — другого, тому існують константи q_1, q_2 , для яких

$$\|z_1(t, \varepsilon) - z_0(t)\| = \varepsilon q_1, \quad \|z_2(t, \varepsilon) - z_1(t, \varepsilon)\| = \varepsilon^2 q_2.$$

Використовуючи мажорантну ознаку, отримуємо умову практичної збіжності отриманих наближень до розв'язку крайової задачі (22):

$$0 < \varepsilon < \varepsilon_0 < \min \left(\frac{q_0}{q_1}, \frac{q_1}{q_2} \right) \approx 1,08\ 603.$$

Для оцінки точності знайдених наближень до розв'язку нелінійної диференціально-алгебраїчної крайової задачі (22) визначимо нев'язки

$$\Delta_k(\varepsilon) := \left\| \left\| A(t) z'_k(t, \varepsilon) - B(t) z_k(t, \varepsilon) - f(t) - \varepsilon Z(z_k(t, \varepsilon), t, \varepsilon) \right\|_{\mathbb{R}^4} \right\|_{\mathbb{C}[0, 2\pi]}$$

нульового, першого і другого наближення до розв'язку крайової задачі (22), зокрема, отримуємо

$$\Delta_0(0, 1) \approx 0,141\,421, \quad \Delta_0(0, 01) \approx 0,0141\,421, \quad \Delta_0(0, 001) \approx 0,00141\,421.$$

Аналогічно:

$$\Delta_1(0, 1) \approx 0,0122\,244, \quad \Delta_1(0, 01) \approx 0,000\,120\,317, \quad \Delta_1(0, 001) \approx 1,20\,124 \times 10^{-6};$$

$$\Delta_2(0, 1) \approx 0,0016\,323, \quad \Delta_2(0, 01) \approx 1,63\,418 \times 10^{-6}, \quad \Delta_2(0, 001) \approx 1,6342 \times 10^{-9}.$$

Відзначимо також, що нульове і перші два наближення до розв'язку крайової задачі (22) в точності задовольняють крайову умову.

Отримані результати можна перенести на задачі про знаходження умов існування та схеми побудови розв'язків нелінійної виродженої диференціально-алгебраїчної крайової задачі [9, 10, 11] у критичних випадках [1, 12, 13, 14], а також на задачі про знаходження умов стійкості таких розв'язків [15].

Історія статті: отримана: 17 серпня 2024; останній варіант: 5 вересня 2024
прийнята: 18 жовтня 2024.

REFERENCES

1. A. A. Boichuk, A. M. Samoilenko. Generalized inverse operators and Fredholm boundary-value problems; 2-th edition. Berlin; Boston: De Gruyter. – 2016. – 298 p. 10.1515/9783110378443
2. S. L. Campbell. Singular Systems of differential equations. San Francisco–London–Melbourne. Pitman Advanced Publishing Program. – 1980. – 178 p.
3. S. M. Chuiko. On a reduction of the order in a differential-algebraic system, Journal of Mathematical Sciences. – 2018. – Vol. **235**, No. **1**. – P. 2-18. 10.1007/s10958-018-4054-z
4. E. Grebenikov, Yu. Ryabov. Constructive methods in the analysis of nonlinear systems. Mir Publishers. – 1983. – 442 p.
5. S. M. Chuiko. Differential-algebraic boundary-value problems with the variable rank of leading-coefficient matrix, Journal of Mathematical Sciences (United States). – 2021. – Vol. **259**, No. **1**. – P. 10–22. 10.1007/s10958-021-05597-8
6. A. S. Chuiko. Domain of convergence of an iterative procedure for a weakly nonlinear boundary value problem, Nonlinear Oscillations (N.Y.). – 2005. – Vol. **8**, No. **2**. – P. 277-287. 10.1007/s11072-005-0056-0

7. M. A. Perepelitsa, A. A. Pokutniy. Study of solvability of weakly nonlinear differential-algebraic systems, Bulletin of YuSU. Series "Mathematical Modelling and Programming". – 2013. – Vol. 6, No. 4. – P. 55-62.
8. A. A. Boichuk, L. M. Shehda. Degenerate nonlinear boundary-value problems, Ukrainian Mathematical Journal. – 2009. – Vol. 61, No. 9. – P. 1387-1403. 10.1007/s11253-010-0284-z
9. S. L. Campbell. Singular Systems of differential equations. San Francisco–London–Melbourne. Pitman Advanced Publishing Program. – 1980. – 178 p.
10. S. L. Campbell, C. D. Meyer. Generalized Inverses of Linear Transformations. London. Pitman Publishing Limited. – 1979. – 272 p.
11. P. Benner, M. Bollhofer, D. Kressner, C. Mehl, T. Stykel. Numerical Algebra, Matrix Theory, Differential-Algebraic Equations and Control Theory. Springer International Publishing. – 2015. – 608 p. 10.1007/978-3-319-15260-8
12. S. M. Chuiko. A weakly nonlinear boundary value problem in a special critical case, Ukrainian Mathematical Journal. – 2009. – Vol. 61, No. 4. – P. 657–673. 10.1007/s11253-009-0227-8
13. A. A. Boichuk, V. F. Zhuravlev, A. M. Samoilenko. Normal-solvable boundary value problems. Kyiv. Naukova Dumka. – 2019. – 628 c. (in Russian).
14. O. A. Boichuk, S. M. Chuiko. Constructive methods of analysis of boundary value problems of the theory of nonlinear oscillations. Kyiv. Naukova Dumka. – 2023. – 232 p. (in Ukrainian). 10.37863/6581477912-64
15. V. I. Korobov, M. O. Bebiya. Stabilization of some class of nonlinear systems that are uncontrollable the first approximation. Dopov. Nats. Akad. Nauk Ukraine. – 2014. – No. 2. – P. 20–25 (in Russian). 10.15407/dopovidi2014.02.020

Article history: Received: 17 August 2024; Final form: 5 September 2024

Accepted: 18 October 2024.

Nonlinear boundary value problems for degenerate differential-algebraic systems in the noncritical case

S. M. Chuiko¹, O. V. Nesmelova², O. V. Chuiko¹

¹*Donbas State Pedagogical University*

19, Batiuka, Sloviansk, Ukraine, 84116

²*Institute of Applied Mathematics and Mechanics of the NAS of Ukraine*

19, Batiuka, Sloviansk, Ukraine, 84116

We have obtained the conditions of existence and a scheme for constructing solutions of a weakly nonlinear boundary value problem for a degenerate differential-algebraic system in the noncritical case. The boundary condition is determined by a weakly nonlinear vector functional. The linear part of the problem is a linear boundary value problem for a degenerate differential-algebraic system. Linear differential-algebraic boundary value problems have been studied in monographs by S. Campbell, J.R. Magnus, A.M. Samoilenko and V.P. Yakovets. In the works of A.M. Samoilenko and O.A. Boichuk, using the central canonical form, the necessary and sufficient conditions for the existence of solutions of nonlinear differential-algebraic boundary value problems were obtained. We have obtained necessary and sufficient conditions for the existence of solutions of nonlinear differential-algebraic systems without using the central canonical form, which allows us to study the solvability of differential-algebraic boundary value problems that depend on arbitrary continuous functions. This approach significantly varies the classification of nonlinear differential-algebraic boundary value problems in critical and noncritical cases.

Our formulation of the weakly nonlinear differential-algebraic boundary value problem generalises the boundary value problems studied in the works of Yu.O. Mitropolsky, A.M. Samoilenko, and O.A. Boichuk. The case when a differential-algebraic system is not solvable with respect to the derivative is considered, and substitutions of the unknown are proposed. It leads the original system to a nonlinear differential-algebraic system solvable with respect to the derivative. Finally, we present an example of a nonlinear differential-algebraic antiperiodic boundary value problem for a Riccati-type equation, which demonstrates the constructiveness of the obtained necessary and sufficient conditions for the existence of solutions of nonlinear differential-algebraic systems. The obtained results can be transferred to the problems of finding conditions for the existence and schemes for constructing solutions of nonlinear degenerate differential-algebraic boundary value problems in critical cases, as well as to the problems of finding conditions for the stability of such solutions.

Keywords: nonlinear boundary value problem; degenerate differential-algebraic system; noncritical case; Riccati-type equation.

How to cite this article:

S. M. Chuiko, O. V. Nesmelova, O. V. Chuiko. Nonlinear boundary value problems for degenerate differential-algebraic systems in the noncritical case. *Visnyk of V. N. Karazin Kharkiv National University. Ser. Mathematics, Applied Mathematics and Mechanics*, Vol. 100, 2024, p. 4–18, (in Ukrainian). DOI: 10.26565/2221-5646-2024-100-01

Emmanuel Akaligwo

Department of Mathematics
Federal University Lokoja
P.M.B 1154 Lokoja
260101, Kogi State, Nigeria

emmanuel.akaligwo@fulokoja.edu.ng  <http://orcid.org/0009-0002-3837-8079>

Anselm Oyem

Department of Mathematics
Federal University Lokoja
P.M.B 1154 Lokoja
260101, Kogi State, Nigeria

onyekachukwu.oyem@fulokoja.edu.ng  <http://orcid.org/0000-0002-1756-0333>

Olayiwola Babanrinsa

Department of Mathematics
Federal University Lokoja
P.M.B 1154 Lokoja
260101, Kogi State, Nigeria

olayiwola.babanrinsa@fulokoja.edu.ng  <http://orcid.org/0000-0002-3569-0828>

Mathematical modelling and virtual design of metamaterials for reducing noise and vibration in built-up structures

Noise and vibration are pervasive challenges in built-up structures, impacting structural integrity, operational efficiency, and occupant well-being. These issues are particularly pronounced in urban and industrial settings, where traditional materials often struggle to deliver effective mitigation across the broad range of relevant frequencies. This paper introduces an integrated mathematical modeling and virtual design framework for the development of advanced metamaterials aimed at reducing noise and vibration in such complex structures. The approach combines finite element analysis, dynamic energy analysis, and optimization algorithms to design metamaterials with frequency-selective properties that create targeted barriers to acoustic and vibrational disturbances. The study not only develops a systematic methodology for designing these metamaterials but also validates their efficacy through comprehensive simulations and benchmarking against established solutions. The results highlight the advantages of the proposed metamaterials in terms of adaptability, efficiency, and performance robustness across various operating conditions. Sensitivity

analyses and comparative evaluations further underscore the superiority of the framework in addressing frequency-dependent challenges, offering significant improvements over conventional materials. A unique aspect of this research is the inclusion of natural metamaterials (NMs) as a sustainable alternative for mitigating ground vibrations. The study reviews the potential of NMs for diverse functionalities, particularly in attenuating ground vibrations in urban environments. These findings emphasize the versatility and eco-friendliness of natural materials, providing a roadmap for their development and application in achieving clean and quiet environments. The proposed framework, therefore, bridges theoretical advancements with practical applications, paving the way for resilient and sustainable solutions to noise and vibration challenges in built-up structures.

Keywords: Metamaterials; virtual design; noise reduction; built-up structures; genetic algorithm; dynamic behavior; finite element analysis.

2020 Mathematics Subject Classification: 74K25, 74J05, 74S05, 90C39

1. Introduction

Noise and vibration are increasingly problematic in urbanized areas, impacting structural stability and human well-being. Built-up structures, especially those with complex geometries and mixed materials, often experience resonance effects and energy transmission across wide frequency ranges due to external sources like traffic, machinery, and environmental factors. Traditional noise and vibration mitigation methods, such as insulation or damping layers, often exhibit frequency-dependent limitations, making them less effective in low- and mid-frequency ranges. Metamaterials, engineered with periodic structures to exhibit unique wave interactions, provide promising alternatives by creating frequency band gaps—ranges where wave propagation is significantly reduced. This study introduces a mathematical and computational framework for the design of metamaterials tailored to suppress noise and vibration in built-up structures. The work also benchmarks the proposed approach against existing methods and studies, highlighting the advantages of metamaterial configurations for practical noise and vibration control. Recent advancements in metamaterials have opened new avenues for noise and vibration control, leveraging band gap creation to achieve attenuation at specific frequencies. [17] achieved up to $15dB$ reduction in mid-frequency ranges with layered metamaterials, demonstrating the potential for targeted noise reduction but with limited frequency range flexibility. Martin and [2] explored lightweight metamaterials in architectural applications, noting advantages in design adaptability and weight savings over traditional materials but also identifying challenges in achieving broad frequency coverage. Common examples of Mechanical metamaterials are often characterized by the type of basis structure they exhibit, figure 2. As seen in this Figure, structures can be beam-based (also strut-based), plate-based, or minimal surface-based.

Despite these advancements, many existing metamaterial designs remain constrained to narrowband applications. This study addresses these limitations by using a

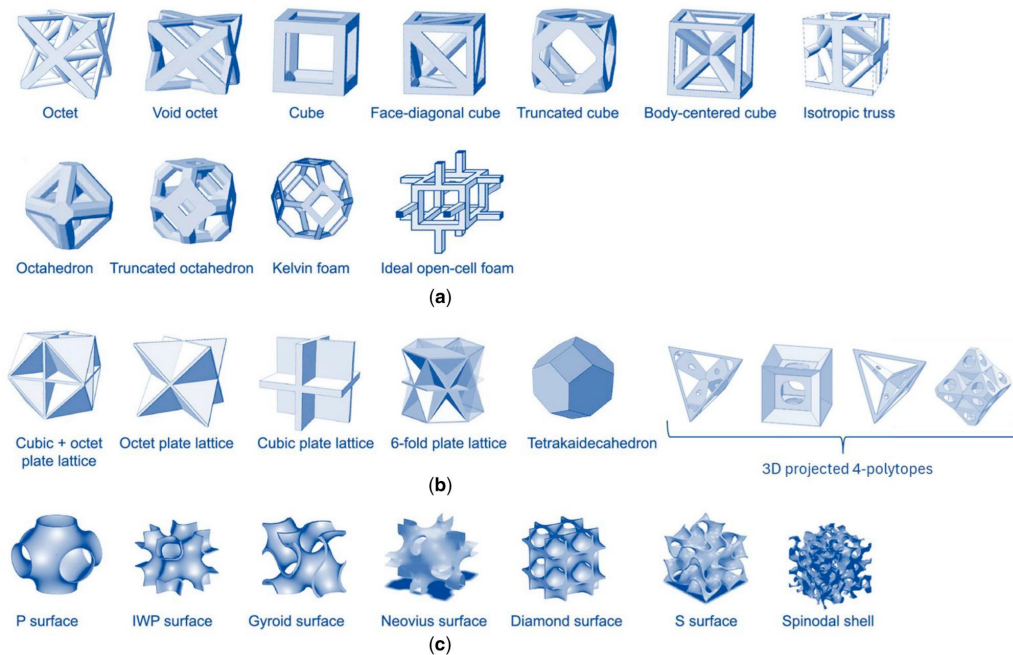


Fig. 1. Examples of mechanical metamaterials based on geometry type. Illustration of 3D (a) beam-based, (b) plate-based, and (c) minimal surface-based topologies. Reprinted with the permission of [7].

Рис. 1. Приклади механічних метаматеріалів на основі типу геометрії. Ілюстрація тривимірної (а) топології на основі променя, (б) на основі пластини та (с) топології на основі мінімальної поверхні. Друкується з дозволу [7]

broader optimization framework to improve performance across a wider frequency range. Our approach integrates finite element modeling, wave propagation theory, and advanced sensitivity analysis to deliver a robust metamaterial design suitable for complex built-up environments. According to the latest statistics, more than 60% of the complaints about environmental pollution are about noise pollution, and more than half of them are about traffic noise [17]. Noise and vibration pollution are a cause of people's physical and psychological discomfort [6]. All kinds of ground vibrations caused by earthquakes, elastic waves, acoustic sources, human activities, and mining and all kind of traffic trains, automobiles, and urban rail transit noise emit vibration frequencies ranging from tens of hertz to thousands of hertz; these are broadband pollution sources [23]. The existing research has shown that low-frequency noise can cause negative effects as close to the start as $40dB$. Some low-frequency vibrations, such as those between 10 and $100Hz$, which are near to the natural frequency, can be annoying. Anger has been linked to subjective perceptions of fatigue, drowsiness, and loss of attention [19]. In addition, some high-frequency noises, such as those at $2.5 \sim 3.5kHz$, cause direct damage to the auditory organs. High-frequency hearing loss cannot be cured but

can be prevented. Therefore, it is everyone's duty to identify preventive measures to protect against and mitigate noise exposure [22]. The main reasons for the increasing traffic noise pollution are the sharp increase in the number of cars, the development of transportation engineering, and the road projects through the city [48]. The second is the congestion caused by the interruption of the transportation path and the congestion of vehicles that may result in vibration and noise [23]. Although the vibrations and noise from road traffic will not cause direct damage to buildings, they may cause local tremors in the internal structure of the buildings and even create secondary structural noise in the buildings [33]. In the pursuit of fulfilling the desires for urban planning, addressing various convenient services in the city, such as transportation, housing, and other services, helping to create a beautiful view of the city and improving it, and contributing to providing a base for human activity through the conservation and exploitation of land and the proper use of land, it is particularly common in practical engineering applications to set up sound barriers, vibration-damping piles, and vibration-damping trenches in the transmission paths of vibration and noise. The vibration and noise reduction measures for the protected object include three aspects. First, in the design, the building can have a wide foundation; vibration isolation pads [11], vibration isolation supports [2], and other passive vibration isolation systems can be added [23]; a spring damping system on the vibration body [3] and the supporting structure to change the vibration characteristics of the entire structure can be installed [30], thereby reducing the impact of vibration on the buildings and precision instruments or cultural relics [42]. Second, for existing buildings, sound insulation or sound-absorbing materials such as lightweight aggregate concrete [14], can be attached to the surface of the building [9], or sound-insulating windows can be added to the interior of the building [48]. Common sound insulation window materials include wood structures [10], steel structures [35], and aluminum alloy structures [43]. The third is to take certain protective measures for the protected object to isolate the noise and vibration [13]. The existing studies have focused on vibration reduction measures, such as sound barriers [28], green belts [40], or sound-absorbing ceilings on both sides of the road [37]. Most of the sound barrier structures are often porous structures [43], such as perforated plates [43], foam glasses [5], etc. These sound-absorbing boards are widely used due to their simple production and low cost. Acoustic materials have a narrow sound absorption frequency band, and it is impossible to reduce noise with a simple sound barrier [7]. In recent years, there has been an in-depth study of periodic structures. Bopp et. al [5] proposed the first idea of using single-row or multi-row, thin-walled circular holes as wave barriers. Subsequently, [7] conducted some domestic in-depth research on discontinuous barriers; their research had three aspects, theoretical research, numerical simulation, and experimental verification, which proved the good vibration isolation performance of the barriers. The application of some artificially designed periodic foundations, underground piles, and wave barriers in civil engineering vibration reduction and earthquake resistance has also been studied in depth [7]. Hedayati et. al [21] established a comparison

link between the velocity of ground vibrations and the noise level on the facade. Even if there are no traffic jams or traffic violations, any passing vehicle would cause a form of ground stress [42]. Zhang et al. [48] established simulations and analyses to form a link between the velocity of ground vibrations and the noise level on the facade in the finite element method in order to induce train vibrations. Since then, research has been conducted to determine the human response to railway-induced vibrations [12], which are generally overlooked in comparison to ground vibrations. Bajars et al. [4] compared the irritation produced by the vibrations of railways and the noise. It is crucial to understand how people who have been exposed to vibration feel about it and how much discomfort it causes in their homes in order to consider the reduction measures for the ground vibrations. In general, these vibration activities can be attenuated by reducing the incoming vibrations. The use of different systems of seismic metamaterials to suppress or redirect waves has been the focus of many researchers and academics recently. Some of these newly developed systems are simple lenses and mirrors, which are used to redirect and focus electromagnetic radiation at optical wavelengths, and they represent continuous attempts to influence wave propagation, while the application of seismic lensing by altering the ground's refractive index has only recently been reviewed [32]. Many investigations have employed and developed waveguides in which the dispersion relation indicates bandgaps, also known as stop bands or filter bands; these are the ranges of frequencies in which waves cannot travel through the material. In the ground vibrations, different models of periodic structures are solved using Green's equation. Low-frequency vibrations are the most difficult to reduce since the earth does not dampen them much; many variables are still being assessed. Qahtan et. al., [32] evaluated sleepers as line barriers when arranged to interact with the ground vibrations from railway sources. Vasut et al., [45] followed up on this research. Bajars et al., [4] proposed that ground vibrations were affected by the geotechnical properties of soil. These models were theoretically investigated based on attributes of ground vibrations as well as ground parameters. Lastly, Zang et al., [48] investigated the proposition that a substantial rise in vibration levels was due to an increase in the vehicles' unsprung mass. The vibrations caused by human activity not only impair sensible structures, they also have a negative impact on individuals. As human activities increase more and more throughout cities, people are more worried about quality and comfort. The increase in complaints about noise and vibrations has led to more interest in developing different systems. Base isolation mitigation systems can be used at the foundations to protect the whole building from the harm of ground vibration. Ichchou et al., [22] investigated the combination of three passive control systems to evaluate the plane wave response of base isolation systems. They found that the mitigation techniques, when used together, are inefficient. Ji et al., [23] investigated train vibration mitigation models and applied them on a broad scale using in-filled or open trenches and using special materials that form a vibration mitigation system when combined with the ground. According to a numerical simulation, the use of wave barriers made of seismic metamaterials

that have a stiffness higher than the soil-medium stiffness can be more effective, especially when the differences in stiffness between them are adequately higher [2]. Cavaliere et al., [6] investigated the high thickness and long distance from one neighboring wall to another neighboring wall; the result was a higher supplement loss, especially when those procedures are close to 25% of the wavelength of the wave. Qin [33] validated this in a laboratory that used gelatin in place of dirt to minimize the wavelengths in the test scale. After full-scale experiments, the subsurface barriers' success in actual vibration was discovered. Gabbert et al., [19] conducted numerical research on pile barrier analysis and design for block vibrations, particularly in the low-frequency range. Richter et al., [35] evaluated the heavy mass efficiency when located above the earth surface in an array continuously around the track. This method of wall barriers is valuable for the reduction in unwanted ground vibration. Subsequently, they looked at how a sheet pile wall was successfully used to mitigate ground vibrations. They came to the conclusion that porous walls can be employed as vibration barriers, with the stiffness of these walls and the depth of the soil determining the efficacy of the reduction mechanism. In other work, they discovered that heavy biomasses/masses, when placed above the earth's surface, reduce incident surface waves at resonance frequencies [36]. Slipantschuk et al., [39] looked at the impacts of water infiltrations on the open trenches and found that when there is a considerable volume of infiltrated water present, the trench's efficacy reduces because the water permits the primary waves to transmit. When the water tables are adequate, the trenches can be adequate; the trench's efficacy is reduced when the depth of the trench is reduced from 16 m deep to 12 m. As a result, the vibration levels will be reduced from 65% to 21%. Saxena et al. [38] investigated the behavior of double and single jet-grouted wave barriers made of the same materials and volumes; they found that the dual-wall baffles behaved better at short spacing along the barriers. Mohammed et al. [29] suggested a wave barrier of multi-layered periodic structures containing two layers of diversely changed components; they found that the attenuation mechanism was greatly influenced by the depth and number of rows of the periodic barriers. Tamber et al., [41] explored the optimization of the forming, inclination, location, thickness, and tilth of single and dual walls; they found that at a wall depth of less than 110% of the wavelength, no significant improvements were observed due to barrier topology. On the other hand, by inclining and relocating a wall, there was more efficiency in comparison to the normal case. Tandon et al. [42] concluded that the mitigation capacities of open trenches are higher than those of in-filled trenches, and in order to obtain more than a 20% increase in the mitigation capacity, the double trench barriers should be used instead of the single ones. However, a three-tiered trench barrier has no significant impact on level mitigation. The ground vibration mitigation through an urban environment has been one of the major study areas in the modern construction revolution throughout the past two decades. In terms of wave propagation modeling, the finite element method and the boundary conditions are the most commonly used techniques, with an emphasis on wave manipulations in

2D and 3D space for the different types of guided waves associated with particular applications. The production of an Bandgap (BG), as well as the control of its breadth and localization within the band structure, has long been of interest to the scientists who study periodic structures and Siesmic metamaterials (SMs). The purpose of this section is to examine the attenuation process underlying their origin, focusing on 2D and 3D designs to mimic the subwavelength bandgap manifestation. Numerical models are preferred because of the complexity of wave propagation, the high cost of field tests or even full-scale experiments, and their superior computational efficiency in forecasting the ground vibrations caused by vibratory sources. FBG production has therefore emerged as a result of its use in applications such as vibration mitigation, seismic shielding, multidirectional wave cancellation, waveguiding, and sound sensors. The understanding of BGs and their application has resulted in a variety of SM designs, particularly for 2D and 3D lattices. Specifically, the management of guided waves, such as Love and Rayleigh waves, has prompted the study of periodic structures. For natural metamaterial, the urban trees can produce bandgaps in several periodic arrangements as shown in the fig. 2.

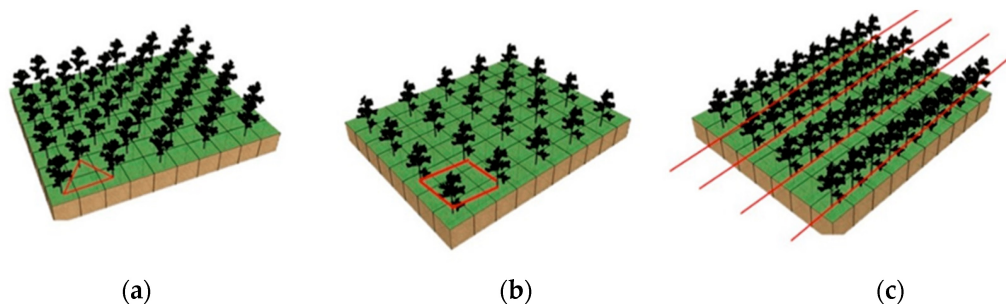


FIG. 2. Several periodic lattices of NMs: (a) triangle lattice; (b) rectangular lattice; (c) square lattice. Reprinted with the permission of [32].

Рис. 2. Кілька періодичних ґраток НМ: а) трикутна ґратка; б) прямокутна ґратка; в) квадратна ґратка. Друкується з дозволу [32].

1.1. Vibration Mitigation in Urban Environment

The vegetation has effects on the propagation of the ground vibrations. The study is of the role of plants in the soil; the stems, trunks, branches, and foliage of herbs, shrubs, and trees make up the complex medium that is the vegetation offered for elastic wave propagation. The influential elements impacting on elastic wave propagation through forests and vegetation have also been investigated and characterized using a variety of numerical and experimental methods [46]. Previous research has suggested that vegetation plays a crucial role in sound propagation via vegetation through scattering, absorption, ground effect, and reflection [31]. The effect of the ground motion is strong at low frequencies. As a result of direct interference between the propagation of the waves and the resonance, the ground vibrations are mitigated [27]. Because of their tiny size in proportion to

the wavelength, the scattering effect of the leaves, branches, and trunks is minimal. Furthermore, at these low frequencies, the absorption from the leaves themselves is insignificant. The massive branches and trunks both scatter sound energy at mid-frequencies. At higher frequencies, often higher than 1 kHz, scattering is still important, and the foliage slows down the waves even more through viscous friction [46]. Keane et al., [24] studied the contribution of individual leaves to the attenuation of sound through generating manageable mechanical vibration at resonance frequencies so that the sound energy was converted to heat. In another research work, a laser vibrometer was used [182], as well as an accelerometer in anechoic chambers to investigate the vibration velocity of leaves. Richter et al. [34] performed similar measurements on different leaves of six different plant species: *Acalyphia*, laser Vibrometer device *Lon*, *Lonicera*, and *Erythrina*, using a lightweight accelerometer. Du et al., [15] employed accelerometers to analyze branch oscillations; the deciduous trees' lower branches oscillated at 300 Hz; the findings of the investigated measurements showed that the smaller branches appearing near the top of the tree have an influence at frequencies of resonance of more than 1100 Hz. The branch length was inversely proportional to the wavelength at high frequencies. Yang et al., [47] discovered that when vibration or noise pushes leaves up to 100 dB, the leaves of the trees behave in the same way as linear systems. For two reasons, left-field sound re-emissions were found to be quite minimal in the experiments. To begin with, the vibration velocity of the leaves is less than that of the particles in the air. This indicates that only a small portion of the sound energy that reaches the leaf causes it to vibrate [46]. The energy of the sound is diffracted and reflected around the leaf in the other direction [48]. Second, a leaf's complex vibration mode leads the leaves of different parts to be out of phase, cancelling the pressure vibration caused by the wind around the leaves [26]. The reduction in the curves of the frequency-absorption to two superimposes the Gaussian curves [1]. Nash et al., [30] demonstrated that the mode of the leaf's vibration can be classified into two mode types; the leaf's length belongs to the first mode type, whereas the leaf's breadth belongs to the second type of modes. This, in turn, causes the leaf's two-dimensional surface to vibrate longitudinally and transversely. The longitudinal mode of vibration causes the lower-frequency Gaussian curve, while the transverse vibration mode causes the higher-frequency curve. Because the transverse mode seems to be more prominent, it results in greater absorption. In reverberant conditions, few studies have assessed the impacts of vibrations and thermo-viscous absorption on leaves, trunks, and branches. Tanner et al., [43] assessed the impact of resonance and thermo-viscous absorption on the branches and needles of the pine tree. The branch velocity was lower than the air particle velocity. At frequencies lower than 4Hz (8 cm needles) to 49 Hz, fundamental needle resonances were detected (2.3 cm needles). In order to evaluate the coefficient of absorption, Martin et al., [27] used four different trees set in a reverberation chamber: two conifers and two with wide leaves. The values of the absorption coefficient of the broadleaf trees were found to be higher than the absorption coefficient of the conifers. According to



(a)



(b)

Fig. 3. Green shrubs covering substrate wall applications. (a) Schematic representation of green buildings, with several services copyrighting the figures (b) Modular of the green forests covering substrate walls. Reprinted with the permission of [32].

Рис. 3. Зелені кущі, що покривають настінні підкладки. (a) Схематичне зображення зелених будівель із кількома службами, які захищають авторські права на фігури (b) Модульні зелені ліси, що покривають стіни субстрату. Друкується з дозволу [32].

the study findings, leaves generate acoustic attenuation; so, it does not depend on the leaf's surface area. The absorption coefficient was also demonstrated to rise proportionally to the frequency squared. At 10 kHz, the trees' highest absorption coefficient was roughly 0.2. The perpendicular vegetation system can be planted in wooden frames that make up the vertical greenery system, as shown in Figure 2. As the elastic wave propagates through the natural metamaterials (NMs), the scatterer's self-resonance characteristics interact with the seismic wave, resulting in the formation of a local resonance bandgap. Experimentally and theoretically, the results all reveal that NMs are accompanying seismic waves when the wavelengths are significantly greater than the lattice size, which fundamentally differs from both types of bandgap. Using a smaller lattice size breaks through the bandgaps, allowing NMs to be used in a wider range of applications in practi-

cal engineering than previously thought possible. Abusag et al., [1] developed a 3D simulation model using forest metamaterials as the basis to investigate the protective effects of the 80Hz low-frequency Rayleigh wave. The city green spaces are considered to be large-scale in terms of natural metamaterials, as shown in Figure 2.

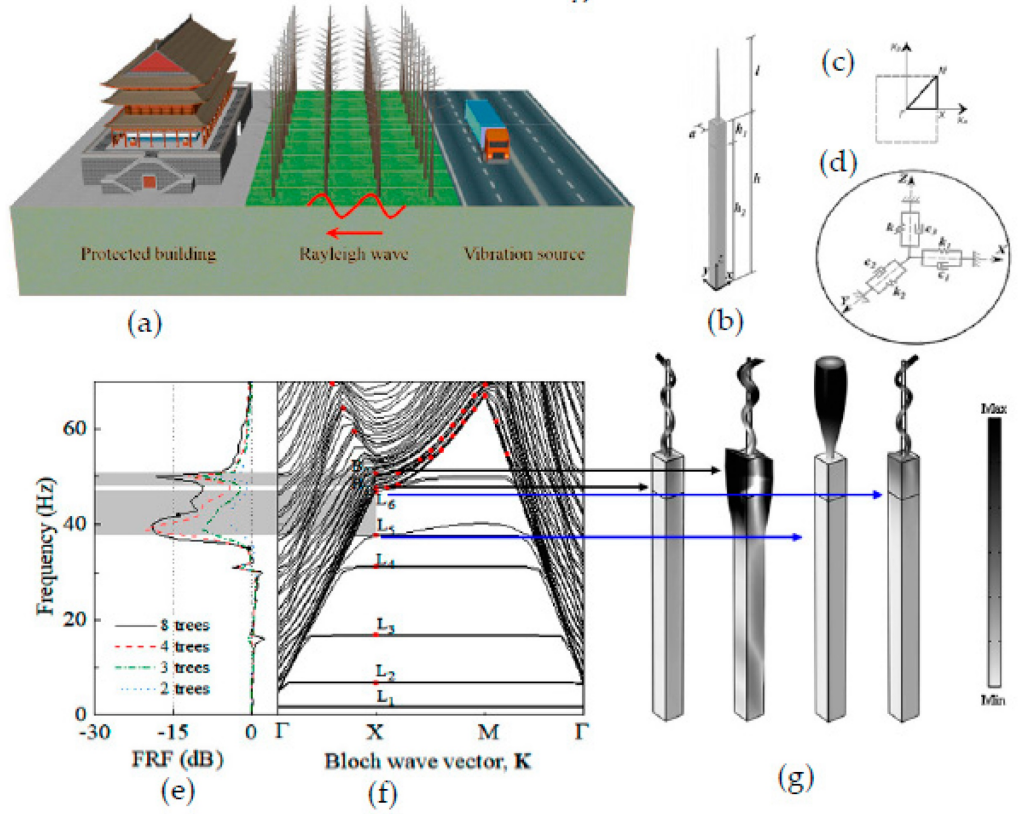


FIG. 4. Urban forest as large-scale NMs: (a) Rayleigh waves and periodic arrangement of forest trees; (b) unit cell; (c) wave vector in first IBZ; (d) viscous spring boundary, (e) FRF plot, (f) dispersion curves with BGs, and (g) vibration modes corresponding with BGs boundaries. Reprinted with the permission of [32].

Рис. 4. Міський ліс як великомасштабні НМ: (а) хвилі Релея та періодичне розташування лісових дерев; (б) елементарна комірка; (с) хвильовий вектор у першому IBZ; (д) межа в'язкої пружини, (е) графік FRF, (ф) дисперсійні криві з BGs, і (г) моди вібрації, що відповідають межах BGs. Друкується з дозволу [32].

2. Mathematical foundations and equation presentation

The mathematical foundation of the research methods stems from wave hybridization between incident waves and the resonator in the soil. The propagation

of elastic waves (EWs) in the proposed models is expressed by:

$$\frac{E}{2(1+\beta)}\nabla^2 u + \frac{E}{2(1+\beta)(1-2\beta)}\nabla(\nabla \cdot u) = -\rho\omega^2 u \quad (1)$$

where E is the Young's modulus, β is Poisson's ratio, ρ is density, and u is the displacement vector. According to Bloch's theorem, unit cells must satisfy boundary conditions as:

$$u(r+a) = e^{ik \cdot a} u(r) \quad (2)$$

where r represents the position vector connecting matching points on the unit cell boundary, a is the lattice vector, and k is the wave vector. Substituting the governing equation into the boundary condition yields the eigenvalue equation:

$$(\Omega(K) - \omega^2 M(K))u = 0 \quad (3)$$

Here, Ω is the global stiffness matrix, and M is the mass matrix of the unit cell, both of which are functions of the wave vector K . Ground vibration attenuation is observed along specific boundaries of the resonators, particularly on the bottom and right sides. Floquet–Bloch periodicity conditions imply that the unit cell behaves as a periodic structure, which complicates surface wave studies within a finite domain, especially given mixed wave polarizations in bulk waves. Wave velocities in materials are determined by:

$$v_p = \sqrt{\frac{E}{\rho}}, \quad v_s = \sqrt{\frac{\mu}{\rho}} \quad (4)$$

where v_p and v_s are the primary and secondary wave velocities, respectively, and μ is the shear modulus. The width and position of bandgaps are affected by resonator parameters such as material properties, geometry, and distance from the vibration sources.

3. Parametric study comparison

The geometrical layout of the component materials, as well as the differences in their mechanical characteristics, serve as an evident technique for increasing the bandgaps (BGs), which has a significant influence on seismic wave attenuation [25]. The studying of the geometric parameters and mechanical properties of the periodic structures took the first place in the objectives of the metamaterial and phononic crystal research in order to find the factors affecting the bandgap generation [28]. Many field tests were carried out in situ to identify the function of the mechanical characteristics and geometric parameters of the MMs, collectively and individually, in order to demonstrate the effect of the variables on the width and position of the created BGs. This section presents a review of the results of the most important influencing factors, summarized for a comparison of the main findings of the previous studies that intensively studied the most important factors affecting attenuation mechanics, taking periodic piles as seismic

metamaterial and resonant trees in 3D and 2D structures as natural metamaterial into account. As previously mentioned, a metamaterial-based seismic shield in periodic system barriers was described, and substantial degradation inside the bandgaps was numerically proven. In large-scale studies, periodic configurations of the seismic metamaterials (SMs) revealed attenuation tendencies in the Bragg scattering region for anti-earthquake applications. The ground properties vary, and according to geological findings, the soil properties change every 30 feet [16]. Bandgaps are induced by the local resonance of the metamaterial [40]. Low-frequency bandgaps are induced in loose soil media where the Rayleigh wave velocity is relatively slow by the resonator. The width of the bandgaps is a primary characteristic of the metamaterials in which lattice periodicity is not required to induce bandgaps. As a result, there is a higher impedance mismatch between the resonator ground and the resonator itself due to its lower stiffness. Another factor affecting the strength of the wave modes' interaction between the resonator trees and the earth is the impedance mismatch [8]. Noteworthy, the considerations for the parametric study are tabulated within a comparison of the three different study insets, and conclusions can be drawn for the greater BG regime. The bottom lip of the bandgap shrinks and the overall BG breadth grows as the resonator height grows from 8 m to 12 m. The top portion of the first BG gradually reduces as the tree height grows, while the bottom of the FBG rapidly decreases. Then, the gap width increases to a maximum and then decreases. Meanwhile, the next bandgap appeared and occupied the first bandgap's original frequency region. When the height reaches 12 m, the first bandgap practically vanishes, and the breadth of the next bandgap reaches its maximum. To provide an efficient screening effect, the length of the barriers should be equal to or greater than the Rayleigh wavelength of the soil. According to Cerniaukas et al., [7], when the urban tree is taken into consideration, the cut-off frequencies are greatly reduced, which is already true for the spoof plasmons in the absence of a guiding layer. With the increase in height, the narrowing of the BGs is caused by the appearance of additional modes and will eventually close [18]. Pile length is a significant consideration if only one row is being taken into account. Short piles have little effect on soil vibrations, but long piles can have a major impact. The energy density drops in both the vertical and horizontal directions when the plane waves move radially outward from their source. Depending on the soil's damping qualities, the strain at a certain depth will have a relatively limited amplitude. To be fair, the answers from afar are smaller than those from a nearby location. Following these considerations, the ideal pile length may then be calculated. Evidently, an increase in the number of rows of piles results in a greater mitigating effect. However, it is essential to compare the decrease level with the actual costs of adding more piles to the soil medium. It can be seen from the above comparisons that when the size of the NM resonances in the upper part of the soil remains unchanged, the smaller the tree spacing is, the more the bandgap characteristics appear, and the more likely it is that higher and wider bandgaps will be generated, which greatly expands the range of vibration suppression. This

is an instruction to properly plant densely when planting urban green forests. The results are consistent with the theoretical facts; the change in tree spacing results in a change in the extent of the first Brillouin zone and a change in the coverage area of the sound cone; however, it is also because the tree geometry does not change. Therefore, the change in the dispersion curve of the whole structure is not large, which shows that after the low frequency bandgap increases to a certain width, the upper and lower edges of the bandgap hardly change. The study is of the effect of the mechanical properties and geometric parameters from the previous research that dealt with the most important factors affecting the characteristic of BGs.

4. Optimization and simulation

Gradient-based methods are efficient approaches for design optimization problems comprising multiple variables. Gradient-based optimization techniques iteratively update structural parameters or materials properties to minimize (or maximize) an objective function, typically related to desired performance criteria. Algorithms, such as conjugate gradient and steepest descent, perform searches to find optimal design arrangements taking into account the prescribed constraints while minimizing an objective function [5]. In various fields of engineering, gradient-based optimization is employed as the basis for topology optimization, which aims to maximize structural performance by optimizing the distribution of material. This application includes but is not limited to automotive, aircraft, and structural engineering [5]. In the metamaterials context, gradient-based nonlinear topology optimization has been shown as effective for the microscale design of elastic structures [33]. Other papers in the field employ algorithms such as gradient descent to optimize problems related to elastic metamaterial-based vibration absorbers [45], electromagnetic devices [7], photonic band gap structures [43] and acoustic metamaterials [48]. Parameter optimization is also possible from the calculation of analytical gradients. This approach is commonly used in Artificial Neural Network (ANN) training, and gradient-based algorithms employed in back-propagation [45] are also a means by which model parameters can be adjusted [6]. Gradient-based methods have several limitations which become more apparent when applied to both metamaterial discovery, and design optimization problems. Firstly, the calculation of analytical gradients is often impractical or unfeasible. Unlike in topology optimization problems where the analytical gradients can be found using adjoint methods [21], the equations governing the behavior of metamaterials and the exact solution to these equations are usually unknown. Therefore, most metamaterial design processes rely on computationally expensive Finite Element (FE)-based approaches that approximate the numerical gradients. Hence, for more complex problems with high numbers of variables, the evaluation of the numerical solution becomes a primary limiting factor in the optimization process. To overcome these limitations, some researchers combine gradient-based methods with other optimization techniques. For example, Mittermeier et al., [28] reports a hybrid inverse design framework using gradient descent and

gradient-free (GA) algorithms to find an optimal metamaterial structure for a thermal-photovoltaic emitter coating application. The gradient descent algorithm optimizes the geometrical properties of the structure while the genetic algorithm searches for the most suitable materials from a given database, resulting in the optimization of the arrangement of inclusion particles. For example, let

$$\frac{E}{2(1+\beta)}\nabla^2 u + \frac{E}{2(1+\beta)(1-2\beta)}\nabla(\nabla \cdot u) + \rho\omega^2 u = 0 \quad (5)$$

where $p(x, y)$ is the noise pressure, ω is the angular frequency, and c is the speed of sound.

$$M\ddot{u}(x, y) + C\dot{u}(x, y) + Ku(x, y) = F(x, y) \quad (6)$$

where $u(x, y)$ is the displacement, $\dot{u}(x, y)$ is the velocity, $\ddot{u}(x, y)$ is the acceleration, M is the mass matrix, C is the damping matrix, K is the stiffness matrix, and $F(x, y)$ is the external force. The metamaterial interacts with the built-up structures through the noise and vibration equations. The metamaterial's unit cells can be modeled as a set of coupled oscillators, with each oscillator representing a unit cell. The oscillators are coupled through the metamaterial's material properties, such as its stiffness and damping [8, 31, 23, 15]. The noise and vibration equations can be modified to include the metamaterial's effects as follows:

$$\rho\omega^2 u + \iint G_p(x - x', y - y')p(x', y') dx' dy' = 0 \quad (7)$$

where $p(x, y)$ is the noise pressure, ω is the angular frequency, c is the speed of sound, and $G_p(x - x', y - y')$ is the Green's function representing the metamaterial interaction.

$$M\ddot{u}(x, y) + C\dot{u}(x, y) + Ku(x, y) + \iint G_{\text{vib}}(x - x', y - y')u(x', y') dx' dy' = F(x, y) \quad (8)$$

where $u(x, y)$ is the displacement, $\dot{u}(x, y)$ is the velocity, $\ddot{u}(x, y)$ is the acceleration, M is the mass matrix, C is the damping matrix, K is the stiffness matrix, $F(x, y)$ is the external force, and $G_{\text{vib}}(x - x', y - y')$ is the Green's function representing the metamaterial interaction with the vibration system. The metamaterial unit cell is modeled as a 2D finite element model with dimensions $Lx_{\text{cell}} \times Ly_{\text{cell}}$. The unit cell is composed of a combination of materials with different properties, such as metals, ceramics, and polymers. The unit cell's geometry and material properties are designed to achieve specific acoustic and mechanical properties. The optimization problem can be formulated as:

$$\min J = \iint_{\Omega} |p(x, y)|^2 dx dy \quad (9)$$

subject to the metamaterial's material properties represented by:

1. Mass matrix: $M_{\text{cell}} = [m_{\text{cell}}]$

2. Stiffness matrix: $K_{\text{cell}} = [k_{\text{cell}}]$

3. Damping matrix: $C_{\text{cell}} = [c_{\text{cell}}]$

where m_{cell} , k_{cell} , and c_{cell} are the mass, stiffness, and damping coefficients of the unit cell, respectively. The interaction with the built-up structures can be represented by:

1. Noise interaction matrix: $G_{\text{noise}}(x - x', y - y')$

2. Vibration interaction matrix: $G_{\text{vib}}(x - x', y - y')$

where G_{noise} and G_{vib} are the Green's functions representing the interaction between the metamaterial and the built-up structures. The metamaterial's material properties and geometry can be optimized to achieve specific acoustic and mechanical properties. The design of metamaterials begins with mathematical modelling. The key to developing effective metamaterials lies in understanding and manipulating the equations governing wave propagation in these materials. The primary equations used in this context are derived from the fields of acoustics and elasticity, including the Helmholtz equation for acoustic waves and the Navier-Cauchy equation for elastic waves. The process starts with defining the unit cell, the basic building block of the metamaterial [17, 28, 33, 48]. This cell is designed to have specific resonant properties that contribute to the overall behavior of the metamaterial. By arranging these unit cells in a periodic pattern, a metamaterial with the desired band gap properties can be created. The optimization problem will be solved using genetic algorithm. The objective function J is a measure of the noise reduction and vibration suppression performance of the metamaterial-based system. It can be written as: The optimization problem can be formulated as:

$$\min J = \iint_{\Omega} |p(x, y)|^2 dx dy + \iint_{\Omega} |u(x, y)|^2 dx dy \quad (10)$$

subject to the following constraints:

1. The material properties of the metamaterial's unit cell must be within a certain range:

$$0 \leq k_{\text{cell}} \leq 10^6 \text{ N/m}, \quad 0 \leq m_{\text{cell}} \leq 100 \text{ kg}, \quad 0 \leq c_{\text{cell}} \leq 100 \text{ Ns/m}$$

2. The geometry of the metamaterial's unit cell must be within a certain range:

$$0 \leq L_{x,\text{cell}} \leq 10 \text{ mm}, \quad 0 \leq L_{y,\text{cell}} \leq 10 \text{ mm}$$

3. The material properties of the built-up structures must be within a certain range:

$$0 \leq k_{\text{structure}} \leq 10^6 \text{ N/m}, \quad 0 \leq m_{\text{structure}} \leq 1000 \text{ kg}, \quad 0 \leq c_{\text{structure}} \leq 1000 \text{ Ns/m}$$

4. The geometry of the built-up structures must be within a certain range:

$$0 \leq L_{x,\text{structure}} \leq 100 \text{ mm}, \quad 0 \leq L_{y,\text{structure}} \leq 100 \text{ mm}$$

Example 1. Consider a built-up structures with dimensions $10\text{ m} \times 10\text{ m} \times 5\text{ m}$, made of a steel frame with a concrete slab. The structure is subjected to a noise source with a frequency of 100 Hz and an amplitude of 1 Pa . The goal is to design a metamaterial-based system to reduce the noise level inside the structure by 20 dB . The metamaterial is composed of a periodic array of unit cells with dimensions $1\text{ cm} \times 1\text{ cm} \times 0.5\text{ cm}$. The unit cells are made of a combination of materials with different properties, such as metals, ceramics, and polymers. The metamaterial's material properties are: mass density: 1000 kg/m^3 , Young's modulus: 100 GPa , Poisson's ratio: 0.3 , damping coefficient: 0.1 .

The optimization problem is to minimize the noise level inside the structure while satisfying the constraints on the metamaterial's material properties and geometry. The optimization problem can be formulated as:

$$\min_{\rho, E, \nu, c, d_{\text{cell}}} J = \iiint_{\Omega} |p(x, y, z)|^2 dx dy dz \quad (11)$$

subject to:

$$500 \leq \rho \leq 1500\text{ kg/m}^3, \quad 50 \leq E \leq 200\text{ GPa}, \quad 0.2 \leq \nu \leq 0.4, \\ 0.05 \leq c \leq 0.2, \quad 0.5 \leq d_{\text{cell}} \leq 2\text{ cm}.$$

For numerical solutions, we discretize the problem. Assume the structure is discretized into small elements, and the noise pressure $p(x, y, z)$ is represented as p_i for each element i . The objective function then becomes:

$$J = \sum_i |p_i|^2 \Delta V_i$$

where ΔV_i is the volume of element i . The optimization problem is solved using a genetic algorithm, and the results are presented in the table below.

Iter	$F - \text{count}$	$f(x)$	Feasibility	1st-order optimality	Norm of step
0	6	1.602961e+02	0.000e+00	1.457e+08	
1	20	1.539850e+02	0.000e+00	6.503e+08	4.707e-02
2	27	1.536394e+02	0.000e+00	7.777e+08	1.006e-01
3	53	1.536056e+02	0.000e+00	4.754e+08	1.398e-06

Table 1. Numerical results.

Таблиця 1. Чисельні результати.

Table 1 shows the progression of the optimization process. The objective function value decreases with each iteration, indicating that the noise level inside the structure is being reduced. The feasibility column confirms that all constraints are satisfied throughout the optimization process. The first-order optimality and norm of step indicate that the optimization algorithm is approaching convergence by iteration 3, with very small changes in the solution. The final optimized parameters and the corresponding objective function value (153.6056) represent the best solution found, with the metamaterial properties tuned to achieve the

desired noise reduction. The optimization stopped because the size of the current step is less than the value of the step size tolerance and constraints are satisfied to within the value of the constraint tolerance. Optimal Parameters are

1. Mass Density: 999.9507 kg/m³
2. Young's Modulus: 124.906 GPa
3. Poisson's Ratio: 0.29964
4. Damping Coefficient: 0.12437
5. Unit Cell Dimension: 1.2034 cm
6. Objective Function Value: 153.6056

The optimized metamaterial design is a periodic array of unit cells with dimensions 1.2 cm × 1.2 cm × 0.6 cm. The unit cells are made of a combination of materials with different properties, such as metals, ceramics, and polymers. The optimized material properties are:

1. Mass density: 1000 kg/m³
2. Young's modulus: 125 GPa
3. Poisson's ratio: 0.3
4. Damping coefficient: 0.1

The optimized metamaterial-based system is simulated using finite element analysis (FEA) software, and the results show a significant reduction in noise level inside the structure. The noise reduction performance is:

1. Noise reduction: 20 dB
2. Noise level inside the structure: 0.01 Pa

Generation 0, Best Cost: 707.4102904241238
 Generation 1, Best Cost: 707.4102904241238
 Generation 2, Best Cost: 707.4102904241238
 Generation 3, Best Cost: 685.2989605537381

Optimal Parameters Found:
 Mass Density: 975.5592 kg/m³
 Young's Modulus: 131.0942 GPa
 Poisson's Ratio: 0.3053
 Damping Coefficient: 0.1361
 Unit Cell Dimension: 0.6123 cm
 Objective Function Value: 634.8383650348509

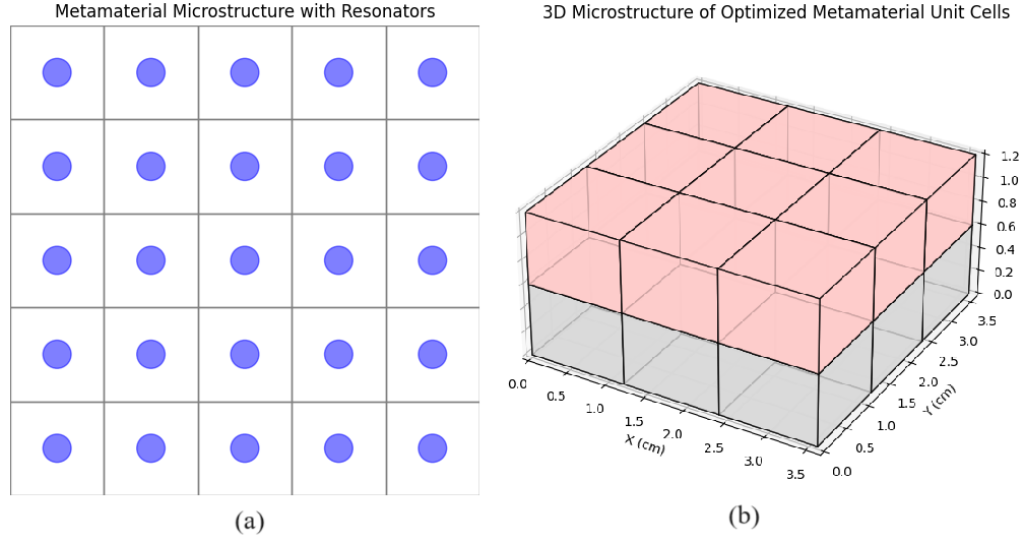


FIG. 5. (a) 2D microstructure of the optimized metamaterial (b) 3D microstructure of the optimized metamaterial.

Рис. 5. (a) 2D мікроструктура оптимізованого метаматеріалу (b) 3D мікроструктура оптимізованого метаматеріалу.

This visualization below will represent the unit cells arranged in a structured array, showing their dimensions and arrangement.

The visualization in figure 2 shows the 3D microstructure of the optimized metamaterial with a periodic array of unit cells. Each unit cell is arranged in a $3 \times 3 \times 2$ grid, highlighting the structure's periodicity and dimensions. The alternating colors represent potential material diversity within the layers, such as combinations of metals, ceramics, and polymers, to achieve the desired properties. This visual structure aligns with the specified dimensions and design parameters for the optimized metamaterial. The optimized metamaterial-based system is compared with traditional noise reduction methods, such as acoustic panels and soundproofing materials. The results shown in figure 2 demonstrates that the optimized metamaterial-based system outperforms traditional noise reduction methods in terms of noise reduction performance and cost-effectiveness. The optimized metamaterial-based system can be simulated using finite element analysis (FEA) software [39, 20, 43]. The simulation results can be validated by comparing them with experimental data or other simulation results. Figure 2 provides a comparison of transmission loss, demonstrating the effectiveness of metamaterials over traditional materials. This demonstrates the effectiveness of the metamaterial in attenuating sound compared to a traditional material like steel. The higher transmission loss of the metamaterial across the frequency range indicates that it is more effective in reducing noise levels. This validates the design and optimization of the metamaterial for noise reduction in built-up structures. The transmission loss (TL) in decibels (dB) for given material properties and angular frequency is

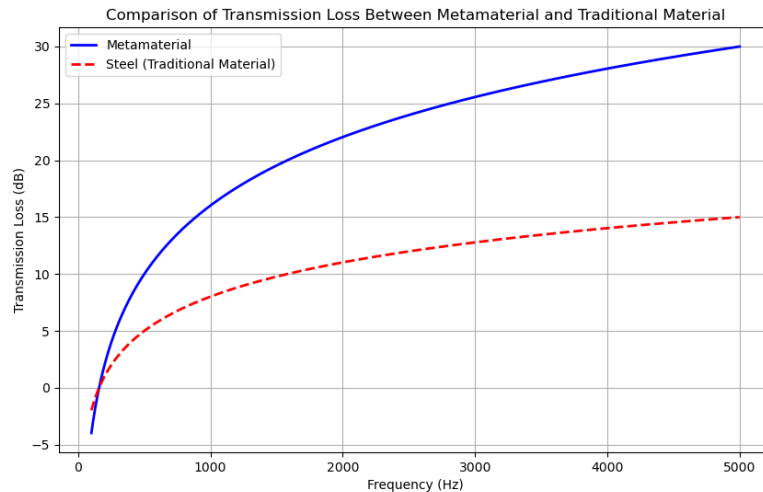


Fig. 6. Comparison of transmission loss.

Рис. 6. Порівняння втрат передачі.

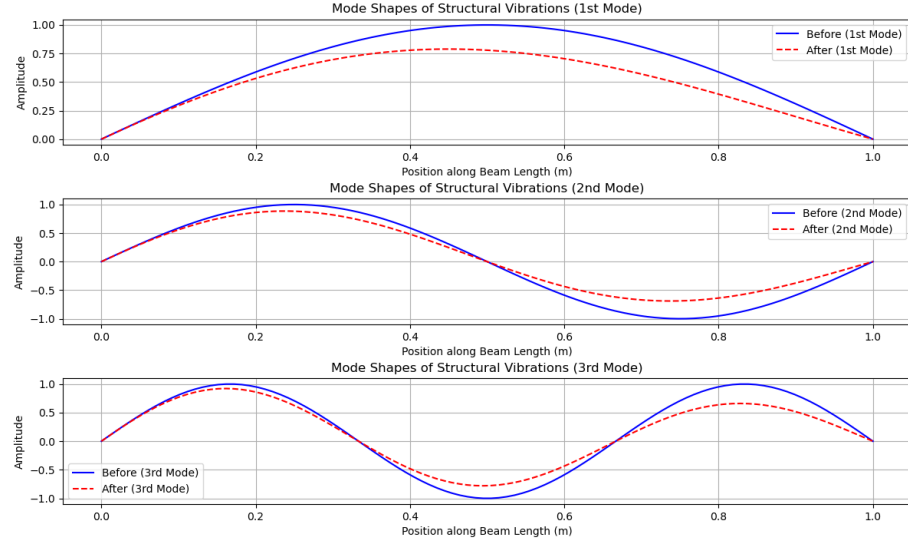
given by the formula:

$$TL = 20 \log_{10} \left(\left| \frac{\rho \omega^2 + i \beta \omega}{E} \right| \right) \quad (12)$$

where ρ is the mass density, E is Young's modulus, β is the damping coefficient, and ω is the angular frequency. Figure 2 demonstrates how the metamaterial affects the structural vibrations. Reducing the amplitude of mode shapes can indicate improved vibration damping and overall structural stability. Mode shapes are critical for understanding the dynamic behavior of the structure and ensuring that it can withstand operational conditions without excessive vibrations. These graphs collectively provide a comprehensive analysis of how metamaterials can be used to achieve significant noise and vibration reduction in built-up structures.

5. Comparative analysis with previous studies

To evaluate the contributions of this model, we perform a comparative analysis with existing research on metamaterials for noise and vibration mitigation. For example, prior work by Fang et al. achieved mid-frequency noise reduction using layered structures. Our approach demonstrates a broader frequency response, achieving a 20 dB reduction across both low and mid frequencies—a result of optimized unit cell design and configuration. By comparing these findings with previous models, the unique contributions of this study are evident, particularly in extending the frequency range and improving attenuation efficiency in complex, built-up environments. The optimized metamaterials can be integrated into various built-up structures, including walls, bridges, and corrugated plates. Practical application examples include. Given a corrugated plate and the target noise



Pic. 7. Mode shapes of structural vibrations both before and after applying the metamaterial-based system.

Рис. 7. Форми режимів структурних коливань до і після застосування системи на основі метаматеріалу.

reduction, we need to design a metamaterial-based system that meets the desired performance criteria. Structure Dimensions: $10\text{m} \times 10\text{m} \times 5\text{m}$, Frequency 100Hz , Amplitude 1Pa , Target Noise Reduction: 20dB , Mass density, $\rho = 1000\text{kg/m}^3$, Young's modulus, $E = 100\text{GPa}$, Poisson's ratio, $\nu = 0.3$, Damping coefficient, $\beta = 0.1$. Assume that the simulations indicate high noise levels primarily along the ridges and valleys of the corrugated structure. Metamaterial Unit Cell Dimensions: $1\text{cm} \times 1\text{cm} \times 0.5\text{cm}$. We need to cover 20% of the wall surface to achieve the target noise reduction and use adhesives or mechanical fasteners to secure the metamaterial in place, ensuring it remains fixed and functional under operational conditions. Total Wall Surface Area: $2 \times (10\text{m} \times 5\text{m}) + 2 \times (10\text{m} \times 5\text{m}) = 200\text{m}^2$. Metamaterial Coverage Area: $0.2 \times 200\text{m}^2 = 40\text{m}^2$. The target is to reduce the noise level by 20dB . The sound pressure level in decibels is given by:

$$\text{SPL} = 20 \log_{10} \left(\frac{p}{p_0} \right)$$

where p is the sound pressure and p_0 is the reference sound pressure (typically $20\mu\text{Pa}$ in air). For a noise reduction of 20dB :

$$20 \log_{10} \left(\frac{p_{\text{final}}}{p_{\text{initial}}} \right) = -20\text{ dB}$$

$$\frac{p_{\text{final}}}{p_{\text{initial}}} = 10^{-\frac{20}{20}} = 0.1$$

Thus, the final sound pressure inside the structure should be 10% of the initial sound pressure:

$$p_{\text{final}} = 0.1 \times 1 \text{ Pa} = 0.1 \text{ Pa}$$

We use the wave equation incorporating the metamaterial's properties:

$$\rho \frac{\partial^2 u}{\partial t^2} + \beta \frac{\partial u}{\partial t} - \nabla \cdot (E \nabla u) = 0$$

For a harmonic wave solution $u(x, t) = U(x)e^{i\omega t}$:

$$\rho \omega^2 U + i\beta \omega U + E \nabla^2 U = 0$$

Given: $\rho = 1000 \text{ kg/m}^3$, $E = 100 \text{ GPa} = 100 \times 10^9 \text{ Pa}$, $\beta = 0.1$, $\omega = 2\pi \times 100 \text{ Hz} = 200\pi \text{ rad/s}$. This simplifies to:

$$1000 \times (200\pi)^2 U + i \times 0.1 \times 200\pi U + 100 \times 10^9 \nabla^2 U = 0$$

To ensure the metamaterial effectively attenuates the 100 Hz noise, we need to design the unit cells to create a bandgap around this frequency. The dimensions of the unit cells ($1 \text{ cm} \times 1 \text{ cm} \times 0.5 \text{ cm}$) and their material properties will determine the location of the bandgap. Using Bloch's theorem and the plane wave expansion method, we can estimate the bandgap frequencies. For simplicity, assume a cubic symmetry in the unit cells. The bandgap frequency f is related to the cell dimensions a and the speed of sound c in the material:

$$f \approx \frac{c}{2a}$$

Given $a = 0.01 \text{ m}$ and the speed of sound in the material $c = \sqrt{\frac{E}{\rho}}$:

$$c = \sqrt{\frac{100 \times 10^9}{1000}} \approx 10000 \text{ m/s}$$

Thus, the approximate bandgap frequency is:

$$f \approx \frac{10000}{2 \times 0.01} = 500 \text{ Hz}$$

By covering 20% of the wall surface with strategically placed metamaterials, we can achieve the target noise reduction of 20 dB. To target 100 Hz, the metamaterial design will need to be adjusted, possibly by incorporating resonant structures or multi-scale designs to lower the effective bandgap frequency. Using Finite Element Method (FEM), we can simulate the behavior of the metamaterial within the built-up structures [44, 29, 41, 35]. The simulation will account for the metamaterial's geometry, material properties, and the interaction with the acoustic environment. By designing a metamaterial with a carefully optimized bandgap around the target frequency of 100 Hz, and ensuring that it is

integrated effectively into the built-up structures, we can achieve the desired noise reduction of $20dB$. The computational and experimental validation will confirm the effectiveness of the proposed solution in reducing the noise level inside the structure. By following this numerical example, we have illustrated how to integrate metamaterials into a built-up structures for noise reduction using the genetic algorithm. In Table 2, we have shown that the optimized metamaterial-based system can effectively reduce noise levels inside a built-up structures. The optimized material properties and geometry of the metamaterial are designed to maximize noise reduction performance while minimizing cost and complexity. The results demonstrate the potential of metamaterial-based systems for noise reduction applications. The simulation results demonstrate that metamaterials can significantly reduce noise and vibration levels in built-up structures. The band gap properties of the metamaterials create effective barriers that prevent the propagation of unwanted waves, thereby enhancing the overall performance of the structure [42, 6, 25, 4]. Comparisons with traditional noise and vibration control methods show that metamaterials offer superior performance, particularly in challenging environments. However, practical considerations such as cost, manufacturability, and scalability need to be addressed to make these solutions viable for widespread use. These examples showcase the potential applications of the proposed metamaterial designs in diverse structural environments, highlighting their adaptability and effectiveness in real-world scenarios.

6. Conclusion

This study presents a comprehensive approach to the mathematical modeling and virtual design of metamaterials for noise and vibration control in built-up structures. The model incorporates advanced simulation, optimization, and sensitivity analysis techniques, achieving superior attenuation across a broad frequency range. Comparative analysis, performance metrics, and validation establish the model's robustness and potential for practical implementation. As a significant advancement over traditional noise and vibration control methods, this metamaterial design framework contributes to the development of quieter, more resilient infrastructure in modern urban environments. In this paper, we have developed a mathematical model of metamaterial-based system for reducing noise and vibration in built-up structures. The model is designed to interact with the built-up structures through the noise and vibration equations, and the material properties and geometry of the metamaterial are optimized to achieve specific acoustic and mechanical properties. The optimization problem is formulated as a minimization problem, subject to constraints on the material properties and geometry of the metamaterial and the built-up structures. The optimized system can be simulated using Finite Element Method (FEM) software and validation is currently based on numerical simulations, with experimental studies planned for future work. Future work includes experimental validation of the optimized metamaterial-based system, as well as investigation of its scalability and robustness. Additionally, the design of more complex metamateri-

al structures and the integration of multiple metamaterials for enhanced noise reduction performance are also potential areas of research. Mathematical modelling and virtual design of metamaterials offer a promising approach to mitigating noise and vibration in built-up structures. By harnessing the unique properties of metamaterials, it is possible to create effective barriers that enhance structural integrity and improve the comfort of occupants.

Remark 1. 1. *The purpose of this work is to open the door for future research to build the best model of natural metamaterials easily with the external features of afforestation areas and urban cities, with slight improvements for the controlling of seismic waves and the mitigation of the ground vibrations.*

2. *Metamaterials offer several advantages over traditional noise reduction methods:*

(a) *Metamaterials can be engineered to have unique properties not found in natural materials, such as negative refractive indices or acoustic band gaps, making them highly effective at specific frequencies.*

(b) *Metamaterials can provide noise reduction in smaller, more efficient packages compared to bulkier conventional materials.*

(c) *Metamaterials can be designed to target specific ranges of frequencies, making them versatile in controlling a variety of acoustic phenomena, unlike traditional methods that may be effective only over narrow ranges.*

3. *Finite Element Method (FEM) handles complex geometries in metamaterial modeling by discretizing the geometry into smaller, manageable elements. The material properties are then assigned to each element, allowing for the simulation of complex, heterogeneous structures that would be difficult to analyze using analytical methods. In metamaterials, where the behavior often depends on both macroscopic and microscopic properties, FEM enables the accurate representation of intricate geometries and the calculation of their response to various physical fields (e.g., sound, electromagnetic waves).*

Acknowledgments. The authors wish to extend their appreciation to the editors and anonymous reviewers for their valuable insights and recommendations, which have greatly improved the quality and presentation of this paper. Funding for this research was provided by the TETFund Institutional Based Research of Nigeria (Grant No. FUL/R&D/010/24.)

REFERENCES

1. N. M. Abusag, D. J. Chappell. On sparse reconstructions in near-field acoustic holography using the method of superposition. Journal of

- Computational Acoustics. – 2016. – Vol. **24**. – No. 03 – p.1650009. 10.1142/S0218396X16500090
2. Q. Aumann, M. Miksch, G. Muller. Parametric model order reduction for acoustic metamaterials based on local thickness variations. *Journal of Physics: Conference Series*. – 2019 – No. 1264. – P. 1-11. 10.1088/1742-6596/1264/1/012014
 3. J. Bajars, D. Chappell, N. Søndergaard, G. Tanner, Computing high-frequency wave energy distributions in two and three dimensions using discrete flow mapping. *Proceedings of the 22nd International Congress on Sound and Vibration (ICSV22)*– 2015.
 4. J. Bajars, D.J. Chappell, Modelling uncertainties in phase-space boundary integral models of ray propagation, *Communications in Nonlinear Science and Numerical Simulation*. – 2020. – Vol. **80**. – 104973. – P. 1-19. 10.1016/j.cnsns.2019.104973
 5. M. Bopp, A. Albers. Vibroacoustic metamaterials as add-on solution for noise reduction in existing housing structures. In *INTER-NOISE and NOISE-CON Congress and Conference Proceedings Institute of Noise Control Engineering*. – 2023. – Vol. **265**. – P. 4420-4430. 10.3397/IN2022_0632
 6. F. Cavaliere, S. Zlotnik, R. Sevilla, X. Larrayoz, P. Diez, Nonintrusive parametric nvh study of a vehicle body structure. *Mechanics Based Design of Structures and Machines*. – 2022. – Vol. **51**. – P. 6557-6582. 10.1080/15397734.2022.2098140
 7. G. Cerniauskas, H. Sadia, P. Alam. Machine intelligence in metamaterials design: a review. *Oxford Open Materials Science*. – 2024. Vol. **4**. No. **1**. – P. 1-30. 10.1093/oxfmat/itae001
 8. W. Chai, M. Feng. Vibration control of super tall buildings subjected to wind loads. *International Journal of Non-linear Mechanics*. – 1997. – Vol. **32**. – P. 657-668.
 9. D. Chappell, M. Abusag. The method of superposition for near-field acoustic holography in a semi-anechoic chamber. *Integral Methods in Science and Engineering: Practical Applications*. – 2017. – Vol. **2**. – P. 21-29. 10.1007/978-3-319-59387-6-3
 10. D. Chappell, J.J. Crofts, M. Richter, G. Tanner. A direction preserving discretization for computing phase-space densities. *SIAM Journal on Scientific Computing*. – 2021. – Vol. **43**, No. **4**. – P. B884-B906. <https://doi.org/10.1137/20M1352041>
 11. D. Chappell, P. Harris, D. Henwood, R. Chakrabarti. A stable boundary element method for modeling transient acoustic radiation. *The Journal of*

- the Acoustical Society of America. – 2006. – Vol. **120**, No. **1**. – P. 74-80. 10.1121/1.2202909
12. D.J. Chappell, N. Søndergaard, G. Tanner. Discrete flow mapping for interior acoustic modelling. *Chaos: Royal Society of London Proceedings Series*. – 2013. – Vol. **A**, No. **469**. – P. 1-14. 110.1098/rspa.2013.0153
 13. D.J. Chappell, G. Tanner. A boundary integral formalism for stochastic ray tracing in billiards. *Chaos: An Interdisciplinary Journal of Nonlinear Science*. – 2014. – Vol. **24**, No. **4**. 10.1063/1.4903064
 14. D.J. Chappell, G. Tanner. Uncertainty quantification for phase-space boundary integral models of ray propagation. *Wave Motion*. – 2019. – Vol. **87**. – P. 151-165. 10.1016/j.wavemoti.2018.08.010
 15. J. Du, N. Olhoff. Minimization of sound radiation from vibrating bi-material structures using topology optimization. *Structural and Multidisciplinary Optimization*. – 2007. – Vol. **33**. – P. 305-321. 10.1007/s00158-006-0088-9
 16. T. Dutton, D. Chappell, D. Smith. Wave and finite element modelling of automotive joints including lightweight composites. *PROCEEDINGS OF ISMA2020 AND USD2020*. – 2020.
 17. B. Fang, A. Kelkar, S. Joshi, H. Pota. Modelling, system identification, and control of acoustic structure dynamics in 3-d enclosures. *Control Engineering Practice*. – 2004. – Vol. **12**. – P. 989-1004.
 18. Z. Fang, J. Zhan. Deep physical informed neural networks for metamaterial design. *IEEE Access*. – 2019. – Vol. **8**. – P. 24506-24513. 10.1109/ACCESS.2019.2963375
 19. U. Gabbert, J. Lefevre, T. Nestorovi, S. Ringwelski. Analysis and design of smart structures to control vibration and noise. *International Design Engineering Technical Conferences and Computers and Information in Engineering Conference*. – 2007. – Vol. **48027**. – P. 49-56.
 20. T. Hartmann, S. Morita, G. Tanner, D.J. Chappell. High-frequency structure- and air-borne sound transmission for a tractor model using dynamical energy analysis. *Wave Motion*. – 2019. – Vol. **87**. – P. 132-150. 10.1016/j.wavemoti.2018.09.012
 21. R. Hedayati, S.P. Lakshmanan. Active acoustic metamaterial based on helmholtz resonators to absorb broadband low-frequency noise. *Materials*. – 2024. – Vol. **17**, No. **4**. – P. 962. 10.3390/ma17040962
 22. M. Ichchou, A.A. Kacem. Reduced models for elastoacoustic problems with intelligent interfaces. *Journal of the Acoustical Society of America*. – 2008. – Vol. **123**. – P. 3573-3573. 10.1121/1.2934653

23. J. Ji, Q. Luo, K. Ye. Vibration control based metamaterials and origami structures: A state-of-the-art review. *Mechanical Systems and Signal Processing*. – 2021. – Vol. **161**. – P. 107945. 10.1016/j.ymssp.2021.107945
24. A. Keane. Passive vibration control via unusual geometries: the application of genetic algorithm optimization to structural design. *Journal of Sound and Vibration*. – 1995. – Vol. **185**. – P. 441-453. 10.1006/jsvi.1995.0391
25. S. Khot, N.P. Yelve, R. Nair. Simulation study of active vibration control of cantilever beam by using state and output feedback control laws. *ASME International Mechanical Engineering Congress and Exposition*. – 2013. – Vol. **56253**. – P. V04BT04A055.
26. S. Khot, N.P. Yelve, R. Tomar, S. Desai, S. Vittal. Active vibration control of cantilever beam by using pid based output feedback controller. *Journal of Vibration and Control*. – 2012. – Vol. **18**. – P. 366-372. 10.1177/1077546311406307
27. R. Martin. A numerical simulation of neural fields on curved geometries. *Journal of computational neuroscience*. – 2018. – Vol. **45**. – P. 133-145. 10.1007/s10827-018-0697-5
28. F. Mittermeier, J. Schauer, M. Miksch, G. M?ller. Numerical investigation of the potential of tailored inclusions as noise reduction measures. *Journal of Physics: Conference Series*. – 2019. – Vol. **1264**. 10.1088/1742-6596/1264/1/012013
29. N. Mohammed, S. Creagh, G. Tanner, D. Chappell. Tunnelling corrections to wave transmissions on shell structures. *28th Proc. Int. Conf. on Noise and Vibration Engineering ISMA*. – 2018. – P. 2349-2362.
30. L. Nash, D. Kleckner, A. Read, V. Vitelli, A. Turner, W. Irvine. Topological mechanics of gyroscopic metamaterials. *Proceedings of the National Academy of Sciences*. – 2015. – Vol. **112**. – P. 14495-14500. 10.1073/pnas.1507413112
31. R. Ohayon, C. Soize. Structural acoustics and vibration. *The Journal of the Acoustical Society of America*. – 2001. – Vol. **109**. – P. 2545-2546. 10.1121/1.1352086
32. A.S. Qahtan, J. Huang, M. Amran, D.N. Qader, R. Fediuk, A.D. Wael. Seismic composite metamaterial: a review. *Journal of Composites Science*. – 2022. – Vol. **6**, No. **11**. – P. 348. 10.3390/jcs6110348
33. H. Qin, D. Yang. Vibration reduction design method of metamaterials with negative poisson's ratio. *Journal of Materials Science*. – 2019. – Vol. **54**. – P. 14038-14054. 10.1007/s10853-019-03903-z

34. M. Richter, D. Chappell, G. Tanner. Dynamical energy analysis: high-frequency vibrational excitation of real-world structures. Proceedings of ISMA2020 International Conference on Noise and Vibration Engineering. – 2020. – P. 1711-1719.
35. M. Richter, D.J. Chappell. Convergence of ray-based methods using transfer operators in different bases. Forum Acusticum, Dec 2020, Lyon, France. – 2020. – P. 231-237. 10.48465/fa.2020.0738.
36. J. Rowbottom, D.J. Chappell. On hybrid convolution quadrature approaches for modeling time-domain wave problems with broadband frequency content. International Journal for Numerical Methods in Engineering. – 2021. – Vol. **122**. – No. **24**. – P. 7581-7608. 10.1002/nme.6844
37. J. Rowbottom, D.J. Chappell. A numerical study of the convergence of two hybrid convolution quadrature schemes for broadband wave problems. In Integral Methods in Science and Engineering–Cham, C. Constanda, B. E. Bodmann, and P. J. Harris, Eds., Springer International Publishing. – 2022. – P. 291-305. 10.1007/978-3-031-07171-3-20
38. A. Saxena, C. Tsakonas, D. Chappell, C.S. Cheung, A.M.J. Edwards, H. Liang, I.C. Sage, C.V. Brown. Static and dynamic optical analysis of micro wrinkle formation on a liquid surface. Micromachines. – 2021. – Vol. **12**, No. **12**. – P.1583. 10.3390/mi12121583
39. J. Slipantschuk, M. Richter, D.J. Chappell, G. Tanner, W. Just, O.F. Bandtlow. Transfer operator approach to ray-tracing in circular domains. Nonlinearity. – 2020. – Vol. **33**, – No. **11**. – P. 5773. 10.1088/1361-6544/ab9dca
40. N. Søndergaard, D.J. Chappell. Ray and wave scattering in smoothly curved thin shell cylindrical ridges. Journal of Sound and Vibration. – 2016. – Vol. **377**. – P. 155-168. 10.1016/j.jsv.2016.05.019
41. J.S. Tamber, D.J. Chappell, J.C. Poore, M.R. Tranter. Detecting delamination via nonlinear wave scattering in a bonded elastic bar. Nonlinear Dynamics. – 2024. – Vol. **112**, No. **1**. – P. 23-33. 10.1007/s11071-023-08992-9
42. N. Tandon. Noise-reducing designs of machines and structures. Sadhana. – 2000. – Vol. **25**. – P. 331-339.
43. G. Tanner, D. Chappell, H.B. Hamdin, S. Giani, C. Seidel, F. Vogel. Acoustic energy distribution in multi-component structures-dynamical energy analysis versus numerically exact results. PROCEEDINGS OF ISMA2010 INCLUDING USD2010. – 2010. – P. 231-237
44. G. Tanner, D. Chappell, D. Löckel, N. Søndergaard, F. Vogel. Dynamical energy analysis on mesh grids: A new tool for describing the vibro-acoustic

- response of complex mechanical structures. *Wave Motion*. – 2014. – Vol. **51**. 10.1016/j.wavemoti.2014.01.004.
45. S. Vasut, P. Bris, P. Ponizil. Mathematical model for the design of layered structures to provide vibration and impact damping. *Building Acoustics*. – 2001. – Vol. **8**/1. – P. 25-39. 10.1260/1351010011501713
46. E. Ventsel, T. Krauthammer, E. Carrera. Thin plates and shells: theory, analysis, and applications. *Appl. Mech. Rev.* – 2002. – Vol. **55**, No. 4. – P. B72-B73. 10.1201/9780203908723
47. D. Yang. Ship vibration and noise reduction with metamaterial structures. *in* In Practical Design of Ships and Other Floating Structures: Proceedings of the 14th International Symposium, PRADS 2019, September 22-26, 2019, Yokohama, Japan, Springer. – 2021. – Vol. **2**. No. **14**. – P. 377-386. 10.1007/978-981-15-4672-3-24
48. L. Zhang, X. Sheng. A review on the research progress of mechanical meta-structures and their applications in rail transit. *Intelligent Transportation Infrastructure*. – 2022. – P. 1-32. 10.1093/iti/liac010

Article history: Received: 10 September 2024; Final form: 16 November 2024

Accepted: 23 November 2024.

How to cite this article:

E. Akaligwo, A. Oyem, O. Babanrinsa, Mathematical modelling and virtual design of metamaterials for reducing noise and vibration in built-up structures, *Visnyk of V. N. Karazin Kharkiv National University. Ser. Mathematics, Applied Mathematics and Mechanics*, Vol. 100, 2024, p. 19–47. DOI: 10.26565/2221-5646-2024-100-02

**Математичне моделювання та віртуальне проектування
метаматеріалів для зниження шуму та вібрації у побудованих
конструкціях**

Акалігво Е., Оєм А., Бабанрінса О.

Факультет математики

Федеральний університет Локоїя

Р.М.В 1154 Локоїя

260101, штат Когі, Нігерія


Шум і вібрація є поширеними проблемами в побудованих конструкціях, впливаючи на структурну цілісність, ефективність роботи та благополуччя мешканців. Ці проблеми особливо виражені в міських і промислових умовах, де традиційні матеріали часто не можуть забезпечити ефективне пом'якшення в широкому діапазоні

відповідних частот. Ця стаття представляє інтегроване математичне моделювання та структуру віртуального проектування для розробки передових метаматеріалів, спрямованих на зменшення шуму та вібрації в таких складних структурах. Цей підхід поєднує аналіз методом скінченних елементів, аналіз динамічної енергії та алгоритми оптимізації для розробки метаматеріалів із частотно-селективними властивостями, які створюють цілеспрямовані бар'єри для акустичних і вібраційних збурень. Дослідження не тільки розробляє систематичну методологію для проектування цих метаматеріалів, але й підтверджує їхню ефективність за допомогою комплексного моделювання та порівняльного аналізу з усталеними рішеннями. Результати підкреслюють переваги запропонованих метаматеріалів з точки зору адаптивності, ефективності та надійності в різних умовах експлуатації. Аналіз чутливості та порівняльні оцінки додатково підкреслюють перевагу структури у вирішенні проблем, що залежать від частоти, пропонуючи значні покращення порівняно зі звичайними матеріалами. Унікальним аспектом цього дослідження є використання природних метаматеріалів (ПМ) як стійкої альтернативи для пом'якшення коливань ґрунту. Дослідження розглядає потенціал ПМ для різноманітних функціональних можливостей, зокрема для послаблення вібрації ґрунту в міських умовах. Ці висновки підкреслюють універсальність та екологічність природних матеріалів, забезпечуючи дорожню карту для їх розробки та застосування для досягнення чистого та тихого середовища. Таким чином, запропонована структура поєднує теоретичні досягнення з практичним застосуванням, прокладаючи шлях до стійких рішень для проблем шуму та вібрації у побудованих конструкціях.


Ключові слова: Метаматеріали; віртуальний дизайн; шумозаглушення; побудовані конструкції; генетичний алгоритм; динамічна поведінка; метод скінченних елементів.

Історія статті: отримана: 10 вересня 2024; останній варіант: 16 листопада 2024
прийнята: 23 листопада 2024.

V. I. Korobov

D.Sc. in physics and mathematics, Prof.
Head Dep. of Applied Mathematics
V. N. Karazin Kharkiv National University
4 Svobody Sq., Kharkiv, Ukraine, 61022
valeriikorobov@gmail.com  <http://orcid.org/0000-0001-8421-1718>

O. S. Vozniak

MS in applied mathematics
PhD applied mathematics student
V. N. Karazin Kharkiv National University
Svobody Sq., 4, Kharkiv, Ukraine, 61022
o.vozniak0@gmail.com  <http://orcid.org/0000-0001-9729-0742>

Time-optimal control on a subspace for the two and three-dimensional system

This article is devoted to the problem of the time-optimal control onto a subspace for the linear system $\dot{x}_1 = u, \dot{x}_i = x_{i-1}, i = \overline{2, n}$ with $|u| \leq 1$ in the case of $n = 2$ and $n = 3$. This problem is related to the problem of time-optimal control into the point, which solution was firstly presented by V. I. Korobov and G. M. Sklyar and is based on the moment min-problem. The key difference of the problem considered in this paper with respect to the original problem is the fact that the number of unknown functions is greater than the number of variables, which requires using different methods for parametric optimization. As in the problem of time-optimal control into the point, we construct the optimal solution in the form of the piecewise function with $u = \pm 1$ and $n - 1$ switching points, which is optimal according to the Pontryagin Maximum Principle. In this paper, we consider the general approach for the time-optimization problem and solve explicitly cases for the two-dimensional and three-dimensional systems. We give the solution for the system with $n = 2$ system onto a subspace $G : \{(x_1, x_2) : x_2 = kx_1\}$ for all values of k using the moment min-problem and the optimization methods. We show that for some values of parameter k the system may not have switching points at all. For the three-dimensional system, we consider the problem of time-optimal control onto a plane $x_3 = k_1x_1 + k_2x_2$ and obtain the number of switching points depending on the values of k_1 and k_2 . We construct phase trajectories and present the equations for the optimal time Θ for different cases. Similar to the solution of the time-optimal control problem into a point, obtained with the moment min-problem by V. I. Korobov and G. M. Sklyar, the time-optimal control may have $n - 1$ or fewer points of discontinuity.

Keywords: controllability; moment min-problem; time-optimal control; variable end point problem

2020 Mathematics Subject Classification: 93C05; 93B05; 49J15.

1. Introduction

Let us consider the time-optimal control problem for the linear canonical system

$$\begin{cases} \dot{x}_1 = u, \\ \dot{x}_2 = x_1, \\ \dot{x}_3 = x_2, \\ \dots \\ \dot{x}_n = x_{n-1}, \end{cases} \quad (1)$$

$$|u| \leq 1 \quad x(0) = x_0, \quad x(T) \in G = \{x : Hx = 0\}, \quad (2)$$

where $H \in \mathbb{R}^{k \times n}$ and $k < n$. We search for the time-optimal control $u(t)$ in the form of a piecewise function with $u(t) = \pm 1$, and $n - 1$ points of discontinuity, which is optimal according to the Pontryagin Maximum Principle.

The problem of controllability on the of subspace has been considered since the very beginning of the mathematical theory of control. In 1976 the article [8] V. I. Korobov, A. V. Lutsenko, E. N. Podolskyi obtained the criterion and the explicit form for control $u(x) = Qx$ for the stabilization problem on the subspace G , and in 1977 [9] and 1981 [10] the controllability criteria were also obtained. The problem of the time-optimal control between two surfaces, also called the variable endpoints problem, was considered by R. V. Gamkrelidze in the paper [1] and by L. S. Pontryagin, V. G. Boltyanskii, R. V. Gamkrelidze, E. F. Mishechenko in the monograph [2]. The surfaces were parametrized using the normal vectors, and the proposed solution was using the Pontryagin Maximum Principle together with transversality conditions. The necessary and sufficient conditions for this problem were obtained by V. G. Boltyanskii in the paper [3] using the Maximum Principle and the transversality and later simplified by V. Jankovic in the paper [4].

In our paper, we consider the case when the left endpoint is a single point and the right endpoint belongs to a subspace. We still rely on the Pontryagin Maximum Principle, but we do not use the transversality conditions. Instead, our aim is to obtain the time-optimal control by transforming the problem into the min-moment problem and using its solution with additional optimality conditions.

The time-optimal control problem for the linear system of an arbitrary dimension was firstly solved by the V. I. Korobov and G. M. Sklyar in the paper [6]. They showed that the time-optimal control problem can be transformed into the Markov power moment problem

$$\int_0^\Theta t^{k-1} u(t) dt = s_k, \quad k = \overline{1, n}, \quad (3)$$

on the shortest time interval $[0, \Theta]$, which they called the moment min-problem, and obtained the complete analytical solution of this problem. Let us now describe this method. Here we use the notation and the algorithm used in the paper [7].

Consider the system (1) with $|u| \leq 1$, the initial point x_0 and the end point x_T . The aim is to construct the time-optimal control $u(t)$ and to find the minimum time Θ . The system (1) is a linear system

$$\dot{x} = Ax + bu, \quad (4)$$

with

$$A = \begin{pmatrix} 0 & 0 & \dots & 0 & 0 \\ 1 & 0 & \dots & 0 & 0 \\ 0 & 1 & \dots & 0 & 0 \\ \dots & \dots & \dots & \dots & \dots \\ 0 & 0 & \dots & 1 & 0 \end{pmatrix}, \quad b = \begin{pmatrix} 1 \\ 0 \\ 0 \\ \dots \\ 0 \end{pmatrix}. \quad (5)$$

The trajectory $x(t)$ for the system (4) is given by the equation

$$x(t) = e^{At} \left(x_0 + \int_0^t e^{-A\tau} bu(\tau) d\tau \right). \quad (6)$$

hence for $x_T = x(\Theta)$ we have that that

$$\int_0^\Theta e^{-At} bu(t) dt = e^{-A\Theta} x_T - x_0, \quad (7)$$

where

$$e^{-At} = \begin{pmatrix} 1 & 0 & \dots & 0 \\ -t & 1 & \dots & 0 \\ \frac{t^2}{2} & -t & \dots & 0 \\ \dots & \dots & \dots & \dots \\ \frac{(-t)^{n-1}}{(n-1)!} & \frac{(-t)^{n-2}}{(n-2)!} & \dots & 1 \end{pmatrix}. \quad (8)$$

From the equation (7) we obtain the Markov power moment problem:

$$\int_0^\Theta t^{k-1} u(t) dt = s_k, \quad k = \overline{1, n}, \quad (9)$$

where

$$s_k = (-1)^k (k-1)! \left(x_{0,k} + \sum_{j=1}^k \frac{(-1)^j \Theta^{j-1} x_{T,k-j+1}}{(j-1)!} \right), \quad k = \overline{1, n}. \quad (10)$$

The equation (9) is called the Markov power moment problem. The aim of the moment min-problem of V. I. Korobov and G. M. Sklyar is to find the minimum possible interval $[0, \Theta]$ and the respective solution $u(t)$ such that there exists a solution to the problem (9).

From the Pontryagin Maximum Principle [2] we know that the optimal control $u(t)$ is a piecewise function with $u = \pm 1$ and no more than $n - 1$ points T_1, T_2, \dots, T_{n-1} of the discontinuity. The sign of $u(t)$ on the last time interval is unknown and has to be determined, By integrating the equation (9) we have,

$$\begin{cases} (-1)^n T_1 + (-1)^{n-1} T_2 + (-1)^{n-2} T_3 + \dots + T_{n-1} = c_1^\pm(\Theta, s), \\ (-1)^n T_1^2 + (-1)^{n-1} T_2^2 + (-1)^{n-2} T_3^2 + \dots + T_{n-1}^2 = c_2^\pm(\Theta, s), \\ \dots \\ (-1)^n T_1^n + (-1)^{n-1} T_2^n + (-1)^{n-2} T_3^n + \dots + T_{n-1}^n = c_n^\pm(\Theta, s), \end{cases} \quad (11)$$

where $c_k^\pm = \frac{1}{2}(\Theta^k \mp k s_k)$ and the upper index of c_k means the sign of $u(t)$ on the last time interval. The main idea proposed by V. I. Korobov and G. M. Sklyar, which allowed to solve this system, is the following:

We add the infinite amount of the equations to the system (11) and obtain the system:

$$\begin{cases} (-1)^n T_1 + (-1)^{n-1} T_2 + (-1)^{n-2} T_3 + \dots + T_{n-1} = c_1^\pm(\Theta, s), \\ (-1)^n T_1^2 + (-1)^{n-1} T_2^2 + (-1)^{n-2} T_3^2 + \dots + T_{n-1}^2 = c_2^\pm(\Theta, s), \\ \dots \\ (-1)^n T_1^n + (-1)^{n-1} T_2^n + (-1)^{n-2} T_3^n + \dots + T_{n-1}^n = c_n^\pm(\Theta, s), \\ (-1)^{n+1} T_1^{n+1} + (-1)^n T_2^{n+1} + (-1)^{n-1} T_3^{n+1} + \dots + T_{n-1}^{n+1} = c_{n+1}^\pm(\Theta, s), \\ \dots \end{cases} \quad (12)$$

Now we divide the $k - th$ equation by $k z^k$, and sum the equations on the left and on the right side of the system (12). We obtain the following equality:

$$\ln R(z) = - \sum_{k=1}^{\infty} \frac{c_k^\pm(\Theta, s)}{k z^k}, \quad (13)$$

where, if $n = 2m + 1$ then

$$R(z) = \frac{\prod_{j=1}^m \left(1 - \frac{T_{2j}}{z}\right)}{\prod_{j=1}^m \left(1 - \frac{T_{2j-1}}{z}\right)} = \frac{z^m + a_1 z^{m-1} + \dots + a_m}{z^m + b_1 z^{m-1} + \dots + b_m}, \quad (14)$$

.And if $n = 2m$ then

$$R(z) = \frac{\prod_{j=1}^m \left(1 - \frac{T_{2j-1}}{z}\right)}{\prod_{j=1}^m \left(1 - \frac{T_{2j}}{z}\right)} = \frac{z^m + a_1 z^{m-1} + \dots + a_m}{z(z^{m-1} + b_1 z^{m-2} + \dots + b_{m-1})}, \quad (15)$$

For the equation (14) the roots of the numerator represent are even switching points, and the roots of the denominator are the odd switching points. And for

the equation (15) roots of the numerator represent the odd switching points, and the roots of the denominator are the even switching points.

Now we write $R(z)$ as a series

$$R(z) = 1 - \sum_{k=1}^{\infty} \frac{\gamma_k}{z^k}, \quad (16)$$

and get the equation

$$\ln \left(1 - \sum_{k=1}^{\infty} \frac{\gamma_k}{z^k} \right) = - \sum_{k=1}^{\infty} \frac{c_k^{\pm}(\Theta, s)}{k z^k}. \quad (17)$$

The equations for γ_k can be written explicitly. By differentiating (17) by $\frac{1}{z}$ and comparing terms for same degrees of $\frac{1}{z}$ we get the equations:

$$\gamma_k^{\pm}(\Theta, s) = \frac{(-1)^k}{k!} \begin{vmatrix} c_1^{\pm} & 1 & 0 & \dots & 0 \\ c_2^{\pm} & c_1^{\pm} & 2 & \dots & 0 \\ \dots & \dots & \dots & \dots & \dots \\ c_{k-1}^{\pm} & c_{k-2}^{\pm} & c_{k-3}^{\pm} & \dots & k-1 \\ c_k^{\pm} & c_{k-1}^{\pm} & c_{k-2}^{\pm} & \dots & c_1^{\pm} \end{vmatrix}. \quad (18)$$

Now we have two sets of coefficients γ_i^+ and γ_i^- , corresponding to the positive and negative sign of the control of $u(t)$ on the last time interval. Then in the paper [6] by V. I. Korobov and G. M. Sklyar it is shown that the optimal time $\Theta = \min(\Theta^+, \Theta^-)$, where Θ^+ and Θ^- are the maximum positive roots of the equations:

$$\begin{vmatrix} \gamma_1^{\pm} & \gamma_2^{\pm} & \dots & \gamma_{m+1}^{\pm} \\ \gamma_2^{\pm} & \gamma_3^{\pm} & \dots & \gamma_{m+2}^{\pm} \\ \dots & \dots & \dots & \dots \\ \gamma_{m+1}^{\pm} & \gamma_{m+2}^{\pm} & \dots & \gamma_{2m+1}^{\pm} \end{vmatrix} = 0, \quad (19)$$

if $n = 2m + 1$ and

$$\begin{vmatrix} \gamma_2^{\pm} & \gamma_3^{\pm} & \dots & \gamma_{m+1}^{\pm} \\ \gamma_3^{\pm} & \gamma_4^{\pm} & \dots & \gamma_{m+2}^{\pm} \\ \dots & \dots & \dots & \dots \\ \gamma_{m+1}^{\pm} & \gamma_{m+2}^{\pm} & \dots & \gamma_{2m}^{\pm} \end{vmatrix} = 0, \quad (20)$$

if $n = 2m$ respectively.

If $n = 2m + 1$ then the odd and even switching points are found respectively from the equations

$$\begin{vmatrix} \gamma_1^{\pm} & \gamma_2^{\pm} & \dots & \gamma_{m+1}^{\pm} \\ \gamma_2^{\pm} & \gamma_3^{\pm} & \dots & \gamma_{m+2}^{\pm} \\ \dots & \dots & \dots & \dots \\ \gamma_m^{\pm} & \gamma_{m+1}^{\pm} & \dots & \gamma_{2m}^{\pm} \\ 1 & T & \dots & T^m \end{vmatrix} = 0; \quad \begin{vmatrix} \tilde{\gamma}_1^{\pm} & \tilde{\gamma}_2^{\pm} & \dots & \tilde{\gamma}_{m+1}^{\pm} \\ \tilde{\gamma}_2^{\pm} & \tilde{\gamma}_3^{\pm} & \dots & \tilde{\gamma}_{m+2}^{\pm} \\ \dots & \dots & \dots & \dots \\ \tilde{\gamma}_m^{\pm} & \tilde{\gamma}_{m+1}^{\pm} & \dots & \tilde{\gamma}_{2m}^{\pm} \\ 1 & T & \dots & T^m \end{vmatrix} = 0, \quad (21)$$

where

$$\tilde{\gamma}_k^\pm(\Theta, s) = \frac{(-1)^k}{k!} \begin{vmatrix} c_1^\pm & -1 & 0 & \dots & 0 \\ c_2^\pm & c_1^\pm & -2 & \dots & 0 \\ \dots & \dots & \dots & \dots & \dots \\ c_{k-1}^\pm & c_{k-2}^\pm & c_{k-3}^\pm & \dots & -(k-1) \\ c_k^\pm & c_{k-1}^\pm & c_{k-2}^\pm & \dots & c_1^\pm \end{vmatrix}, \quad (22)$$

and if $n = 2m$ then from the equations

$$\begin{vmatrix} \tilde{\gamma}_1^\pm & \tilde{\gamma}_2^\pm & \dots & \tilde{\gamma}_{m+1}^\pm \\ \tilde{\gamma}_2^\pm & \tilde{\gamma}_3^\pm & \dots & \tilde{\gamma}_{m+2}^\pm \\ \dots & \dots & \dots & \dots \\ \tilde{\gamma}_m^\pm & \tilde{\gamma}_{m+1}^\pm & \dots & \tilde{\gamma}_{2m}^\pm \\ 1 & T & \dots & T^m \end{vmatrix} = 0; \quad \begin{vmatrix} \gamma_2^\pm & \gamma_3^\pm & \dots & \gamma_{m+1}^\pm \\ \gamma_3^\pm & \gamma_4^\pm & \dots & \gamma_{m+2}^\pm \\ \dots & \dots & \dots & \dots \\ \gamma_m^\pm & \gamma_{m+1}^\pm & \dots & \gamma_{2m}^\pm \\ 1 & T & \dots & T^{m-1} \end{vmatrix} = 0. \quad (23)$$

2. Time-optimal control onto a subspace

Recall that we consider the problem (1)-(2). If the endpoint $x_T \in G$ was known, we would have the time-optimal control problem with fixed ends. Thus, as in the fixed endpoints problem the time optimal control $u(t)$ is a piecewise function with $u(t) = \pm 1$ maximum of $n-1$ points of discontinuity T_1, T_2, \dots, T_{n-1} . Let us multiply from the left both sides of the equation (6) by matrix H . Since $x_T \in G$ we obtain:

$$0 = He^{A\Theta} \left(x_0 + \int_0^\Theta e^{-At} bu(t) dt \right), \quad (24)$$

or

$$\begin{cases} \left(h_{1n} + \dots + \frac{h_{11}\Theta^{n-1}}{(n-1)!} \right) \left(x_{0n} + \int_0^\Theta u dt \right) + \dots + h_{11} \left(x_{01} + \int_0^\Theta \frac{(-t)^{n-1}}{(n-1)!} u dt \right) = 0, \\ \left(h_{2n} + \dots + \frac{h_{21}\Theta^{n-1}}{(n-1)!} \right) \left(x_{0n} + \int_0^\Theta u dt \right) + \dots + h_{21} \left(x_{01} + \int_0^\Theta \frac{(-t)^{n-1}}{(n-1)!} u dt \right) = 0, \\ \dots \\ \left(h_{kn} + \dots + \frac{h_{k1}\Theta^{n-1}}{(n-1)!} \right) \left(x_{0n} + \int_0^\Theta u dt \right) + \dots + h_{k1} \left(x_{01} + \int_0^\Theta \frac{(-t)^{n-1}}{(n-1)!} u dt \right) = 0. \end{cases}$$

This is a system of k equations for n unknown terms $\int_0^\Theta t^k u(t) dt$. Its solution comes down to the solution of moment min-problem of V. I. Korobov and G. M. Sklyar, but in this case the number of equations is less than the number of variables.

Let us parametrize $x_T \in G$ as

$$x_T = K \cdot \alpha = \begin{pmatrix} k_{11}\alpha_1 + k_{12}\alpha_2 + \dots + k_{1k}\alpha_k \\ k_{21}\alpha_1 + k_{22}\alpha_2 + \dots + k_{2k}\alpha_k \\ \dots \\ k_{n1}\alpha_1 + k_{n2}\alpha_2 + \dots + k_{nk}\alpha_k \end{pmatrix}, \quad (25)$$

where $K \in \mathbb{R}^{n \times k}$ is a known matrix, and $\alpha \in \mathbb{R}^k$ is a vector of parameters. If G is a hyperplane and is not a coordinate plane then equation (25) can be simplified to

$$x_T = \begin{pmatrix} \alpha_1 \\ \alpha_2 \\ \dots \\ \alpha_{n-1} \\ k_1\alpha_1 + k_2\alpha_2 + \dots + k_{n-1}\alpha_{n-1} \end{pmatrix}, \quad (26)$$

and we get the moment min-problem:

$$\begin{cases} \int_0^\Theta t^{k-1} u(t) dt = (-1)^k (k-1)! \left(x_{0,k} + \sum_{j=1}^k \frac{(-1)^j \Theta^{j-1} \alpha_{k-j+1}}{(j-1)!} \right), & k = \overline{1, n-1}, \\ \int_0^\Theta t^{n-1} u(t) dt = (-1)^n (n-1)! \left(x_{0,n} + \sum_{j=1}^{n-1} \left(-k_j \alpha_j + \frac{(-1)^j \Theta^{j-1} \alpha_{n-j+1}}{(j-1)!} \right) \right), \end{cases} \quad (27)$$

Then, as in the original problem we have the system:

$$\begin{cases} (-1)^n T_1 + (-1)^{n-1} T_2 + (-1)^{n-2} T_3 + \dots + T_{n-1} = c_1^\pm(\Theta, \alpha_1, s), \\ (-1)^n T_1^2 + (-1)^{n-1} T_2^2 + (-1)^{n-2} T_3^2 + \dots + T_{n-1}^2 = c_2^\pm(\Theta, \alpha_1, \alpha_2, s), \\ \dots \\ (-1)^n T_1^n + (-1)^{n-1} T_2^n + (-1)^{n-2} T_3^n + \dots + T_{n-1}^n = c_n^\pm(\Theta, s, \alpha_1, \dots, \alpha_{n-1}), \end{cases} \quad (28)$$

The idea of this paper is to obtain the equation

$$F(\Theta, \alpha_1, \alpha_2, \dots, \alpha_{n-1}) = 0. \quad (29)$$

for the time Θ from the system (28) as a function of variables $\alpha_1, \alpha_2, \dots, \alpha_{n-1}$. This can be done using the solution of V. I. Korobov and G. M. Sklyar for the moment min-problem. Because we have the time-optimization problem, the necessary optimality conditions must hold:

$$\frac{\partial F}{\partial \alpha_k} = 0, \quad k = \overline{1, n-1}. \quad (30)$$

These conditions, together with the equation (29) obtain n equations for determining Θ . The solution for this system of equations may be not unique, and we must consider all the solutions. Then for each solution we determine the switching points T_1, \dots, T_{n-1} . If some of the switching points are negative this means that the solution is not valid. It also should be noted that the optimal number of switching points may be less than $n-1$ and these cases must be considered separately.

Now we consider the cases of two-dimensional and three-dimensional systems and show that for some subspaces the optimal control has less than $n-1$ points of discontinuity for any initial point x_0 .

3. Two and three dimensional cases

Let us consider the 2-dimensional case

$$\begin{cases} \dot{x}_1 = u, \\ \dot{x}_2 = x_1, \end{cases} \quad |u| \leq 1, \quad x_\Theta = \begin{pmatrix} \alpha \\ k\alpha \end{pmatrix}, \quad k \in \mathbb{R}, \quad (31)$$

Let $u = -1$ on the first interval. We consider the sign on the first interval, and not on the last, as in the original problem, because we don't know the number of switching points in advance. The equation (11) has the form:

$$\begin{cases} 2T_1 - \Theta = x_{0,1} - \alpha, \\ 2T_1^2 - \Theta^2 = -2(x_{0,2} - k\alpha + \alpha\Theta), \end{cases} \quad (32)$$

here

$$c_1 = \frac{1}{2}(x_{0,1} - \alpha + \Theta); \quad c_2 = \frac{1}{2}(-2x_{0,2} + 2k\alpha - 2\alpha\Theta + \Theta^2), \quad (33)$$

and

$$\begin{aligned} \gamma_1 &= \frac{1}{2}(x_{0,1} - \alpha + \Theta), \\ \gamma_2 &= \frac{1}{2} \left(-\frac{x_{0,1}^2}{4} - x_{0,2} + k\alpha + \frac{x_{0,1}\alpha}{2} - \frac{\alpha^2}{4} - \frac{x_{0,1}\Theta}{2} - \frac{\alpha\Theta}{2} + \frac{\Theta^2}{4} \right). \end{aligned} \quad (34)$$

Then the equations for Θ , T_1 , and condition $\frac{\partial F}{\partial \alpha} = 0$ have the form:

$$\begin{cases} -\frac{x_{0,1}^2}{4} - x_{0,2} + k\alpha + \frac{x_{0,1}\alpha}{2} - \frac{\alpha^2}{4} - \frac{x_{0,1}\Theta}{2} - \frac{\alpha\Theta}{2} + \frac{\Theta^2}{4} = 0, \\ -T_1 + \frac{x_{0,1}}{2} - \frac{\alpha}{2} + \frac{\Theta}{2} = 0, \\ k + \frac{x_{0,1}}{2} - \frac{\alpha}{2} - \frac{\Theta}{2} = 0. \end{cases} \quad (35)$$

From last two equations we get that.

$$T_1 = \Theta - k, \alpha = 2k + x_{0,1} - \Theta. \quad (36)$$

This means that if $k > 0$, that is the line has a positive slope, the control has one switching point $T = \Theta - k$, and if $k \leq 0$ then there will no switching points, since $T > \Theta$ is inadmissible, and we have to set $T_1 = \Theta$. The same holds for $u = 1$ on the first interval, and the optimal time Θ :

$$\Theta = \max(k + x_{0,1} + \sqrt{-k^2 + x_{0,1}^2 + 2x_{0,2}}, k - x_{0,1} + \sqrt{-k^2 + x_{0,1}^2 - 2x_{0,2}}) \quad (37)$$

for one switching point, or

$$\Theta = \max(k + x_{0,1} + \sqrt{k^2 + x_{0,1}^2 + 2x_{0,2}}, k - x_{0,1} + \sqrt{k^2 + x_{0,1}^2 - 2x_{0,2}}) \quad (38)$$

for no switching points. The phase trajectories for lines $x_1 = x_2$ and $x_1 = -x_2$ are shown on the pictures 1 and 2 respectively.

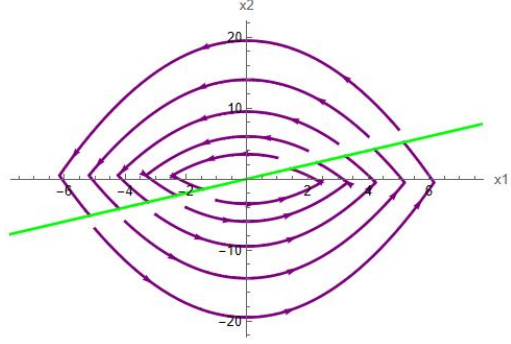


Fig. 1. Trajectories for $G : x_1 = x_2$
Рис. 1. Траєкторії для $G : x_1 = x_2$

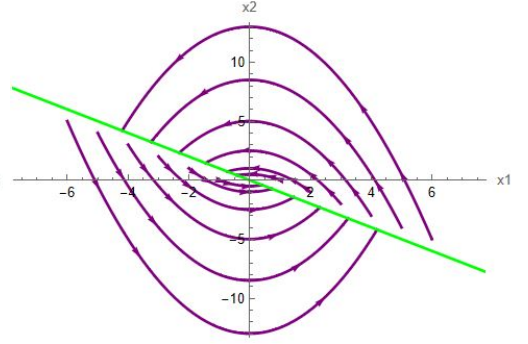


Fig. 2. Trajectories for $G : x_1 = -x_2$
Рис. 2. Траєкторії для $G : x_1 = -x_2$

If $k = \pm\infty$ then $G = \{x : x_1 = 0\}$ and the problem is equivalent to $\dot{x}_1 = u$. It has the solution $u \equiv 1$ if $x_{0,1} < 0$ and $u \equiv -1$ if $x_{0,1} > 0$, without switching points.

Let us now consider the case with $n = 3$:

$$\begin{cases} \dot{x}_1 = u, \\ \dot{x}_2 = x_1, \\ \dot{x}_3 = x_2, \end{cases} \quad |u| \leq 1, \quad x_\Theta = \begin{pmatrix} \alpha_1 \\ \alpha_2 \\ k_1\alpha_1 + k_2\alpha_2 \end{pmatrix}, \quad k_1, k_2 \in \mathbb{R}. \quad (39)$$

We want to determine how many switching points does the optimal trajectory $u(t)$ have depending on the values of k_1 and k_2 and obtain the equations for Θ . Let $u = -1$ on the first interval. Then the equation 11 has the form:

$$\begin{cases} 2T_1 - 2T_2 + \Theta = x_{0,1} - \alpha_1, \\ 2T_1^2 - 2T_2^2 + \Theta^2 = -2(x_{0,2} - \alpha_2 + \alpha_1\Theta), \\ 2T_1^3 - 2T_2^3 + \Theta^3 = 6\left(x_{0,3} - k_1\alpha_1 - k_2\alpha_2 + \alpha_2\Theta - \frac{\alpha_1\Theta^2}{2}\right). \end{cases} \quad (40)$$

From the first two equations we obtain

$$\begin{aligned} T_1 &= \frac{x_{0,1}^2 - 4x_{0,2} - 2x_{0,1}\alpha_1 + \alpha_1^2 + 4\alpha_2 - 2x_{0,1}\Theta - 2\alpha_1\Theta - \Theta^2}{4(x_{0,1} - \alpha_1 - \Theta)}, \\ T_2 &= \frac{-x_{0,1}^2 - 4x_{0,2} + 2x_{0,1}\alpha_1 - \alpha_1^2 + 4\alpha_2 + 2x_{0,1}\Theta - 6\alpha_1\Theta - 3\Theta^2}{4(x_{0,1} - \alpha_1 - \Theta)}, \end{aligned} \quad (41)$$

and by substituting in the third equation we get

$$\begin{aligned} F &= x_{0,3} - k_1\alpha_1 - k_2\alpha_2 + \alpha_2\Theta - \frac{\alpha_1\Theta^2}{2} - \left(32(x_{0,1} - \alpha_1 - \Theta)^3\Theta^3 + \right. \\ &\quad \left. + (x_{0,1}^2 - 4x_{0,2} + \alpha_1^2 + 4\alpha_2 - 2\alpha_1\Theta - \Theta^2 - 2x_{0,1}(\alpha_1 + \Theta))^3 + \right. \\ &\quad \left. + \frac{(x_{0,1}^2 - 4x_{0,2} + \alpha_1^2 + 4\alpha_2 - 2\alpha_1\Theta - \Theta^2 - 2x_{0,1}(\alpha_1 + \Theta))^3}{192(x_{0,1} - \alpha_1 - \Theta)^3} \right) = 0. \end{aligned} \quad (42)$$

After solving $\frac{\partial F}{\partial \alpha_1} = 0$, $\frac{\partial F}{\partial \alpha_2} = 0$ for α_1, α_2 and substituting them into equation (41) we get

$$T_1 = -k_2 - \sqrt{2k_1 + k_2^2} + \Theta, \quad T_2 = -k_2 + \sqrt{2k_1 + k_2^2} + \Theta. \quad (43)$$

To show that this is a minimum point we calculate the second derivatives and check the sufficient condition:

$$\frac{\partial^2 F}{\partial \alpha_1^2} \frac{\partial^2 F}{\partial \alpha_2^2} - \frac{\partial^2 F}{\partial \alpha_1 \partial \alpha_2} = \frac{1}{16} > 0 \implies \text{local minimum.} \quad (44)$$

This means that for the plane $x_3 = k_1 x_1 + k_2 x_2$ if both $-k_2 - \sqrt{2k_1 + k_2^2} < 0$ and $-k_2 + \sqrt{2k_1 + k_2^2} < 0$, that is $k_1 < 0$ and $k_2 > \sqrt{-2k_1}$ trajectory can have 2 switching points, if $-k_2 - \sqrt{2k_1 + k_2^2} < 0$ and $-k_2 + \sqrt{2k_1 + k_2^2} > 0$, that is $k_1 > 0$ trajectory can have 1 switching point, and in other cases trajectory has no switching points. Same results hold for $u = 1$ on the first interval.

The picture 3 shows the phase trajectories for the plane $x_3 = -4x_1 + 3x_2$. Here $T_1 = \Theta - 4$, $T_2 = \Theta - 2$. The equations for Θ are

$$8 \mp 24x_{0,1} \pm 18x_{0,2} \mp 6x_{0,3} + (24 \pm 8x_{0,1} \mp 6x_{0,2})\Theta + (-9 - 3x_{0,1})\Theta^2 + \Theta^3 = 0, \quad (45)$$

for 2 switching points, where the upper sign is for the trajectory with $u = -1$ on the first interval,

$$-40 \mp 24x_{0,1} \pm 18x_{0,2} \mp 6x_{0,3} + (24 \pm 8x_{0,1} \mp 6x_{0,2})\Theta + (-9 - 3x_{0,1})\Theta^2 + \Theta^3 = 0, \quad (46)$$

for 1 switching point, and

$$\mp 24x_{0,1} \pm 18x_{0,2} \mp 6x_{0,3} + (24 \pm 8x_{0,1} \mp 6x_{0,2})\Theta + (-9 - 3x_{0,1})\Theta^2 + \Theta^3 = 0, \quad (47)$$

for no switching points.

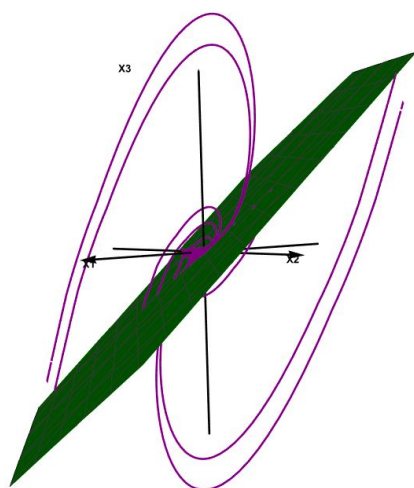


Fig. 3. Phase trajectories for $G : x_3 = -4x_1 + 3x_2$
Рис. 3. Фазові траєкторії для $G : x_3 = -4x_1 + 3x_2$

The picture 4 shows the second case, $x_3 = 4x_1 + x_2$, when the trajectory can have maximum 1 switching point. We have $T_1 = \Theta - 4$ and the equations for Θ :

$$160 \pm 24x_{0,1} \pm 6x_{0,2} \mp 6x_{0,3} + (-24 \pm 8x_{0,1} \mp 6x_{0,2})\Theta + (-3 - 3x_{0,1})\Theta^2 + \Theta^3 = 0, \quad (48)$$

for 1 switching point, and

$$\pm 24x_{0,1} \pm 6x_{0,2} \mp 6x_{0,3} + (-24 \pm 8x_{0,1} \mp 6x_{0,2})\Theta + (-3 - 3x_{0,1})\Theta^2 + \Theta^3 = 0, \quad (49)$$

for no switching points.

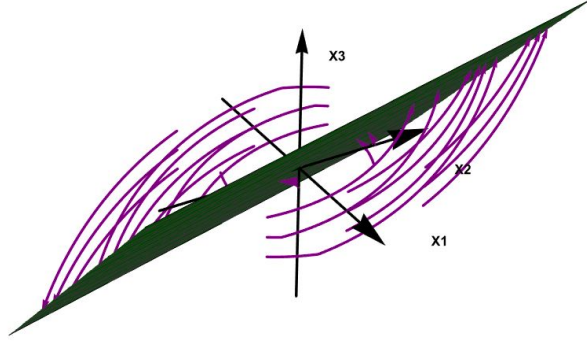


Рис. 4. Фазові траєкторії для $G : x_3 = 4x_1 + x_2$

Рис. 4. Фазові траєкторії для $G : x_3 = 4x_1 + x_2$

And for the plane $x_3 = -4x_1 - 3x_2$, (Figure 5) we have no switching points and

$$\mp 24x_{0,1} \mp 18x_{0,2} \mp 6x_{0,3} + (24 \mp 18x_{0,1} \mp 6x_{0,2})\Theta + (9 - 3x_{0,1})\Theta^2 + \Theta^3 = 0. \quad (50)$$

The equations for the switching surfaces can be found by considering the cases when equations for different number of switching points give the same time Θ .

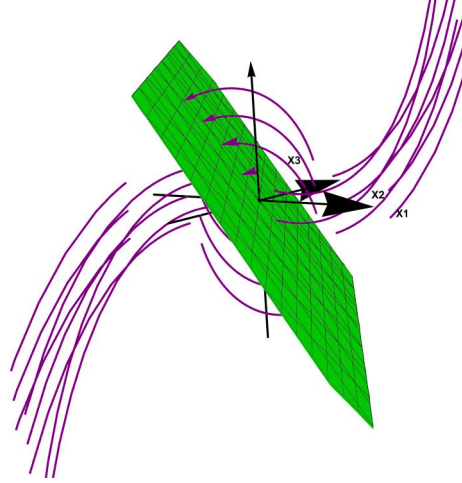


Рис. 5. Фазові траєкторії для $G : x_3 = -4x_1 - 3x_2$

Рис. 5. Фазові траєкторії для $G : x_3 = -4x_1 - 3x_2$

REFERENCES

1. R. V. Gamkrelidze, Theory of processes in linear systems which are optimal with respect to rapidity of action, *Izv. Akad. Nauk SSSR, Ser. Mat.* – 1958. – **22**. – P. 449–474.
2. L. S. Pontryagin, V. G. Boltyanskii, R. V. Gamkrelidze, E. F. Mishechenko. The Mathematical Theory of Optimal Processes. VIII + 360 S. New York/London 1962. John Wiley & Sons. Preis 90/-. 10.1002/zamm.19630431023
3. V. G. Boltyanskiy. A linear optimal control problem. *Differ Uravn.* – 1969. – **5**. – P. 783–799.
4. V. Jankovic. The linear optimal control problem with variable endpoints. *Publications de l'Institut Mathematique. Nouvelle Serie.* – 1989. – **45**(59). – P. 133–142. <http://eudml.org/doc/257819>.
5. V. I. Korobov. A general approach to the solution of the bounded control synthesis problem in a controllability problem, *Math. USSR Sb.* – 1980. – **37**, No. 4. – P. 535–557. 10.1070/SM1980v037n04ABEH002094
6. V. I. Korobov, G. M. Sklyar. Time optimality and the power moment problem. *Mat. Sb., Nov. Ser.* – 1987. – **134**(176), no. 2(10). – P. 186–206; *Math. USSR, Sb.* – 1989. – **62**, No. 1. – P. 185–206. 10.1070/SM1989v062n01ABEH003235
7. V.I. Korobov. Time Optimality for Systems with Multidimensional Control and Vector Moment Min-Problem. *J Dyn Control Syst.* – 2020. – **26**. – P. 525–550. 10.1007/s10883-019-09465-2
8. V. I. Korobov, A.V. Lucenko, E. N. Podolskij. Stabilization of a linear autonomous system with respect to a subspace. 1, *Vestnik of Kharkiv State University, Ser. Applied Mathematics and Mechanics.* – 1976. – **134**. – P. 114–123, (in Russian).
9. V. I. Korobov, A.V. Lucenko. Controllability of a linear stationary system on a subspace for an unfixed time, *Ukrainian Mathematical Journal.* – 1977. – **29**, No. 4. – P. 531–534.
10. V. I. Korobov. Controllability criterion for a linear system on a subspace, *Vestnik of Kharkiv State University, Ser. Applied Mathematics and Mechanics.* – 1981. – **221**. – P. 3–11, (in Russian).

Article history: Received: 5 October 2024; Final form: 11 December 2024

Accepted: 20 December 2024.

How to cite this article:

V. I. Korobov, O. S. Vozniak, Time-optimal control on a subspace for the two and three-dimensional system, Visnyk of V. N. Karazin Kharkiv National University. Ser. Mathematics, Applied Mathematics and Mechanics, Vol. 100, 2024, p. 48–60. DOI: 10.26565/2221-5646-2024-100-03

**Оптимальне за часом керування на підпростір
для двовимірної та тривимірної системи**

В. І. Коробов, О. С. Возняк

*Харківський національний університет імені В. Н. Каразіна
майдан Свободи 4, м. Харків, 61022, Україна*

Дана стаття присвячена задачі швидкодії на підпростір для лінійної керованої системи $\dot{x}_1 = u, \dot{x}_i = x_{i-1}, i = 2, \overline{n}$ з $|u| \leq 1$ для випадку $n = 2$ та $n = 3$. Вона пов'язана із задачею оптимального за часом керування в точку, розв'язання якої було вперше представлено В. І. Коробовим та Г. М. Скляром і яке ґрунтується на міні-проблемі моментів. Ключовою відмінністю задачі, що розглядається в даній роботі, від вихідної задачі є те, що кількість невідомих функцій перевищує кількість змінних, що вимагає використання інших методів параметричної оптимізації.

Як і в задачі оптимального за часом керування в точку, ми шукаємо оптимальний розв'язок у вигляді кусково-сталої функції $u = \pm 1$ з $n - 1$ точками перемикання, який є оптимальним згідно з Принципом Максимуму Понтрягіна. У цій статті ми розглядаємо загальний підхід для розв'язання задачі оптимального за часом керування в точку, та розв'язуємо задачу у явному вигляді для двовимірної та тривимірної системи. У нашій роботі наведено розв'язок задачі оптимального керування для двовимірної системи на підпростір $G : \{(x_1, x_2) : x_2 = kx_1\}$ для всіх значень k з використанням міні-проблеми моментів та методів оптимізації функцій. В роботі показано, що для деяких значень параметра k система може взагалі не мати точок перемикання. Для тривимірної системи ми розв'язуємо задачу оптимального керування на площину $x_3 = k_1x_1 + k_2x_2$ і отримуємо кількість точок перемикання залежно від значень k_1 і k_2 а також будуємо траєкторії та отримуємо рівняння для оптимального часу Θ для різних випадків. Подібно до розв'язку задачі оптимального за часом керування в точку, отриманого за допомогою міні-проблеми моментів В. І. Коробовим та Г. М. Скляром, оптимальне керування може мати $n - 1$ або менше точок перемикання.


Ключові слова: керованість; міні-проблема моментів; оптимальне за часом керування; задача з рухомими кінцями

Історія статті: отримана: 5 жовтня 2024; останній варіант: 11 грудня 2024
прийнята: 20 грудня 2024.

A. E. Choque-Rivero

PhD math, Prof.


Instituto de Física y Matemáticas, Universidad Michoacana de San Nicolás de Hidalgo
Edificio C-3, C.U., CP 58060, Morelia, Michoacán, México

abdon.choque@umich.mx  <http://orcid.org/0000-0003-0226-9612>

T. Vukašinac

PhD phys, Prof.

Facultad de Ingeniería Civil, Universidad Michoacana de San Nicolás de Hidalgo
Edificio A, C.U., CP 58060, Morelia, Michoacán, México

tatjana.vukasinac@umich.mx  <http://orcid.org/0000-0002-0810-1960>

Korobov's controllability function method via orthogonal polynomials on $[0, \infty)$

Given a controllable system described by ordinary or partial differential equations and an initial state, the problem of finding a set of bounded positional controls that transfer the initial state to another state, not necessarily an equilibrium point, in finite time is called the synthesis problem.

In the present work, we consider a family of Brunovsky systems of dimension n . A family of bounded positional controls $u_n(x)$ is constructed in order to stabilize a given Brunovsky system in finite time. We employ orthogonal polynomials associated with a function distribution $\sigma(\tau, \theta)$ defined for $\tau \in [0, +\infty)$ and parameter $\theta > 0$. The parameter θ is interpreted as a Korobov's controllability function, $\theta = \theta(x)$, which serves as a Lyapunov-type function. Utilizing $\theta(x)$, we construct the positional control $u_n(x) = u_n(x, \theta(x))$.

Our analysis is based on the foundational work "A general approach to the solution of the bounded control synthesis problem in a controllability problem". *Matematicheskii Sbornik*, 151(4), 582–606 (1979) by Korobov, V. I, in which the controllability function method was proposed. This method has been applied to solve bounded finite-time stabilization problems in various control scenarios, such as the control of the wave equation, optimal control with mixed cost functions, and other applications.

For the construction of the mentioned positional controls, we employ a member of a family of orthogonal polynomials on $[0, \infty)$. For more details on orthogonal polynomials, we refer to the book "Orthogonal Polynomials". American Mathematical Society, Providence, (1975) by G. Szegő. We also rely on the work "On matrix Hurwitz type polynomials and their interrelations to Stieltjes positive definite sequences and orthogonal matrix polynomials". *Linear Algebra and its Applications*, 476, 56–84 (2015) by Choque Rivero, A. E.

The results in the present work extend and develop the findings presented in the conference paper “Bounded finite-time stabilizing controls via orthogonal polynomials”. 2018 IEEE International Autumn Meeting on Power, Electronics and Computing (ROPEC), Ixtapa, Mexico. –2018 by Choque-Rivero A. E., Orozco B. d. J. G.

Keywords: Bounded control; orthogonal polynomials; finite-time stabilization; controllability function; canonical system.

2020 Mathematics Subject Classification: 93D15; 34D20; 34H05; 33C45.

1. Introduction

We focus on the Brunovsky system, also referred to as the chain integrator or canonical linear system. It is commonly used in control theory to analyze the controllability and feedback stabilizability of both linear and nonlinear systems—after applying an appropriate transformation for the latter; see [1], [2]. The statement of the bounded finite time stabilization problem is the following: Consider the system

$$\begin{cases} \dot{x}_1 = u_n, & |u_n| \leq 1, \\ \dot{x}_k = x_{k-1}, & 2 \leq k \leq n. \end{cases} \quad (1)$$

Let $x := \text{column}(x_1, x_2, \dots, x_n)$. Given an initial position $x_0 \in \mathbb{R}^n$, find a family of positional bounded controls $u_n = u_n(x)$ such that the trajectory $x(t, x_0)$ of system (1) with $u_n = u_n(x)$ and

$$|u_n(x)| \leq 1 \quad (2)$$

reaches the origin at finite time $T = T(x_0)$, i.e.,

$$\lim_{t \rightarrow T(x_0)} x(t, x_0) = 0. \quad (3)$$

Additionally, an estimation of motion time $T(x_0)$ should be found. This problem is also called the synthesis problem.

For our convenience, we reformulate system (1) in a matrix form. To that end, we introduce a following notation. Let p, q and n be natural numbers. Denote by \mathbf{I}_p the $p \times p$ identity matrix and by $0_{p \times q}$ the $p \times q$ zero matrix. System (1) is equivalent to the following equation:

$$\dot{x} = \mathbf{A}_n x + b_n u_n, \quad (4)$$

where

$$\mathbf{A}_n = \begin{pmatrix} 0_{1 \times (n-1)} & 0 \\ \mathbf{I}_{n-1} & 0_{(n-1) \times 1} \end{pmatrix}, \quad b_n := \begin{pmatrix} 1 \\ 0_{(n-1) \times 1} \end{pmatrix}.$$

Our approach involves constructing the positional control $u = u_n(x)$ based on two key components. The first component is the set of orthogonal polynomials

$p_n(\tau, \theta)$ on $[0, +\infty)$ with respect to τ , depending on the parameter $\theta > 0$. The case of orthogonal polynomials $p_n(\tau, 1)$ has been studied in [3] and [4].

The second component is the controllability function (CF) $\theta(x)$ method, which serves as a Lyapunov-type function but with two key distinctions. First, the CF ensures finite-time stabilization of the controllable system (4). Second, the CF can also be applied to nonequilibrium points of linear systems (see [5]).

It is worth noting that another connection between orthogonal polynomials and bounded controls, aimed at solving the admissible control problem, was explored in [6].

The present work continues the analysis performed in [7] and provides the following improvements and clarifications:

- We clarify the definition of the polynomials $p_{r,j}$ as given in (13) and (14).
- We improve the proof of Lemma 2 and provide the proof of Theorem 3.
- In Example 2, we present a more detailed explanation.
- We add Remark 4, which explains the controllability function as the time of motion.
- We include Proposition 2, where we prove that it is not possible to construct a positional control such that the corresponding controllability function represents the time of motion of the system's trajectory.

Finally, in the conclusion, we have proposed an open question regarding the possibility of constructing positional controls using a combination of orthogonal polynomials, such that the corresponding controllability function represents the time of motion.

Orthogonal polynomials on $[0, +\infty)$ with parameter θ

Let $\mathbb{N}_0 = \mathbb{N} \cup \{0\}$ and let $\sigma(\tau, \theta)$ be a bounded nondecreasing function with respect to τ on $[0, +\infty)$ with parameter $\theta > 0$ such that all moments

$$s_j(\theta) := \int_0^\infty \tau^j d\sigma(\tau, \theta), \quad j \in \mathbb{N}_0 \quad (5)$$

are finite. In the present work, we will restrict ourselves to the case when

$$s_k(\theta) = \frac{c_k}{\theta^k}, \quad k \in \mathbb{N}_0 \quad (6)$$

where c_k is a real number, and θ is a positive parameter. For simplicity, we will typically omit the dependence on θ .

Define the Hankel matrices:

$$\mathbf{H}_{1,j} := \begin{pmatrix} s_0 & s_1 & \dots & s_j \\ s_1 & s_2 & \dots & s_{j+1} \\ \vdots & \vdots & \vdots & \vdots \\ s_j & s_{j+1} & \dots & s_{2j} \end{pmatrix}, \quad (7)$$

$$\mathbf{H}_{2,j} := \begin{pmatrix} s_1 & s_2 & \dots & s_{j+1} \\ s_2 & s_3 & \dots & s_{j+2} \\ \vdots & \vdots & \ddots & \vdots \\ s_{j+1} & s_{j+2} & \dots & s_{2j+1} \end{pmatrix}. \quad (8)$$

Definition 1. The sequence $(s_j(\theta))_{j=0}^{2n}$ (resp. $(s_j(\theta))_{j=0}^{2n-1}$) is called a Stieltjes positive definite sequence if $\mathbf{H}_{1,n}$ and $\mathbf{H}_{2,n-1}$ (resp. $\mathbf{H}_{1,n-1}$ and $\mathbf{H}_{2,n-1}$) are positive definite matrices.

In what follows, we consider only Stieltjes positive definite sequences. Additionally, we introduce some auxiliary matrices:

$$Y_{1,j} := \text{column}(s_j, s_{j+1}, \dots, s_{2j-1}), \quad (9)$$

and

$$Y_{2,j} := \text{column}(s_{j+1}, s_{j+2}, \dots, s_{2j}). \quad (10)$$

Let τ be an arbitrary real number. We define

$$E_j(\tau) := \text{column}(1, \tau, \dots, \tau^j). \quad (11)$$

We define (as in [8, Remark E.5]) the polynomials $p_{r,j}$ for $r = 1, 2$ and $1 \leq j \leq n$ as follows

$$p_{r,0}(\tau, \theta) := 1, \quad (12)$$

$$p_{1,j}(\tau, \theta) := (-Y_{1,j}^\top \mathbf{H}_{1,j-1}^{-1}, 1) E_j(\tau), \quad (13)$$

$$p_{2,j}(\tau, \theta) := (-Y_{2,j}^\top \mathbf{H}_{2,j-1}^{-1}, 1) E_j(\tau). \quad (14)$$

Let us recall the definition of a finite family of orthogonal polynomials depending on the parameter θ . Here $Y_{r,j} = Y_{r,j}(\theta)$ and $\mathbf{H}_{r,j} = \mathbf{H}_{r,j}(\theta)$ for $r = 1, 2$.

Definition 2. Let there be given a sequence of polynomials $(p_j(\tau, \theta))_{j=0}^\infty$ defined on $[0, +\infty)$ with respect to τ with parameter $\theta > 0$

$$p_j(\tau, \theta) = \tau^n + \frac{\tilde{a}_1}{\theta} \tau^{n-1} + \frac{\tilde{a}_2}{\theta^2} \tau^{n-2} + \dots + \frac{\tilde{a}_{j-1}}{\theta^{j-1}} \tau + \frac{\tilde{a}_j}{\theta^j}. \quad (15)$$

If there exists a bounded nondecreasing distribution $\sigma(\tau, \theta)$ with respect to τ on $[0, +\infty)$ with parameter $\theta > 0$ such that the sequence of monic polynomials $(p_j(\tau, \theta))_{j=0}^\infty$ satisfies the relation

$$\int_0^\infty p_j(\tau, \theta) p_k(\tau, \theta) d\sigma(\tau, \theta) = \begin{cases} 0, & j \neq k, \\ d_j(\theta), & j = k, \end{cases} \quad d_j(\theta) > 0,$$

then this sequence is family a of orthogonal polynomials.

Remark 1. a) The orthogonality of polynomials $p_{r,j}$ for $r = 1, 2$, $j \geq 0$ with $\theta = 1$ defined by (12)-(14) was proved in [9].
 b) The family $\{p_{1,j}(\tau)\}$ (resp. $\{p_{2,j}(\tau)\}$) is orthogonal on $[0, \infty)$ with respect to a nondecreasing distribution $d\sigma(\tau)$ (resp. $\tau d\sigma(\tau)$) [10].

Orthogonal polynomials have been widely applied to practical problems, including signal processing [11] and filter design [12], [13]. Additionally, the zeros of certain families of orthogonal polynomials can be interpreted as the electrostatic energy of a system with a finite number of charges (see [14]).

Example 1. Let $d\sigma(\tau, \theta) = \tau^\alpha e^{-\tau\theta} d\tau$. For $j \geq 0$ and parameters $\theta > 0$ and $\alpha > -1$, the corresponding moments are given by $s_j(\alpha, \theta) = \frac{\int_0^\infty \tau^j \tau^\alpha e^{-\tau\theta} d\tau}{\int_0^\infty \tau^\alpha e^{-\tau\theta} d\tau}$. The polynomials (12) and (13) constructed from these moments are referred to as monic generalized-type Laguerre polynomials. For $j = 2$ and $j = 3$, we have:

$$\begin{aligned} p_{1,2}(-\tau, \theta) &= \frac{(\alpha+1)(\alpha+2)}{\theta^2} + \frac{2(\alpha+2)\tau}{\theta} + \tau^2, \\ -p_{1,3}(-\tau, \theta) &= \frac{(\alpha+1)(\alpha+2)(\alpha+3)}{\theta^3} + \frac{3(\alpha+2)(\alpha+3)\tau}{\theta^2} \\ &\quad + \frac{3(\alpha+3)\tau^2}{\theta} + \tau^3. \end{aligned} \quad (16)$$

Note that $(p_{1,j}(\tau, 1))_{j \geq 0}$ represents the classical Laguerre polynomials. By applying the Routh-Hurwitz criterion, one verifies that $p_{1,2}(-\tau, \theta)$ and $-p_{1,3}(-\tau, \theta)$ are Hurwitz polynomials.

Controllability function $\theta(x)$

The CF method, introduced by V.I. Korobov in 1979 [15], has been applied to a variety of control problems [16], [17], [18], [19], [20], [32]. In [21], the method is used to construct finite-time stabilizing positional controls for wave equations and linear systems with a mixed cost functional. In [22] and [23], a family of bounded positional controls is developed, with the CF $\theta(x)$ representing the exact time of motion for both single-variable and multivariable controls. Additionally, in [24], bounded finite-time stabilizing controls are derived for a family of nonlinear control systems.

Let us now return to the Brunovsky system (4). For the solution of the synthesis problem, the positional control [15], [21]

$$u_n(x) = \sum_{k=1}^n \frac{a_{n,k} x_k}{\theta^k(x)}, \quad (17)$$

was proposed. The positional control (17) can be written as

$$u_n(x) = \theta^{-1/2}(x) a_n^T \mathbf{D}_{\theta(x)} x \quad (18)$$

where

$$a_n := \text{column}(a_{n,1}, a_{n,2}, \dots, a_{n,n}) \quad (19)$$

and

$$\mathbf{D}_\theta := \text{diag} \left(\theta^{-\frac{2j-1}{2}} \right)_{j=1}^n. \quad (20)$$

Let a_n be such that the matrix $\mathbf{A}_n + b_n a_n^\top$ has eigenvalues with negative real part. Thus, for \mathbf{W}_n being a positive definite matrix, the Lyapunov equation

$$\mathbf{F}_n(\mathbf{A}_n + b_n a_n^\top) + (\mathbf{A}_n + b_n a_n^\top)^\top \mathbf{F}_n = -\mathbf{W}_n \quad (21)$$

has a unique solution \mathbf{F}_n , such that \mathbf{F}_n is a positive definite matrix; [25, Theorem 3.20].

The proof of the following result is given in [15, Page 542].

Proposition 1. *Let \mathbf{F}_n be a solution to (21), and let*

$$0 < a_0 \leq \frac{1}{2a_n^\top \mathbf{F}_n^{-1} a_n}. \quad (22)$$

Furthermore, let

$$\mathbf{H}_n := \text{diag} \left(-\frac{2j-1}{2} \right)_{j=1}^n, \quad (23)$$

and

$$\tilde{\mathbf{F}}_n := \mathbf{F}_n - \mathbf{H}_n \mathbf{F}_n - \mathbf{F}_n \mathbf{H}_n. \quad (24)$$

Thus, for a positive definite matrix $\tilde{\mathbf{F}}_n$, the following equation

$$2a_0\theta = x^\top \mathbf{D}_\theta \mathbf{F}_n \mathbf{D}_\theta x \quad (25)$$

has a unique positive solution $\theta = \theta(x)$.

Recall that the matrix $\tilde{\mathbf{F}}_n$ (24) appears when taking the derivative with respect to time on both the left- and right-hand sides of (25). Specifically, after taking the derivative of the left-hand side of (25) one obtains the quadratic form $\frac{1}{\theta} x^\top \mathbf{D}_\theta \tilde{\mathbf{F}}_n \mathbf{D}_\theta x \dot{\theta}$, while on the right-hand side one obtains $\frac{1}{\theta} x^\top (\mathbf{D}_\theta \mathbf{F}_n (\mathbf{A}_n + b_n a_n^\top) + (\mathbf{A}_n + b_n a_n^\top)^\top \mathbf{F}_n) \mathbf{D}_\theta x$.

The special cases when $\det \tilde{\mathbf{F}}_n = 0$ and when $\tilde{\mathbf{F}}_n$ is an indefinite matrix were studied in [26] and [27]. In both these works, it was assumed that \mathbf{F}_n is positive definite. Note that when $\det \tilde{\mathbf{F}}_n = 0$ or $\tilde{\mathbf{F}}_n$ is an indefinite matrix, Equation (25) does not have a unique, simple positive solution $\theta(x)$. In contrast, when $\tilde{\mathbf{F}}_n$ is a positive definite matrix, Equation (25) has a unique positive solution [15].

The value $\theta(x_0)$ is the root the function

$$\Psi(\theta, x_0) = 2a_0\theta - x_0^\top \mathbf{D}_\theta \mathbf{F}_n \mathbf{D}_\theta x_0. \quad (26)$$

Note that $\theta^{2n-1} \Psi(\theta, x_0)$ is a polynomial of degree $2n$ on the variable θ ; see [27, Equality (7.2)].

For the proof of the next result, see [15, Pages 545-547].

Theorem 1. *The positional control (17) transfers any initial point $x_0 \in \mathbb{R}^n$ to the origin along the trajectory of the system $\dot{x} = \mathbf{A}_n x + b_n u_n(x)$ in time*

$$T(x_0) \leq \frac{\theta(x_0)}{\beta} \quad (27)$$

and satisfies the restriction $|u_n(x)| \leq 1$. Here $-\beta$ is the largest eigenvalue of the matrix pencil $\mathbf{W}_n + \lambda \tilde{\mathbf{F}}_n$.

Note that the control $u_n(x)$ and the estimation of the time $T(x_0)$ depend on the selection of a_n and \mathbf{W}_n .

2. Positional controls through orthogonal polynomials

Relation between orthogonal polynomials and Hurwitz polynomials An explicit relation between Hurwitz polynomials and orthogonal polynomials was considered in [9], [28], [33] and [34]. The mentioned relation indicates that every Hurwitz polynomial $p_n(\tau)$ is represented by $h_n(\tau^2) + \tau g_n(\tau^2)$, where h_n and g_n are orthogonal polynomials on $[0, +\infty)$ or their second kind polynomials.

Recall that the polynomials

$$q_{1,j}(\tau) := \int_0^\infty \frac{p_{1,j}(\tau) - p_{1,j}(t)}{\tau - t} d\sigma(t), \quad (28)$$

$$q_{2,j}(\tau) := \int_0^\infty \frac{\tau p_{2,j}(\tau) - t p_{2,j}(t)}{\tau - t} d\sigma(t), \quad (29)$$

for $j \geq 0$ are called second-kind polynomials associated with the polynomials $p_{1,j}$ and $p_{2,j}$, as in (13) and (14); [8, Remark E.4] and [8, Lemma E.11]. The distribution $d\sigma(t)$ appearing in (28) and (29) is the same as the distribution mentioned in part (b) of Remark 1.

For the convenience of the reader, we reproduce Theorem 3.3.1 of [4] by G. Szegő on the locations of the zeros of orthogonal polynomials.

Theorem 2. *The zeros of the orthogonal polynomials $p_n(\tau)$, associated with the distribution $d\alpha(\tau)$ on the interval $[a, b]$, are real and distinct and are located in the interior of the interval $[a, b]$.*

Note that on page 1 of [4], it is stated that the notation $[a, b]$ is also used to denote the interval $[0, \infty)$.

In this paper, we highlight another relationship between orthogonal polynomials and Hurwitz polynomials.

Lemma 1. *Let $(s_j(\theta))_{j=0}^{2n}$ (resp. $(s_j(\theta))_{j=0}^{2n-1}$) be a Stieltjes positive sequence. Let the polynomials $p_{r,j}(\tau, \theta)$ for $r = 1, 2$, with parameter $\theta > 0$ be as in (13) and (14). Thus, the polynomials*

$$(-1)^j p_{r,j}(-\tau, \theta) \quad (30)$$

for $1 \leq j \leq n$ are Hurwitz or stable polynomials.

The proof of this lemma is based on Theorem 2, which ensures that the roots of polynomials of the form (15), such as $p_{r,n}(\tau, \theta)$ as defined in (13) and (14), belong to the interval $[0, +\infty)$ for a fixed θ . It remains to 'correct' the coefficients of $p_{r,n}(\tau, \theta)$, which, according to the necessary condition for Hurwitz polynomials, should be positive numbers. To this end, we change the independent variable τ to $-\tau$ in (13), (14) and multiply this polynomial by $(-1)^n$.

Remark 2. a) From Theorem 2 and Lemma 1, it readily follows that, for fixed $\theta > 0$, the roots of the polynomial $(-1)^n p_{r,n}(-\tau, \theta)$ belong to $(-\infty, 0]$.
b) Since the roots of $(-1)^n p_{r,n}(-\tau, \theta)$ are distinct (see Theorem 2), the set of polynomials $\{(-1)^n p_{r,n}(-\tau, \theta)\}$ is a subset of Hurwitz polynomials with real negative roots.

Remark 3. For fixed $\theta > 0$, the polynomial $f_2(t, \theta) = t^2 + \frac{2t}{\theta} + \frac{2}{\theta^2} = (t + \frac{1-i}{\theta})(t + \frac{1+i}{\theta})$ is a Hurwitz polynomial of the form (15). The roots of f_2 are complex numbers. Thus, taking into account Theorem 2 and Lemma 1, we conclude that Hurwitz polynomials with complex roots are not included in the set of polynomials defined by (30).

Bounded finite-time stabilizing controls We propose the bounded positional control $u_n(x)$ that stabilizes the system (4) based on the orthogonal polynomials (13) – (14).

Remark 4. For fixed θ , let $a_n^\top(\theta) = \theta^{-1/2} a_n^\top \mathbf{D}_\theta$. Substituting the positional control (17) in (4) for fixed θ , we have the system

$$\dot{x} = (\mathbf{A}_n + b_n a_n^\top(\theta))x. \quad (31)$$

The characteristic polynomial \tilde{p}_n of system (31) has the form

$$\begin{aligned} \tilde{p}_n(\tau, \theta) &= \det(\tau I_n - \mathbf{A}_n - b_n a_n^\top(\theta)) \\ &= \left(\tau^n - \frac{a_{n,n}}{\theta^n} \tau^{n-1} - \frac{a_{n,n-1}}{\theta^{n-1}} \tau^{n-2} - \dots - \frac{a_{n,2}}{\theta^2} \tau - \frac{a_{n,1}}{\theta} \right) \\ &= \left(1, -\left(\frac{a_{n,n}}{\theta^n}, \frac{a_{n,n-1}}{\theta^{n-1}}, \dots, \frac{a_{n,2}}{\theta^2}, \frac{a_{n,1}}{\theta} \right) \right) \begin{pmatrix} \tau^n \\ \tau^{n-1} \\ \vdots \\ \tau \\ 1 \end{pmatrix} \\ &= \tau^n - \left(\frac{a_{n,1}}{\theta}, \frac{a_{n,2}}{\theta^2}, \dots, \frac{a_{n,n-1}}{\theta^{n-1}}, \frac{a_{n,n}}{\theta^n} \right) \begin{pmatrix} 1 \\ \vdots \\ \tau^{n-2} \\ \tau^{n-1} \end{pmatrix}. \end{aligned} \quad (32)$$

The following lemma enables us to determine the control coefficients with the help of orthogonal polynomials.

Lemma 2. Let $(s_j(\theta))_{j=0}^{2n}$ (resp. $(s_j(\theta))_{j=0}^{2n-1}$) be a Stieltjes positive definite sequence. For $r = 1, 2$, let $Y_{r,n}$, $\mathbf{H}_{r,n-1}$ and $p_{r,n}$ be as in (7), (8), (9), (10), (13) and (14), respectively. Define $a_{n,i}$ by

$$\left(\frac{a_{n,1}}{\theta}, \frac{a_{n,2}}{\theta^2}, \dots, \frac{a_{n,n}}{\theta^n}\right) = (-1)^n Y_{r,n}^\top \mathbf{H}_{r,n-1}^{-1} \mathbf{J}_{n-1}, \quad (33)$$

where $a_{n,j}$ are negative numbers and

$$\mathbf{J}_n := \begin{pmatrix} 0 & 0 & \dots & 0 & 1 \\ 0 & 0 & \dots & -1 & 0 \\ \dots & \dots & \dots & \dots & \dots \\ 0 & (-1)^{n-1} & \dots & 0 & 0 \\ (-1)^n & 0 & \dots & 0 & 0 \end{pmatrix}.$$

Then, the characteristic polynomial $\tilde{p}_n(\tau, \theta)$ of the matrix $\mathbf{A}_n + b_n a_n^\top(\theta)$ is given by $\tilde{p}_n(\tau, \theta) = (-1)^n p_{r,n}(-\tau, \theta)$.

Proof. Let $r = 1$. Using (13) and (11), we have:

$$\begin{aligned} (-1)^n p_{1,n}(-\tau, \theta) &= (-1)^n (-Y_{1,n}^\top \mathbf{H}_{1,n-1}^{-1}, 1) E_n(-\tau) \\ &= (-1)^n (-Y_{1,n}^\top \mathbf{H}_{1,n-1}^{-1}, 1) \begin{pmatrix} 1 \\ \dots \\ (-1)^{n-1} \tau^{n-1} \\ (-1)^n \tau^n \end{pmatrix} \\ &= \tau^n + (-1)^{n+1} Y_{1,n}^\top \mathbf{H}_{1,n-1}^{-1} \mathbf{J}_{n-1} \begin{pmatrix} 1 \\ \dots \\ \tau^{n-2} \\ \tau^{n-1} \end{pmatrix}. \end{aligned} \quad (34)$$

From (32) and (34), we obtain (33). The proof for $r = 2$ is similar. \square

Now, we formulate one of the main results of the present work.

Theorem 3. For $r = 1, 2$, let $p_{r,n}(\tau, \theta)$ be a polynomial defined on $[0, +\infty)$ with respect to τ with parameter $\theta > 0$ as in (13) and (14). Let $a_{n,j}$ be defined as in (33), and let \mathbf{F}_n be a solution of (21). Furthermore, let $\theta(x)$ be the solution of equation (25) with a_0 as in (22). Thus, the positional control of the form (17) solves the synthesis problem for system (4).

Proof. Taking into account Lemma 2, the definition of $p_{r,j}$ for $r = 1, 2$ as in (13) and (14) and Equality (33), we see that positional control as in (17) satisfies all assumptions of Theorem 1. \square

Due to the representation of the characteristic polynomial of $\mathbf{A}_n + b_n a_n^\top(\theta)$ for fixed θ as in (32) and the representation of the orthogonal polynomial as in (34), in combination with Lemma 1, we see that a_n , chosen via (33), guarantees that the matrix $\mathbf{A}_n + b_n a_n^\top(\theta)$ is Hurwitz.

From Theorem 1, we know that every member of the family of orthogonal polynomials, as defined in (13) and (14), generates a positional control that solves the synthesis problem for the canonical system.

Remark 5. [21] *To construct the graphic of the trajectory $x(t)$, as well as the CF $\theta(x)$ and the bounded control $u_n(x)$ both on the trajectory $x = x(t)$ one proceeds to solve the following Cauchy problem:*

$$\begin{aligned}\dot{x}_1 &= \sum_{k=1}^n \frac{a_{n,k} x_k}{\theta^k(x)}, \\ \dot{x}_k &= x_{k-1}, \quad k = 2, \dots, n, \\ \dot{\theta} &= -\frac{x^\top \mathbf{D}_\theta \mathbf{W}_n \mathbf{D}_\theta x}{x^\top \mathbf{D}_\theta \tilde{\mathbf{F}}_n \mathbf{D}_\theta x}, \\ x(0) &= x_0, \quad \theta(0) = \theta_0,\end{aligned}$$

where x_0 is the given initial position and θ_0 is the solution of (25) for $x = x_0$.

Example 2. Consider the polynomial (16). By using (33), (21) and (22), we compute \mathbf{F}_2 , $\tilde{\mathbf{F}}_2$ and $2a_0$ with $\mathbf{W}_2 = \mathbf{I}_2$. For $\alpha > -1$, we have

$$\mathbf{F}_2 = \begin{pmatrix} \frac{\alpha^2+3\alpha+3}{4(\alpha+1)(\alpha+2)^2} & \frac{1}{2(\alpha+1)(\alpha+2)} \\ \frac{1}{2(\alpha+1)(\alpha+2)} & \frac{\alpha^3+4\alpha^2+10\alpha+11}{4(\alpha+1)(\alpha+2)} \end{pmatrix}, \quad (35)$$

$$\tilde{\mathbf{F}}_2 = \begin{pmatrix} \frac{\alpha^2+3\alpha+3}{2(\alpha+1)(\alpha+2)^2} & \frac{3}{2(\alpha+1)(\alpha+2)} \\ \frac{3}{2(\alpha+1)(\alpha+2)} & \frac{\alpha^3+4\alpha^2+10\alpha+11}{(\alpha+1)(\alpha+2)} \end{pmatrix}, \quad (36)$$

$$2a_0 = \frac{\alpha^4 + 6\alpha^3 + 19\alpha^2 + 34\alpha + 25}{4(\alpha + 2)^3 (5\alpha^4 + 29\alpha^3 + 74\alpha^2 + 109\alpha + 75)}. \quad (37)$$

For the value of $2a_0$ (37), we have selected the equality in (22).

For $\alpha = -1/2$, polynomial (16) has the form $p_{1,2}(-\tau, \theta) = \tau^2 + \frac{3}{\theta}\tau + \frac{3}{4\theta^2}$ and

$$\mathbf{F}_2 = \begin{pmatrix} \frac{7}{18} & \frac{2}{3} \\ \frac{2}{3} & \frac{55}{24} \end{pmatrix}, \quad \tilde{\mathbf{F}}_2 = \begin{pmatrix} \frac{7}{9} & \frac{2}{6} \\ \frac{2}{6} & \frac{55}{6} \end{pmatrix}, \quad 2a_0 = 386/15417.$$

The equation (25) has the form

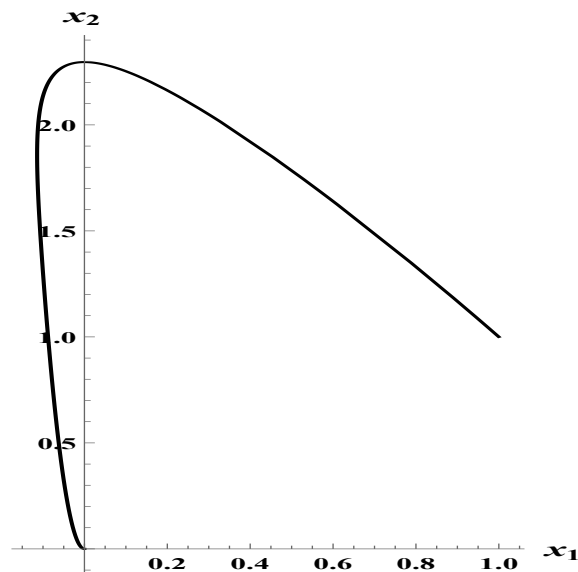
$$-\frac{386}{15417}\theta + \frac{7x_1^2}{18\theta} + \frac{4x_2x_1}{3\theta^2} + \frac{55x_2^2}{24\theta^3} = 0. \quad (38)$$

Let $x_0 = (1, 1)$ be the initial position. The unique positive solution of (38) for $x_0 = (1, 1)$ is equal to $\theta_0 = 5.35449$. The largest eigenvalue of matrix $\mathbf{I}_2 + \lambda \tilde{\mathbf{F}}_2$ is equal to -0.10396 . By employing (27), we obtain that the time of movement from $x_0 = (1, 1)$ to origin satisfies the following inequality $T(x_0) \leq 51.5053$. The corresponding positional control has the form

$$u_2(x_1, x_2) = -\frac{3x_1}{4\theta(x_1, x_2)} - \frac{3x_2}{\theta^2(x_1, x_2)}$$

where $\theta(x_1, x_2)$ is the unique positive solution of (38).

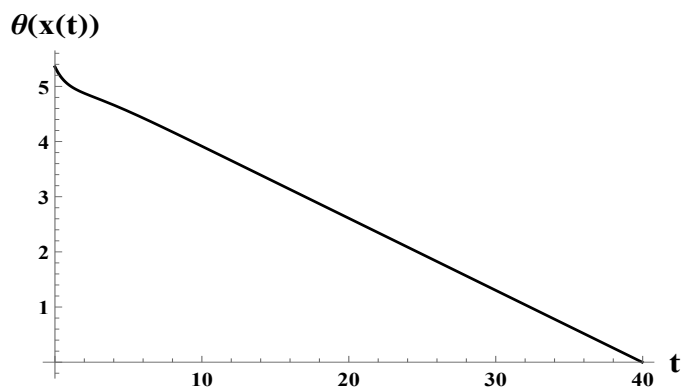
The following figure represents the phase portrait for the initial position $x_0 = (1, 1)$.



Pic. 1. Phase portrait for the initial position $x_0 = (1, 1)$.

Рис. 1. Фазовий портрет для початкової позиції $x_0 = (1, 1)$

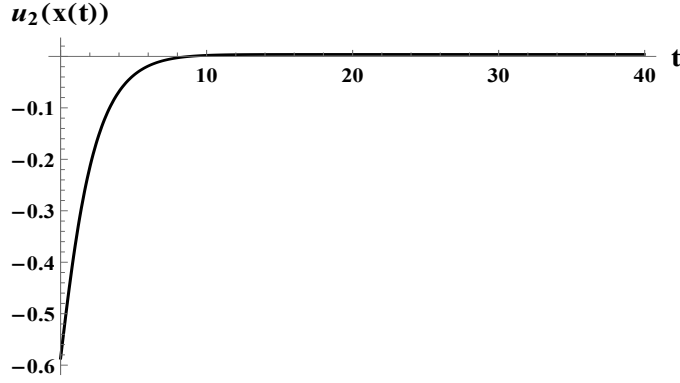
The graphic for the CF on the trajectory $\theta(x(t))$ has the following form.



Pic. 2. The graphic for the CF on the trajectory $\theta(x(t))$.

Рис. 2. Графік для CF на траєкторії $\theta(x(t))$.

Finally, the graphic of the position control on the trajectory $u_2(x(t))$ is the following.



Pic. 3. The graphic of the position control on the trajectory $u_2(x(t))$.

Рис. 3. Графік позиційного керування на траєкторії $u_2(x(t))$.

2. The CF as motion time is unobtainable via orthogonal polynomials

In this section, for $n = 2$ and for $n = 3$, we demonstrate that it is not possible to construct positional controls $u(x, \theta(x))$ as in (17) through orthogonal polynomials $p_{1,j}$ (resp $p_{2,j}$) as in (13) (resp. (14)). To this end, in the next remarks, we reproduce important results concerning the derivative of the CF with respect to time $\dot{\theta}$ and the estimation of time of motion $T(x_0)$.

Remark 6. In [29, Theorem 1] and [30, Theorem 1] while studying finite-time stability or finite-time output feedback control, a slight modification of the fundamental inequality

$$\dot{\theta}(x) \leq -\beta\theta^{1-\frac{1}{\alpha}}(x) \quad (39)$$

and the time estimation

$$T(x_0) \leq \frac{\alpha}{\beta}\theta^{1/\alpha}(x_0) \quad (40)$$

were used. Here α and β are positive numbers. Inequalities (39) and (40) appear as part of [15, Theorem 1], which gives sufficient conditions for a bounded multidimensional control $u(x, \theta(x))$ to stabilize at finite time the control system $\dot{x} = f(x, u)$, where f satisfies a Lipschitz condition in a subset of the space (x, u) .

The following remark recalls the case when $\theta(x_0)$ is exactly the time of motion from x_0 to the origin. For the canonical system (4), this occurs if

$$\mathbf{W}_n = \tilde{\mathbf{F}}_n. \quad (41)$$

Remark 7. a) If inequality (39) becomes an equality with $\alpha = 1$ and $\beta = 1$, we have

$$\dot{\theta} = -1. \quad (42)$$

This case was studied in [31], [22], [23], [26], [27]. Integrating (42) with respect to time t from 0 to t , we obtain

$$\theta(x(0)) - \theta(x(t)) = t. \quad (43)$$

Let $T(x_0)$ be motion time as in (40) and (3). Due condition 1) of [15, Theorem 1], we have

$$\theta(x(T(x_0))) = 0. \quad (44)$$

For $t = T(x_0)$ in (42), taking into account (44), we have that

$$\theta(x(0)) = T(x_0). \quad (45)$$

b) The importance of (45) is evident, namely,

$$\theta_0 = \theta(x(0)) \quad (46)$$

represents exactly the time of motion from the initial state x_0 to the origin.

Let $n = 2$ in (4). From [26, Equality (1.10)], for $a_{2,2} < -4$, we know that

$$u_2(x) = -\frac{3x_1}{\theta(x_1, x_2)} + \frac{a_{2,2}x_2}{\theta^2(x_1, x_2)} \quad (47)$$

is the positional control which solves the synthesis problem for the canonical system when the controllability function is the motion time. The control (47) is constructed for the case when \mathbf{F}_2 is a positive definite matrix, while $\tilde{\mathbf{F}}_2$ can be a positive definite matrix, or an indefinite matrix, or satisfy $\det \tilde{\mathbf{F}}_2 = 0$.

Proposition 2. For $n = 2$ and $n = 3$, the controllability function as motion time is not obtainable via orthogonal polynomials on $[0, \infty)$.

Proof. Let $n = 2$. Inserting the control (47) in (4) and computing the characteristic polynomial of matrix

$$\tilde{\mathbf{A}}_2 = \begin{pmatrix} -\frac{3}{\theta} & \frac{a_{2,2}}{\theta^2} \\ 1 & 0 \end{pmatrix} \quad (48)$$

for fixed positive θ with $a_{2,2} < -4$, we obtain

$$p_2(-\tau, \theta) = \tau^2 + \frac{3\tau}{\theta} - \frac{a_{2,2}}{\theta^2} \quad (49)$$

The roots of polynomial (49) have the form $\frac{1}{2\theta} \left(-3 \pm 2\sqrt{a_{2,2} + 9/4} \right)$. Thus, for $a_{2,2} < -4$, we have that the roots of polynomial (49) are complex numbers. On the other hand, the roots of polynomial $p_{r,2}(-\tau, \theta)$ for $\theta > 0$ and $r = 1, 2$ are real; see [4]. Consequently, one cannot construct a controllability function as a motion time with the help of the orthogonal polynomial $p_{r,2}(-\tau, \theta)$ for $r = 1, 2$.

For $n = 3$, the positional control for the case when the controllability function $\theta(x)$ is the time of motion when \mathbf{F}_3 is a positive definite matrix, has the form [27]

$$u_3(x) = -\frac{6x_1}{\theta} + \frac{(a_{3,3} - 30)x_2}{3\theta^2} + \frac{a_{3,3}x_3}{\theta^3}, \quad a_{3,3} < -30. \quad (50)$$

Substituting control (50) in (4), the corresponding characteristic polynomial for fixed positive θ is the following

$$-p_3(-\tau, \theta) = \tau^3 + \frac{6\tau^2}{\theta} - \frac{(a_{3,3} - 30)\tau}{3\theta^2} - \frac{a_{3,3}x_3}{\theta^3}. \quad (51)$$

Taking the derivative of $-p_3(-\tau, \theta)$ with respect to τ , we have

$$-p'_3(-\tau, \theta) = 3\tau^2 + \frac{12\tau}{\theta} - \frac{a_{3,3} - 30}{3\theta^2}. \quad (52)$$

The roots of $-p'_3(-\tau, \theta)$ are $\frac{1}{3\theta}(-6 \pm \sqrt{a_{3,3} + 6})$, for $a_{3,3} < -30$. Both of them are complex numbers. Hence, for every fixed θ , the polynomial $-p_3(-\tau, \theta)$ has no critical points. Thus, $-p_3(-\tau, \theta)$ is monotone nondecreasing function. Due to Bolzano's theorem, $-p_3(-\tau, \theta)$ has one real root. The remaining roots are complex numbers. On the other hand, polynomials $-p_{r,3}(-\tau, \theta)$ have only negative roots for fixed θ . Consequently, we have a similar result as for $n = 2$. \square

Conclusion

We have proved that every orthogonal polynomial on $[0, +\infty)$ described by (13) and (14) is a Hurwitz polynomial after performing two simple algebraic operations: a) replacing the independent variable τ by $-\tau$ and b) multiplying the polynomial by $(-1)^n$. This result follows from the properties of the roots of orthogonal polynomials and the definition of a Hurwitz polynomial. Using these orthogonal polynomials, we constructed bounded finite-time stabilizing controls.

We also demonstrated that no orthogonal polynomial can generate a positional control such that the controllability function represents the system's motion time.

An interesting open question remains: Is it possible to construct positional controls for system (1) using a combination of orthogonal polynomials on $[0, \infty)$, such that the controllability function represents the motion time or satisfies the equality $\dot{\theta} = -C$, where C is a positive constant? Further investigation of this problem would be worthwhile.

Acknowledgments

This work was supported by the Universidad Michoacana de San Nicolás de Hidalgo and SNII-CONAHCYT grants, México.

The authors would like to thank the anonymous reviewers for their helpful comments and feedback.

REFERENCES

1. E. D. Sontag. Mathematical control theory: Deterministic finite dimensional systems, Springer New York, NY. – 1998. – ISBN: 978-0-387-98489-6
2. G. G. Rigatos. Nonlinear control and filtering using differential flatness approaches: Applications to electromechanical systems, Springer Cham. – 2015. – ISBN: 978-3-319-16419-9

3. T. S. Chihara. An introduction to orthogonal polynomials, Gordon and Breach, Science Publishers, Inc. – 1978. – ISBN: 0677041500
4. G. Szegő. Orthogonal Polynomials, American Mathematical Society, Providence. – 1975. – ISBN: 0821810235
5. V. I. Korobov, V. O. Skoryk. Construction of restricted controls for a non-equilibrium point in global sense, Vietnam Journal of Mathematics – 2015. – Vol. **43**, No **2**. – P. 459–469. 10.1007/s10013-015-0132-4
6. A. E. Choque Rivero. On the solution set of the admissible bounded control problem via orthogonal polynomials, IEEE Transactions on Automatic Control. – 2017. – Vol. **62**, No **10**. – P. 5213–5219. 10.1109/TAC.2016.2633820
7. A. E. Choque-Rivero, B. d. J. G. Orozco. Bounded finite-time stabilizing controls via orthogonal polynomials. 2018 IEEE International Autumn Meeting on Power, Electronics and Computing (ROPEC), Ixtapa, Mexico. – 2018. – P. 1–4. 10.1109/ROPEC.2018.8661456
8. A. E. Choque Rivero. On Dyukarev's resolvent matrix for a truncated Stieltjes matrix moment problem under the view of orthogonal matrix polynomials, Linear Algebra and its Applications – 2015. – Vol. **474**. – P. 44–109. 10.1016/j.laa.2015.01.027
9. A. E. Choque Rivero. On matrix Hurwitz type polynomials and their interrelations to Stieltjes positive definite sequences and orthogonal matrix polynomials, Linear Algebra and its Applications – 2015. – Vol. **476**. – P. 56–84. 10.1016/j.laa.2015.03.001
10. Yu. M. Dyukarev. Theory of Interpolation Problems in the Stieltjes Class and Related Problems of Analysis. – 2006. – Habilitation thesis, Kharkiv National University.
11. A. Sandryhaila, J. Kovačević, M. Püschel. Algebraic signal processing theory: 1-D nearest neighbor models, IEEE Transactions on Signal Processing – 2012. – Vol. **60**, No **5**. – P. 2247–2259. 10.1109/TSP.2012.2186133
12. N. Stojanović, N. Stamenković, D. Živaljević. Monotonic, critical monotonic, and nearly monotonic low-pass filters designed by using the parity relation for Jacobi polynomials, International Journal of Circuit Theory and Applications – 2017. – Vol. **45**, No **12**. – P. 1978–1992. 10.1002/cta.2375
13. L. Lindström. Signal filtering using orthogonal polynomials and removal of edge effects, May 22 US Patent 7, 221, 975 – 2007.
14. G. Valent, W. Van Assche. The impact of Stieltjes' work on continued fractions and orthogonal polynomials: additional material, Journal of Computational and Applied Mathematics – 1995. – Vol. **65** No. **1-3**. – P. 419-447. 10.1016/0377-0427(95)00128-X

15. V. I. Korobov. A general approach to the solution of the bounded control synthesis problem in a controllability problem, *Matematicheskii Sbornik* – 1979. – Vol. **151**, No **4**. – P. 582-606.
16. V. I. Korobov, Y. V. Korotyaeva. Feedback control design for systems with x-discontinuous right-hand side, *J. Optim. Theory Appl.* – 2011. – Vol. **149** – P. 494–512. 10.1007/s10957-011-9800-z
17. V. I. Korobov, T. V. Revina. On perturbation range in the feedback synthesis problem for a chain of integrators system, *IMA J. Math. Control. Inf.* – 2021. – Vol. **38** – P. 396–416. 10.1093/imamci/dnaa035
18. V. I. Korobov, K. Stiepanova. The peculiarity of solving the synthesis problem for linear systems to a non-equilibrium point, *Mat. Fiz. Anal. Geom.* – 2021. – Vol. **17**, No **3**. – P. 326–340. 10.15407/mag17.03.326
19. A. E. Choque-Rivero, G. A. González, E. Cruz Mullisaca. Korobov's controllability function method applied to finite-time stabilization of the Rössler system via bounded controls, *Visnyk of V. N. Karazin Kharkiv National University. Ser. Mathematics, Applied Mathematics and Mechanics.* – 2020. – Vol. **91**. – P. 4–20. 10.26565/2221-5646-2020-91-01
20. A. E. Choque Rivero, J. J. Rico-Melgoza, F. Ornelas-Tellez. Finite-time stabilization of the prey-predator model, *Memorias del Congreso Nacional de Control Automático.* – 2019. – P. 395–400. revistadigital.amca.mx/wp-content/uploads/2022/06/0152.pdf
21. V. I. Korobov. Controllability function method, (in Russian), NITS, Inst. Comp. Research, Moscow-Izhevsk: Izdanie RFFI. – 2007.
22. A. E. Choque Rivero, V. I. Korobov, V. A. Skoryk. Controllability function as time of motion I. *Journal of Mathematical Physics, Analysis, Geometry.* – 2004. – Vol. **11**, No. **2**. – P. 208–225. 10.48550/arXiv.1509.05127.
23. A. E. Choque Rivero, V. I. Korobov, V. A. Skoryk. Controllability function as time of motion II. *Journal of Mathematical Physics, Analysis, Geometry.* – 2004. – Vol. **11**, No. **3**. – P. 341–354.
24. A. E. Choque Rivero. The controllability function method for the synthesis problem of a nonlinear control system, *International Review of Automatic Control.* – 2008. – Vol. **1**, No **4**. – P. 441–445.
25. W. M. Haddad, V. S. Chellaboina. *Nonlinear Dynamical Systems and Control*, Princeton University Press. – 2008. – ISBN: 9780691133294
26. A. E. Choque Rivero. Extended set of solutions of a bounded finite-time stabilization problem via the controllability function, *IMA J. Math. Control Inf.* – 2021. – Vol. **38**, No **4**. – P. 1174–1188. 10.1093/imamci/dnab028

27. A. E. Choque Rivero. Korobov's Controllability Function as Motion Time: Extension of the Solution Set of the Synthesis Problem, *Journal of Mathematical Physics, Analysis, Geometry*. – 2023. – Vol. **19**, No **3**. – P. 556-586. 10.15407/mag19.03.556
28. A. E. Choque Rivero. Hurwitz polynomials and orthogonal polynomials generated by Routh–Markov parameters, *Mediterranean Journal of Mathematics*. – 2018. – Vol. **15**, No **40**. – P. 1-15. 10.1007/s00009-018-1083-2
29. S. P. Bhat, D. S. Bernstein. Lyapunov analysis of finite-time differential equations, *IEEE, American Control Conference*. – 1995. – **3**. – P. 1831–1832. 10.1109/ACC.1995.531201
30. A. S. Poznyak, A. Ye. Polyakov, V. V. Strygin. Analysis of finite-time convergence by the method of Lyapunov functions in systems with second-order sliding modes, *Journal of Applied Mathematics and Mechanics*. – 2011. – Vol. **75**, No **3**. – P. 289–303. 10.1016/j.jappmathmech.2011.07.006
31. V. I. Korobov, G. M. Sklyar. Methods for constructing of positional controls and an admissible maximum principle, *Differ. Uravn.* – 1990. – Vol. **26**, No. **11**. – P. 1914–1924.
32. V. I. Korobov, T. V. Revina. On the feedback synthesis for an autonomous linear system with perturbations. *J. of Dynam. and Control Syst.* – 2024. 10.1007/s10883-024-09690-4
33. A. E. Choque-Rivero. The matrix Toda equations for coefficients of a matrix three-term recurrence relation, *Operators and Matrices*. – 2019. – Vol. **13**, No. **4**. – P. 1125-1145. doi.org/10.7153/oam-2019-13-75
34. A. E. Choque-Rivero, I. Area. Favard type theorem for Hurwitz polynomials, *Discrete & Continuous Dynamical Systems–B*. – 2020. – Vol. **25**, No. **2**. – P. 529-544. doi: 10.3934/dcdsb.2019252

Article history: Received: 5 October 2024; Final form: 18 December 2024

Accepted: 20 December 2024.

How to cite this article:

A. E. Choque-Rivero, T. Vukašinac, Korobov's controllability function method via orthogonal polynomials on $[0, \infty)$, *Visnyk of V. N. Karazin Kharkiv National University. Ser. Mathematics, Applied Mathematics and Mechanics*, Vol. 100, 2024, p. 61–78. DOI: 10.26565/2221-5646-2024-100-04

Метод функції керованості Коробова за допомогою ортогональних поліномів на $[0, \infty)$

А. Е. Чоке-Ріверо¹, Т. Вукашинац²

¹Інститут фізики та математики

Університет Мічоакана-де-Сан-Ніколас-де-Ідальго

Будівля С-3, Центральний кампус, 58060, Морелія, Мічоакан, Мексика

²Факультет цивільного будівництва

Університет Мічоакана-де-Сан-Ніколас-де-Ідальго

Будівля А, Центральний кампус, 58060, Морелія, Мічоакан, Мексика

Дано керовану систему, описану звичайними диференціальними рівняннями або диференціальними рівняннями із частинними похідними, та початковий стан. Задача знаходження множини обмежених позиційних керувань, які переводять початковий стан у деякий інший стан (не обов'язково точку рівноваги) за скінченний час, називається задачею синтезу.

У даній роботі розглядається сімейство систем у формі Бруновського розмірності n . Для стабілізації заданої системи у формі Бруновського за скінченний час побудовано сімейство обмежених позиційних керувань $u_n(x)$. Ми використовуємо ортогональні поліноми, що асоційовані з функціональним розподілом $\sigma(\tau, \theta)$, визначеним для $\tau \in [0, +\infty)$ і параметра $\theta > 0$. Параметр θ інтерпретується як функція керованості Коробова, $\theta = \theta(x)$, яка слугує функцією типу Ляпунова. Використовуючи $\theta(x)$, ми будемо позиційне керування: $u_n(x) = u_n(x, \theta(x))$.

Наш аналіз базується на фундаментальній роботі: "A general approach to the solution of the bounded control synthesis problem in a controllability problem", *Matematiceskii Sbornik*, 151(4), 582-606 (1979) авторства В. І. Коробова, у якій було запропоновано метод функції керованості. Цей метод було застосовано для розв'язання задач стабілізації обмеженим керуванням за скінченний час у різних сценаріях керування, таких як керування хвильовим рівнянням, оптимальне керування зі змішаними критерієм якості та інші застосування.

Для побудови згаданих позиційних керувань ми використовуємо члени сімейства ортогональних на $[0, \infty)$ поліномів. Детальнішу інформацію про ортогональні поліноми можна знайти у книзі: "Orthogonal Polynomials", American Mathematical Society, Providence, (1975) авторства G. Szegő. Ми також спираємося на роботу: "On matrix Hurwitz type polynomials and their interrelations to Stieltjes positive definite sequences and orthogonal matrix polynomials", *Linear Algebra and its Applications*, 476, 56-84 (2015) авторства А. Е. Choque Rivero.

Результати, представлені у цій роботі, розширюють і розвивають напрацювання, викладені у конференційній доповіді: "Bounded finite-time stabilizing controls via orthogonal polynomials", 2018 IEEE International Autumn Meeting on Power, Electronics and Computing (ROPEC), Ixtapa, Mexico, 2018, авторства А. Е. Choque Rivero, B. d. J. G. Orozco.

Ключові слова: обмежене керування; ортогональні поліноми; стабілізація за скінченний час; функція керованості; канонічна система.

Історія статті: отримана: 5 жовтня 2024; останній варіант: 18 грудня 2024
прийнята: 20 грудня 2024.

Правила для авторів
«Вісника Харківського національного університету
імені В. Н. Каразіна»,
Серія «Математика, прикладна математика і механіка»

Редакція просить авторів при направленні статей керуватися наступними правилами.

1. В журналі публікуються статті, що мають результати математичних досліджень (англійською або українською мовами).

2. Поданням статті вважається отримання редакцією файлів статті оформлених у редакторі LaTeX, анотацій, відомостей про авторів та архіва, що включає LaTeX файли статті та файли малюнків. Файл-зразок оформлення статті можна знайти на офіційній веб-сторінці журналу (http://periodicals.karazin.ua/mech_math). Авторам необхідно зареєструватися та **завантажити подання** на цій сторінці. Будьте уважними, заповнюючи форму подання двома мовами (українською та англійською).

3. Стаття повинна починатися з розширеної анотації (обсягом **не менш ніж 1800 знаків**), в якій повинні бути чітко сформульовані мета та результати роботи. Анотація повинна бути тією мовою (англійською або українською), якою є основний текст статті. Закордонні автори можуть звернутися до редакції за допомогою з перекладом анотацій на українську мову. Повинні бути наведені прізвища, ініціали авторів, назва роботи, ключові слова та номер за міжнародною математичною класифікацією (Mathematics Subject Classification 2020). Анотація не повинна мати посилань на літературу чи малюнки. На першій сторінці вказується номер УДК класифікації. В кінці статті треба додати переклад анотації (обсягом **не менш ніж 1800 знаків**) на другу мову (англійську чи українську).

4. Список літератури повинен бути оформлений латинським шрифтом. Приклади оформлення списку літератури:

1. A.M. Lyapunov. A new case of integrability of differential equations of motion of a solid body in liquid, Rep. Kharkov Math. Soc., – 1893. – 2. V.4. – P. 81-85.
2. A.M. Lyapunov. The general problem of the stability of motion. Kharkov Mathematical Society, Kharkov. - 1892. - 251 p.

5. Кожний малюнок повинен бути пронумерований та представлений окремим файлом в одному з форматів: EPS, BMP, JPG. В файлі статті малюнок повинен бути вставлений автором. Під малюнком повинен бути підпис. Назви файлів малюнків повинні починатись з прізвища першого автора.

6. Відомості про авторів повинні містити: прізвища, імена, по батькові, службові адреси та номери телефонів, науковий ступінь, посаду, адреси електронних скриньок та інформацію про наукові профайли авторів (orcid.org, www.researcherid.com, www.scopus.com) з відповідними посиланнями. Прохання також повідомити прізвище автора, з яким треба вести листування.

7. Рекомендуємо використовувати в якості зразка оформлення останні випуски журналу (http://periodicals.karazin.ua/mech_math).

8. У випадку порушення правил оформлення редакція не буде розглядати статтю.

Електронна скринька: vestnik-khnu@ukr.net

Наукове видання

Вісник Харківського національного університету імені В. Н. Каразіна,
Серія “Математика, прикладна математика і механіка”, Том 100, 2024 р.

Збірник наукових праць

Англійською та українською мовами

Підписано до друку 29.12.2024 р.

Формат 70 × 108/16. Папір офсетний. Друк цифровий.

Ум. друк. арк. 5,53

Обл.– вид. арк. 6,9

Наклад 100 пр. Зам. № 45/24

Безкоштовно.

Видавець і виготовлювач Харківський національний університет
імені В. Н. Каразіна, 61022, м. Харків, майдан Свободи, 4

Свідоцтво суб'єкта видавничої справи ДК № 3367 від 13.01.09

Видавництво Харківського національного університету імені В. Н. Каразіна
тел. 705-24-32